Institut für Nutzpflanzenwissenschaften und Ressourcenschutz (INRES)

Characterization of the phenylboronic acid-induced defects in primary roots of maize (*Zea mays* L.) and the association of boron homeostasis with the benzoxazinoid pathway

Dissertation

zur Erlangung des Grades

Doktorin der Agrarwissenschaften (Dr. agr.)

der Agrar-, Ernährungs- und Ingenieurwissenschaftlichen Fakultät

der Rheinischen Friedrich-Wilhelms-Universität Bonn

von

Liuyang Chu

aus

Hunan, China

Bonn, 2026

Referentin: PD Dr. Michaela Matthes

Korreferent: Prof. Dr. Gabriel Schaaf

Tag der mündlichen Prüfung: 20.03.2026

Angefertigt mit Genehmigung der Agrar-, Ernährungs- und Ingenieurwissenschaftlichen Fakultät der Universität Bonn

Content

List of figures

List of tables

Abbreviations

2-CPBA	2-Carboxyphenylboronic acid
5HIONG	Indoline-2-one-5-β-D-glucopyranoside
2,4-D	2,4-Dichlorophenoxyacetic acid
ABA	Abscisic acid
ACC	1-Aminocyclopropane-1-carboxylic acid
AIR	Alcohol-insoluble residues
ANOVA	Analysis of variance
Api	D-apiose
ARF	AUXIN RESPONSE FACTOR
At	*Arabidopsis thaliana*
AUX1	AUXIN-RESISTANT 1
AUX/IAA	AUXIN/ INDOLE-3-ACETIC ACID
BA	Branching area
BBA	1-Butylboronic acid
BLUPs	Best linear unbiased predictors
BN	Branch number
BOR	High boron requiring
bx	*benzoxazinless*
BZ	Branching zone
CS	Central spike
DAB	3,3'-Diaminobenzidine
DAP	Days after planting
DAT	Days after treatment
DIBOA	2,4-Dihydroxy-1,4-benzoxazin-3-one
DIMBOA	2,4-Dihydroxy-7-methoxy-1,4-benzoxazin-3-one
DNA	Deoxyribonucleic acid
dRG-II	Dimeric rhamnogalacturonan II
EPG	Endopolygalacturonase
Glc	Glucoside
GWAS	Genome-wide association study
HBOA	2-Hydroxy-1,4-benzoxazin-3-one

HG	Homogalacturonan
HION	3-Hydroxy-indolin-2-one
HPLC	High-performance liquid chromatography
^{1}H-NMR	Proton nuclear magnetic resonance
IAA	Indole-3-acetic acid
IGP	Indole-3-glycerolphosphate
ION	Indolin-2-one
Kyn	L-Kynurenine
LBD	LATERAL ORGAN BOUNDARIES DOMAIN
LD	Linkage disequilibrium
LRD	Lateral root density
LRN	Lateral root number
LRP	Lateral root primordia
MAF	Minor allele frequency
mRG-II	Monomeric rhamnogalacturonan II
mRNA	Messenger ribonucleic acid
mur1	*murus1*
MZ	Maturation zone
NIP	Nodulin 26-like intrinsic protein
OGAs	Oligogalacturonic acids
ORF	Open reading frame
PAGE	Polyacrylamide gel electrophoresis
PBA	Phenylboronic acid
PIN	PIN-FORMED
PL	Peduncle length
PM	Plasma membranes
PME	Pectin methylesterase
PPBo	4-Phenoxyphenylboronic acid
PR	Primary root tip
PRL	Primary root length
QQ	Quantile-quantile
QTL	Quantitative trait locus

RG-I	Rhamnogalacturonan I
RG-II	Rhamnogalacturonan II
RNA	Ribonucleic acid
ROS	Reactive oxygen species
rte	*rotten ear*
SA	Salicylic acid
SAUR	SMALL AUXIN UP-REGULATED RNA
SEC	Size-exclusion chromatography
SNP	Single nucleotide polymorphism
spi1	*sparse inflorescence1*
TAA	TRYPTOPHAN AMINOTRANSFERASE OF ARABIDOPSIS
TL	Tassel length
tls1	*tassel-less1*
TRIBOA	2,4,7-Trihydroxy-1,4-benzoxazin-3-one
UTR	Untranslated region
UV	Ultraviolet
vt2	*vanishing tassel2*
WT	Wild type
XTH	XYLOGLUCAN TRANSGLYCOSYLASE/HYDROLASE
YFP	YELLOW FLUORESCENT PROTEIN
YUC	YUCCA
Zm	*Zea mays*

Abstract/Zusammenfassung

Abstract

Boron is an essential micronutrient for plants. *In planta*, boron predominantly resides in the primary cell wall, crosslinking the pectic polysaccharide rhamnogalacturonan II (RG-II), which is vital for maintaining cell wall integrity. Non-optimal levels of boron negatively affect the development of plants and reduce crop yield. In adaptation to variable soil boron conditions, plants have developed mechanisms to maintain boron homeostasis, of which the best known are boron transporters. In the cereal crop and model plant maize (*Zea mays* L.), the importance of boron during reproductive development is well studied, and genes encoding boron transporters have been characterized. However, the effects of boron deficiency on the maize root, and regulators of boron homeostasis in maize next to boron transporters, remain largely obscure.

To assess boron deficiency-induced defects in maize roots, one strategy is to induce boron deficiency using a chemical approach. Phenylboronic acid (PBA) was hypothesized to inhibit RG-II dimerization and therefore might mimic boron deficiency. However, the characterization of PBA as a boron deficiency mimic *in planta* has not been demonstrated.

To identify new regulators of boron homeostasis in maize, one strategy is to assess natural variation of boron concentration in association panels, and to subsequently analyze the phenotypic variation with the genetic variation through genome-wide association analysis (GWAS).

This thesis characterized the boron deficiency-induced defects in maize roots, tested the usability of PBA as a boron deficiency mimic, and identified additional regulators of boron homeostasis in maize leaves using GWAS.

In chapter 2, the primary root defects induced by boron deficiency and by PBA were characterized and compared. Both boron deficiency and PBA induced defects in primary root length, lateral root density, auxin levels and reactive oxygen species levels. Although the PBA-induced defects were similar to the boron deficiency-induced defects, the severity was different. Notably, PBA did not inhibit nor promote RG-II crosslinking *in vitro*, and PBA did not incorporate into pectin *in vivo*. Specifically, the PBA-induced lateral root density defects appeared linked to functions of the boric acid moiety. Using the ratios of primary root length and lateral root density between PBA treatment and no-PBA control, putative targets of PBA related to phytohormones, cell wall modification, endocytosis, and root development were

detected through GWAS.

In chapter 3, a GWAS of boron levels in maize ear leaves was conducted to identify novel genetic regulators of boron homeostasis. Integrated analysis of the GWAS results and gene expression data highlighted *benzoxazinless3* (*bx3*) as a promising candidate, suggesting an association between leaf boron homeostasis and the benzoxazinoid pathway, a well-characterized defense pathway. The loss-of-function mutation of *bx3* in maize and the overexpression of *BX1* and *BX2* in Arabidopsis, a species that does not endogenously express the benzoxazinoid pathway, both resulted in elevated boron levels in leaves. Furthermore, the product of the BX3 enzyme function, 3-hydroxy-indolin-2-one (HION), was found to form a complex with boric acid *in vitro*. Our study, therefore, detected a novel connection between boron homeostasis and the benzoxazinoid pathway, likely through *bx3* and the direct substrate and product of BX3, furthermore suggesting a potential target for crop engineering for better adaptability to low soil boron levels.

Zusammenfassung

Bor ist ein essentieller Mikronährstoff für Pflanzen. In Pflanzen befindet sich Bor überwiegend in der primären Zellwand, wo es das pektische Polysaccharid Rhamnogalacturonan II (RG-II) vernetzt. Diese Vernetzung ist entscheidend für die Aufrechterhaltung der Zellwandintegrität. Nicht-optimale Konzentrationen von Bor beeinträchtigen die Pflanzenentwicklung und verringern den Ernteertrag. Zur Aufrechterhaltung der Borhomöostase haben Pflanzen unterschiedliche Mechanismen entwickelt, von denen die bekanntesten über Bortransporter wirken. Bei der Nutz- und Modellpflanze Mais (*Zea mays* L.) ist die Bedeutung von Bor während der reproduktiven Entwicklung gut untersucht. Zusätzlich sind auch die Bortransporter in Mais charakterisiert. Dennoch bleiben die Auswirkungen von Bormangel auf die Maiswurzel sowie Regulatoren der Bor-Homöostase neben den Transportern weitgehend unklar.

Um Bormangel-bedingte Defekte in Maiswurzeln zu untersuchen, besteht eine Strategie darin, Bor-Mangelbedingungen chemisch zu induzieren. Es wird angenommen, dass Boronsäuren, wie Phenylborsäure (PBA), die Dimerisierung von RG-II blockieren und dadurch Bormangel imitieren. Eine Charakterisierung von PBA in Bezug auf dessen Fähigkeit Bormangel *in planta* zu induzieren wurde jedoch bisher nicht durchgeführt.

Zur Identifizierung neuer Regulatoren der Bor-Homöostase in Mais können beispielsweise genomweite Assoziationsanalysen (GWAS) durchgeführt werden. Dabei wird die natürliche Variation von Merkmalen, z. B. die Borkonzentration, in genetischen Populationen erfasst und anschließend die phänotypische Variation mit genetischen Informationen der Population assoziiert.

Diese Dissertation charakterisierte die durch Bormangel verursachten Defekte in Maiswurzeln, prüfte die Verwendbarkeit von PBA zur Induzierung von Bormangel und identifizierte neue Regulatoren der Bor-Homöostase in Mais.

In Kapitel 2 wurden die durch Bormangel und durch PBA induzierten Primärwurzeldefekte charakterisiert und verglichen. Sowohl Bormangel als auch PBA führten zu Defekten in der Primärwurzel-Länge, der Dichte der Seitenwurzeln, sowie dem Gehalt an Auxin und reaktiver Sauerstoffspezies. Obwohl die durch PBA induzierten Defekte denjenigen des Bormangels ähnelten, unterschieden sie sich in ihrer Ausprägung. Auffällig war, dass PBA *in vitro* weder die RG-II-Vernetzung hemmte noch förderte und *in vivo* nicht in Pektin eingebaut wurde. Insbesondere schienen die durch PBA hervorgerufenen Defekte in der Seitenwurzel-Dichte mit Funktionen der Borsäure-Gruppe zusammenzuhängen. Durch die Analyse der Verhältnisse von Primärwurzel-Länge und Seitenwurzel-Dichte zwischen PBA-Behandlung und

Kontrollbedingungen konnten mittels GWAS potenzielle PBA-Zielgene identifiziert werden, die im Zusammenhang mit Phytohormonen, Zellwandmodifikation, Endozytose und Wurzelentwicklung standen.

In Kapitel 3 wurde eine GWAS der Borgehalte in Mais-Kolbenblättern durchgeführt, um neue genetische Regulatoren der Bor-Homöostase zu identifizieren. Die integrierte Analyse der GWAS-Ergebnisse mit öffentlich verfügbaren Genexpressionsdaten hob *benzoxazinless3* (*bx3*) als vielversprechendes Kandidatengen hervor und deutete auf eine Verbindung zwischen der Bor-Homöostase in Blättern und dem Benzoxazinoid-Stoffwechselweg hin. Sowohl die Funktionsverlust-Mutation von *bx3* in Mais als auch die gleichzeitige Überexpression von *BX1* und *BX2* in Arabidopsis, einer Art, die den Benzoxazinoid-Stoffwechselweg endogen nicht exprimiert, führten zu erhöhten Borgehalten in Blättern. Darüber hinaus wurde festgestellt, dass das Produkt der BX3-Enzymfunktion, 3-Hydroxy-Indolin-2-on, *in vitro* einen Komplex mit Borsäure bilden kann. Somit zeigte unsere Studie, dass der Benzoxazinoid-Stoffwechselweg in Mais mit der Bor-Homöostase verknüpft ist, wahrscheinlich über *bx3* sowie das direkte Substrat und Produkt von BX3. Somit wurde in dieser Dissertation ein potenzielles Ziel für die Pflanzenzüchtung zur besseren Anpassungsfähigkeit von Mais an geringe Borgehalte im Boden identifiziert.

1 Introduction

Boron is a metalloid element identified as an essential micronutrient for plants (Warington, 1923; Marschner, 2023). In the form of boric acid $B(OH)_3$, boron is accessible to roots and can be transported and utilized by plants (Matthes et al., 2020). Optimal levels of boron are important for the growth and development of many plants, and boron presents a narrow window between deficient and toxic concentrations (Goldberg, 1997).

1.1 Boron deficiency and toxicity phenotypes

Although boron is ubiquitous on earth, it is distributed heterogeneously. The dissolved forms of boron are mainly boric acid $B(OH)_3$ and the borate anion $B(OH)_4^-$, both highly soluble in water, making boron easily leached from soil by rainfall. As a consequence, boron deficiency in soils is a prominent abiotic stress worldwide (Shorrocks, 1997; Brdar-Jokanović, 2020). This stress is predicted to get even more severe with climate change, as intense rainfall or drought can either leach boron from soil or restrict boron uptake (García-Sánchez et al., 2020; Li et al., 2023). In semi-arid environments, especially in soil irrigated with boron-rich water, and in soil developed from marine and volcanic clay, boron levels exceed plant requirements and cause boron toxicity symptoms in crops, and ultimately yield losses (Ponnamperuma and Yuan, 1966; Martínez-Alvarez et al., 2017; Brdar-Jokanović, 2020; Zhao et al., 2024).

1.1.1 Boron deficiency phenotypes

When the availability of boron is limited for plants, the root and shoot meristems, groups of undifferentiated cells that generate post-embryonic tissues and organs (Lindsay et al., 2024), are affected. Both meristem types halt their growth under such conditions, leading to inhibition of root elongation, leaf expansion, and flower development. (Fig. 1.1; Bolaños et al., 2023; Chu et al., 2025b).

Root shortening is one of the earliest responses observed under boron deficiency (Warington, 1923; Dell and Huang, 1997). Early inhibition of root length is attributed to impaired cell division and inhibited cell elongation (Martin-Rejano et al., 2011). The root meristem length was rapidly reduced under boron deficiency in advance of primary root length reduction (Poza-Viejo et al., 2018). In Arabidopsis, boron deficiency-induced root defects also include enhanced root hairs, cell death and swollen root tips (Oiwa et al., 2013; Camacho-Cristobal et al., 2015). These defects were repeatedly observed in various dicotyledons (Bolaños et al., 2023; Chu et al., 2025b). In cereal crops like maize, knowledge regarding the root responses to boron deficiency is limited. A few studies investigated boron deficiency-induced root defects with

partially contradicting results, since maize root systems either were unaffected by boron deficiency (Lordkaew et al., 2011; Bienert et al., 2023) or showed reductions in primary root length, lateral root number, and lateral root density (Eltinge, 1936; Wilder et al., 2022). These inconsistencies might reflect genotypic and tissue-specific variation of boron deficiency susceptibility in maize roots.

In the shoot, typical boron deficiency symptoms include growth arrest, leaf chlorosis and loss of apical dominance (Fig. 1.1). Dicotyledonous plants like Arabidopsis and oilseed rape (*Brassica napus*) developed small, rolled and brittle young leaves, short internodes and bushy shoot appearances under boron deficiency (Takano et al., 2006; Tanaka et al., 2008; Zhang et al., 2014; Pommerrenig et al., 2018). Maize developed white stripes between leaf veins, irregularly arranged vascular bundles, and narrow wrinkle leaves under boron deficiency (Lordkaew et al., 2011; Chatterjee et al., 2014; Durbak et al., 2014; Bienert et al., 2023). The reproductive development is particularly sensitive to boron deficiency. In Arabidopsis, boron limitation inhibited development of flowers and siliques, and even caused seed setting failure (Noguchi et al., 1997; Takano et al., 2006; Muro et al., 2025). Similarly, in oilseed rape, boron deficiency caused malformed flowers with wrinkled petals and separated anther-stigma, or withered flower buds, resulting in the "flowering-without-seed-setting" symptom (Xu et al., 2002; Zhang et al., 2017; Verwaaijen et al., 2023; Tölle et al., 2025). In maize, both the tassel and the ear were completely missing under severe boron deficiency (Leonard et al., 2014; Durbak et al., 2014). In less severe cases of boron deficiency in maize, pollen sterility and small or deformed cobs were observed, while there was no significant decrease in the dry weight of vegetative tissues (Lordkaew et al., 2011). The sensitivity of reproductive development to boron deficiency is conserved among many other crops, including rice (*Oryza sativa*), wheat (*Triticum aestivum*) and barley (*Hordeum vulgare*; Garg et al., 1979; Dell and Huang, 1997; Nakagawa et al., 2007). The boron deficiency-induced defects in reproductive development consequently lead to drastic losses of grain yield and quality (Brdar-Jokanović, 2020).

1.1.2 Boron toxicity phenotypes

Boron toxicity leads to symptoms including inhibited root and shoot growth, leaf chlorosis or necrosis, and reduced fertility (Fig. 1.1; Camacho-Cristóbal et al., 2008; Marschner, 2023). In Arabidopsis roots, excessive boron inhibited root growth in a dose-dependent manner, particularly affecting the root meristem zone (Aquea et al., 2012; Tapia-Quezada et al., 2022). Similar responses were observed also in cereals like barley and rice (Reid et al., 2004; Choi et al., 2007; de Abreu Neto et al., 2017). In maize, negative effects of boron toxicity on root length

(Esim et al, 2013; Sakcali et al., 2015) were observed. Boron toxicity could reduce the number of maize roots and enhance the lateral root elongation, without causing adverse defects in shoot growth (Wilder et al., 2022).

In plant shoots, boron toxicity caused chlorosis and necrosis in older leaves. The leaf symptoms were pronounced at the leaf tips and start with spots (Ponnamperuma and Yuan, 1966; Reid et al., 2004). Reduction of chlorophyll and water content in the shoot induced by high boron treatment have also been repeatedly reported (Macho-Rivero et al., 2017; Macho-Rivero et al., 2018; Martínez-Mazón et al., 2023). Boron toxicity also caused deformities in fruits (Xu et al., 2021; Yang et al., 2022). In rice, boron toxicity led to reduction of tillers, indicating involvement of impaired meristem maintenance (de Abreu Neto et al., 2017). In maize, excessive boron reduced shoot length and leaf area significantly, induced necrosis at the leaf margins, and inhibited root growth (Esim et al., 2013).

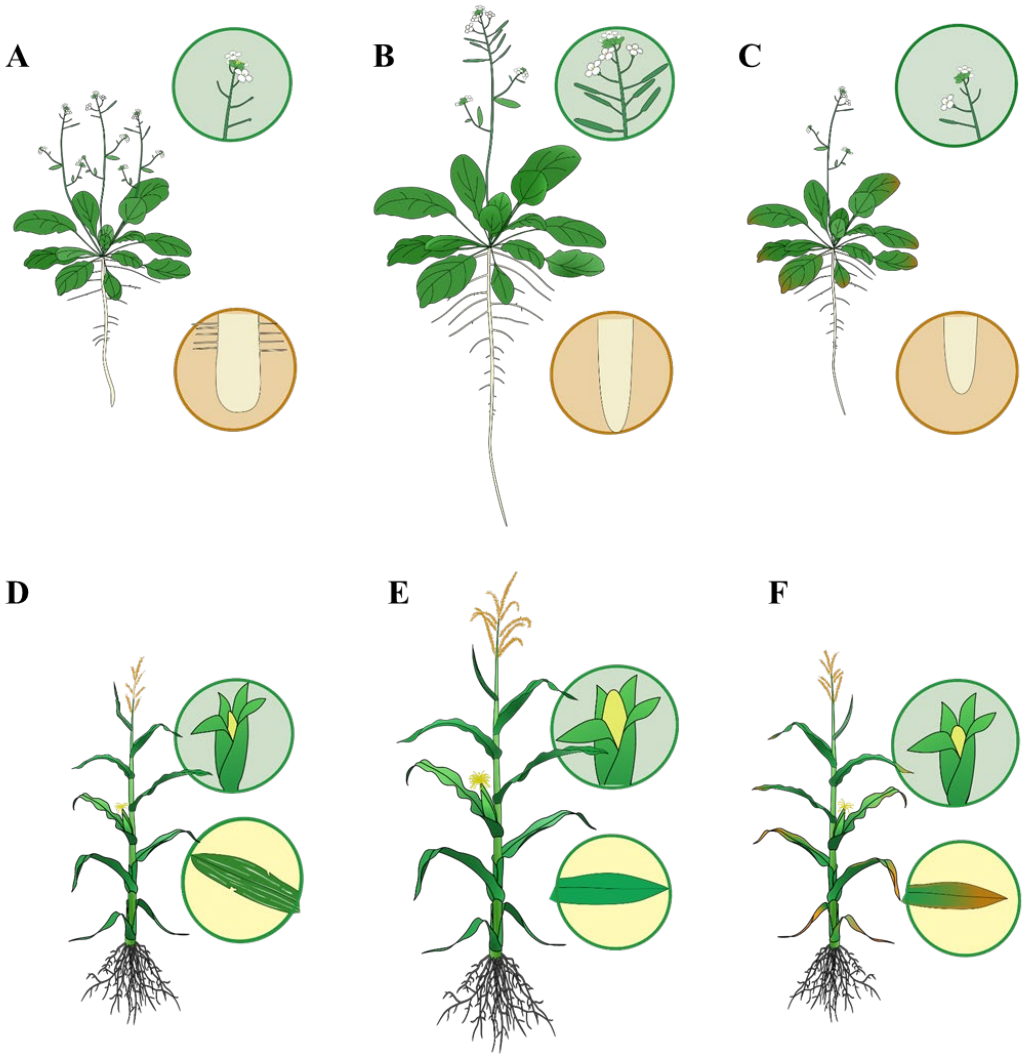

Figure 1.1. Typical boron deficiency and toxicity phenotypes in Arabidopsis and maize. A-C, Arabidopsis phenotypes

observed under different boron growing conditions. A, Arabidopsis grown under boron-deficient condition. The plant is small, the leaves especially the younger leaves are rolled, the shoot apical dominance is lost, the fertility is reduced, the root is short and stunted with dense root hairs developed, the root tip is enlarged. B, Arabidopsis grown with optimal levels of boron achieves optimal growth. C, Arabidopsis grown under boron-toxic condition. The plant growth is inhibited, the fertility is reduced, necrosis is developed at the leaf tips and margins, especially at the older leaves, the root elongation is inhibited. D-F, Maize phenotypes observed under different boron growing conditions. D, Maize grown in boron-deficient soil. The leaves are small, thick, brittle and with chlorotic stripes, especially in the younger leaves; the cob is small; the fertility is reduced. E, Maize grown with adequate levels of boron results in optimal growth. F, Maize grown under boron-toxic condition. Necrosis is developed in the leaves, from older leaves to younger ones, from leaf tips and margins to the whole leaf. Boron toxicity reduced the size of tassels and ears.

1.2 Transport of boron

Boron is taken up and translocated in plants through multiple transport pathways. Uncharged boric acid can diffuse across plasma membranes along the concentration gradient (Dordas et al., 2000; Stangoulis et al., 2001). Meanwhile, the facilitated transport and active transport of boron are important for efficient boron uptake and translocation in plants grown with insufficient soil boron levels (Fig. 1.2). The directional transport of boron is mediated by two classes of boron channels/transporters: the NODULIN INTRINSIC PROTEIN (NIP) family and the HIGH BORON REQUIRING (BOR) family (Shao et al., 2021; Jothi and Takano, 2023).

There are three NIP channels identified in Arabidopsis that can accelerate boric acid import: NIP5;1 in the root tip epidermis and mature root endodermis, NIP6;1 in the stem node phloem region and NIP7;1 in the anther tapetum (Takano et al., 2006; Tanaka et al., 2008; Routray et al., 2018). Under boron deficiency, NIP5;1 is polarly localized in the soil-side plasma membrane to import boric acid. The *NIP5;1* ortholog *tassel-less1* (*tls1*) was characterized in maize (Leonard et al., 2014; Durbak et al., 2014). Orthologs of *tls1* have also been identified in other crops including rice, barley, and oilseed rape (Mitani et al., 2008; Schnurbusch et al., 2010; Hanaoka et al., 2014; Liu et al., 2015; Hua et al., 2016; Shao et al., 2021; Zhou et al., 2021; Song et al., 2021; He et al., 2021).

BORs actively export boron out of the cytosol against concentration gradients. The main boron efflux transporter found in the Arabidopsis root is BOR1 (Noguchi et al., 1997; Takano et al., 2002). Under boron deficiency, BOR1 is localized in the stele-side plasma membrane, exporting boron into the stele, increasing the boron concentration in xylem for translocation to the shoot (Takano et al., 2002). Orthologs of *BOR1* in maize are *rotten ear* (*rte*) and *rte2* (Chatterjee et al., 2014; Chatterjee et al., 2017). Orthologs have additionally been characterized in many other major crops including rice, barley and oilseed rape (Nakagawa et al., 2007; Sutton et al., 2007; Zhang et al., 2017; Chen et al., 2018).

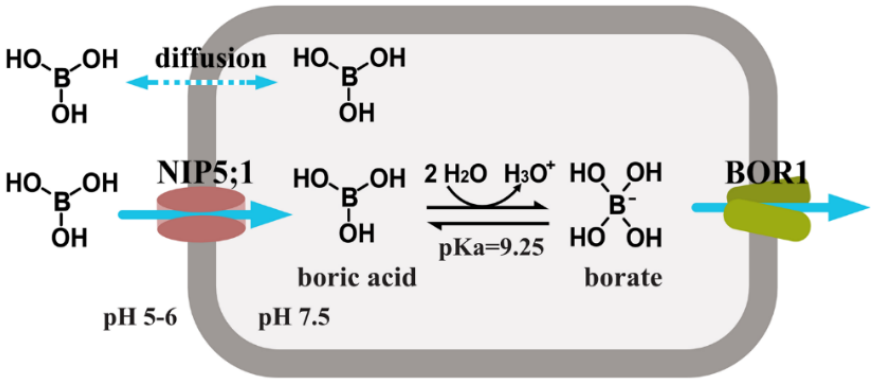

Figure 1.2: Boron transport model in the plant cell. Boric acid passively permeates plasma membranes (indicated by the dashed arrow) and the boric acid channel NODULIN INTRINSIC PROTEIN5;1 (NIP5;1) facilitates boron transport into the cytosol. At the cytosolic pH (pH 7.5), boric acid is converted to borate. Borate is actively exported by the boron transporter HIGH BORON REQUIRING1 (BOR1). Modified from (Takano and Tanaka, 2023).

1.3 Molecular functions of boron

In boron-deficient plants, 81% - 98% of boron is located in the cell wall (Matoh et al., 1992; Hu et al., 1996; Pommerrenig et al., 2022). Most of the observed boron deficiency phenotypes can be linked to cell wall defects and the best characterized molecular function of boron is to crosslink the pectic polysaccharide rhamnogalacturonan II (RG-II) (Kobayashi et al., 1996; Matoh et al., 1996; O'Neill et al., 1996).

RG-II, homogalacturonan (HG) and RG-I comprise the main pectic domains in the primary cell wall (Bharadwaj et al., 2020). As the most complex polysaccharide yet identified in nature (Bar-Peled et al., 2012), RG-II is comprised of a HG backbone linked with four sidechains (A to D) and two substituents, all together comprised of 12 different monosaccharides (Barnes et al., 2021). Side chain A and B each has a D-apiose (Api) residue harboring *cis*-diols on the furanose ring. Particularly with the Api on side chain A, boron forms stable diesters and links two monomeric RG-II (mRG-II) to form a dimeric RG-II (dRG-II) molecule (Kobayashi et al., 1996; O'Neill et al., 1996; Ishii and Ono, 1999; Ishii and Matsunaga, 2001).

Although RG-II in the cell walls is at low abundance (Matsunaga et al., 2004), its dimerization is crucial for cell wall properties. When RG-II dimerization is impaired, the cell wall mechanical strength is altered, wall pore size is enlarged, cell adhesion is disrupted, cell elongation and expansion are inhibited (Fleischer et al., 1999; O'Neill et al., 2001; O'Neill et al., 2004; Kakegawa et al., 2005). To investigate the RG-II dimerization status, pectin can be purified from cell wall components and RG-II can be released from pectin by endopolygalacturonase (Marfà et al., 1991). Afterwards, RG-II dimerization can be determined quantitatively by size-exclusion chromatography (SEC; Fleischer et al., 1999) or semi-quantitatively by

polyacrylamide gel electrophoresis (PAGE; Chormova et al., 2014; Fig. 1.3).

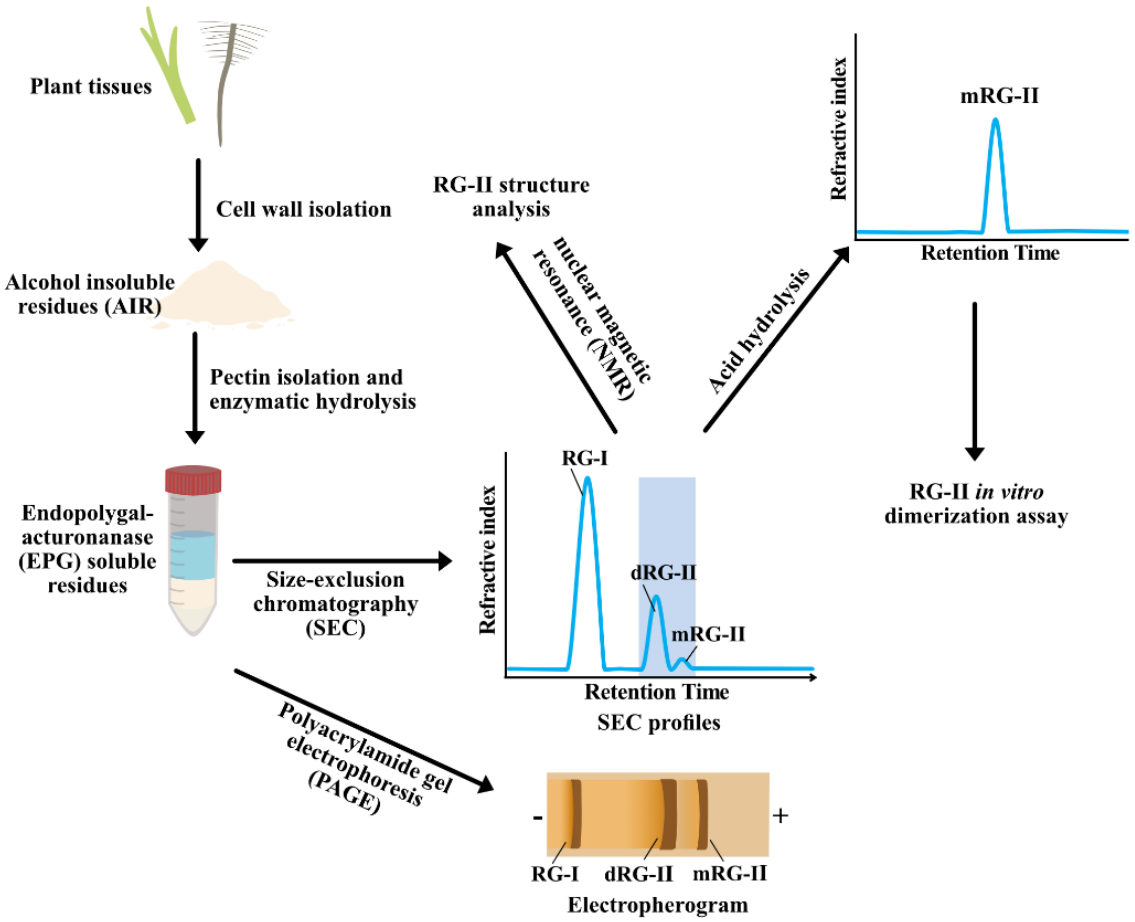

Figure 1.3 Simplified workflow for isolating rhamnogalacturonan II (RG-II) and analyzing its dimerization. Cell walls were isolated from homogenized plant tissues as alcohol insoluble residues (AIR). Pectin fractions were purified from AIR with a series of solvents and enzymes. The endopolygalacturonase (EPG) was used to cleave the homogalacturonan backbone, releasing RG-I and RG-II from the pectic chains. The different pectin domains enriched in the EPG soluble residues can be separated by size exclusion chromatography (SEC) or polyacrylamide gel electrophoresis (PAGE). Fractions enriched in RG-II can be purified for further structure analysis via e.g., nuclear magnetic resonance (NMR), or be monomerized for *in vitro* dimerization experiments.

Defects of RG-II side chains or boron deprivation can both impair RG-II dimerization. Excess boric acid was shown to partially rescue the dimerization defects observed in sidechain mutants. The underlying mechanism, however, remains unknown (Hays et al., 2025). The boron-mediated RG-II crosslinking is thought to happen predominantly in the endomembrane system (Begum and Fry, 2022; 2023), but it remains obscure, what modulates RG-II dimerization. *In vitro* analysis indicated that RG-II is not dimerized by boric acid spontaneously (O'Neill et al., 1996), but requires certain ions or cationic chaperones, such as arabinogalactan proteins, which are located in the plasma membrane (Sanhueza et al., 2022; Begum and Fry, 2023). In addition, boron binding affinity chromatography found many membrane-associated proteins in the Arabidopsis and the maize root that might interact with boron (Wimmer et al., 2009). Boron

can also mediate binding between RG-II and glycosylinositol phosphorylceramides (GIPC; Voxeur and Fry, 2014). GIPC are major components of plant membrane microdomains (Markham et al., 2013). These findings suggest a possible function of boron in the cell wall-membrane continuum.

Under adequate boron, more than 60% of cellular boron was not bound to cell walls (Hu et al., 1996; Pommerrenig et al., 2022), implying boron functions in non-cell-wall compartments. Based on observations that defects in pectin crosslinking cannot explain all phenotypes observed under boron-deficient conditions and that there are striking differences of phenotypes observed in mutants defective in boron uptake compared with wild-type plants grown under boron-deficient conditions, molecular functions of boron independent of diol binding and structural functions have been proposed, as reviewed in (Matthes et al., 2020).

From such hypotheses, especially phytohormone-related functions appear intriguing as they might provide a molecular explanation for the boron-related phenotypes, especially the meristem development defects. Particularly, alterations of auxin, including auxin biosynthesis, levels, transport and signaling, in response to boron deficiency, have raised interests (Chu et al., 2025b). In Arabidopsis roots, boron deficiency induced an increase of auxin signaling (Li et al., 2015; Camacho-Cristobal et al., 2015; Herrera-Rodriguez et al., 2022; Tao et al., 2023). This increase was thought to be related to altered auxin transport rather than auxin biosynthesis in the roots (Li et al., 2015; Tao et al., 2023). In the maize shoot, the auxin efflux marker PIN-FORMED1a (PIN1a):Yellow Fluorescent Protein showed alterations of distribution, accumulation and localization in the shoot apical meristem and in the developing tassel meristem of the maize boron transporter mutant *tls1* (Matthes et al., 2023), suggesting that PIN1a-mediated auxin transport was reduced in the boron-deficient maize shoot. In the Arabidopsis RG-II dimerization defective mutant *murus1* (*mur1*), the plasma membrane localization of auxin transporters PIN3, PIN4 and AUXIN-RESISTANT 1 were reduced compared to that in the wildtype, while boric acid supplementation partially rescued the localization defects (Jewaria et al., 2025). Other phytohormones like ethylene, cytokinin, brassinosteriods, jasmonic acid, and abscisic acid (ABA) were reported to be responsive to boron deficiency as well. Some of them were even considered to mediate the development of boron deficiency-induced phenotypes (Eggert and von Wirén, 2017; Chen et al., 2023). However, the phytohormone responses under boron deficiency conditions were shown to be variable in different tissues, species and genotypes or at different time points (Chu et al., 2025b). It remains unresolved how boron deficiency is perceived, and how the phytohormone cascades are molecularly regulated in response to boron deficiency.

1.4 Approaches to study boron deficiency in plants

Due to the ubiquity of boron in the natural environment, it's difficult to create boron-deficient experimental conditions for plant research. One of the commonly used approaches to experimentally induce boron deficiency is to prepare boron-free/low-boron media (Asad et al., 1997). Boron can be removed from aqueous media by boron-specific resins, such as the weak base anion exchange resin Amberlite IRA-743 (Kunin and Preuss, 1964; Wang et al., 2014).

Another approach to induce boron deficiency on a plant level is to use boron transporter mutants. Those mutants are inherently boron-deficient and consequently show enhanced boron deficiency-related phenotypes with impaired boron transport (Noguchi et al., 1997; Takano et al., 2006; Hanaoka et al., 2014; Leonard et al., 2014; Chatterjee et al., 2014; Durbak et al., 2014). For example, the mutant of the maize boric acid channel gene, *tls1* (*NIP5;1* ortholog), was used to reveal the involvement of auxin and cytokinin in the boron deficiency-induced phenotypic defects and boron functions during meristem development via genetic studies (Matthes et al., 2022; Matthes et al., 2023). The mutant of the Arabidopsis boron transporter gene *BOR1* was used to assess the effects of boron on fertility through reciprocal crosses and grafting (Noguchi et al., 1997; Muro et al., 2025). However, it is difficult to decipher the primary or secondary molecular responses caused by boron deficiency with these mutants.

Since the best characterized function of boron is to crosslink RG-II, boron deficiency could theoretically be artificially mimicked by interrupting crosslinking of RG-II. Boronic acids, including phenylboronic acid (PBA), have been proposed as boron deficiency mimics (Bassil et al., 2004). PBA has a benzene ring and a boric acid moiety (Fig.1.4A). The boric acid moiety allows PBA *cis*-diol binding affinity, but with only two hydroxyl groups, PBA should not be able to crosslink RG-II. According to the theory that there is a dRG-II—mRG-II interconversion *in planta* (O'Neill et al., 1996), PBA, with a pKa of 8.8, which is lower than that of boric acid ($pKa_{boric\ acid}$ = 9.25; Figs. 2.2; 2.4A), was proposed to compete with or even displace borate at its binding sites (Bassil et al., 2004). Therefore, PBA might inhibit RG-II dimerization (Fig. 1.4C). PBA or PBA-derived boronic acids were reported to form borate ester bonds with *cis*-diol-containing saccharides or polysaccharides, and have been extensively studied for sugar recognition and affinity separation (Yan et al., 2004; Jiang et al., 2006; Furikado et al., 2014).

In planta, PBA induced phenotypes similar to boron deficiency, such as disrupted cell-to-cell wall adhesion (Bassil et al., 2004), inhibited maize root elongation (Housh et al., 2020), impaired apple pollen tube elongation (Fang et al., 2016), and inhibited Arabidopsis hypocotyl bending similar to boron deficient *mur1* (Jewaria et al., 2025). These phenotypes pointed to the

cell wall structural alteration as hypothesized. Additionally, relations to the phytohormone auxin were implied by the inhibitory effects of PBA on auxin transport (Matthes and Torres-Ruiz, 2016), and of PBA derivatives on auxin biosynthesis (Kakei et al., 2015). Particularly, PBA stabilized BOR1 in the plasma membranes against the high-boron-induced protein degradation (Matthes and Torres-Ruiz, 2016). However, a recent study detected dRG-II through PAGE of pectin fragments isolated from PBA-treated Arabidopsis, introducing the new hypothesis that PBA might crosslink RG-II (Fig. 1.4C; Hays et al., 2024).

Yet, for both hypotheses, no direct or quantitative analysis of the PBA—RG-II interactions had ever been conducted. Moreover, the boron-carbon bond in PBA is prone to reactive oxygen species (ROS), for example, H_2O_2. As a result, PBA can be deboronated by H_2O_2 in aqueous solution (Fig. 1.4B; Graham et al., 2021). Therefore, the utility of PBA as boron deficiency mimic *in planta* or the effects of PBA on RG-II dimerization need thorough characterization.

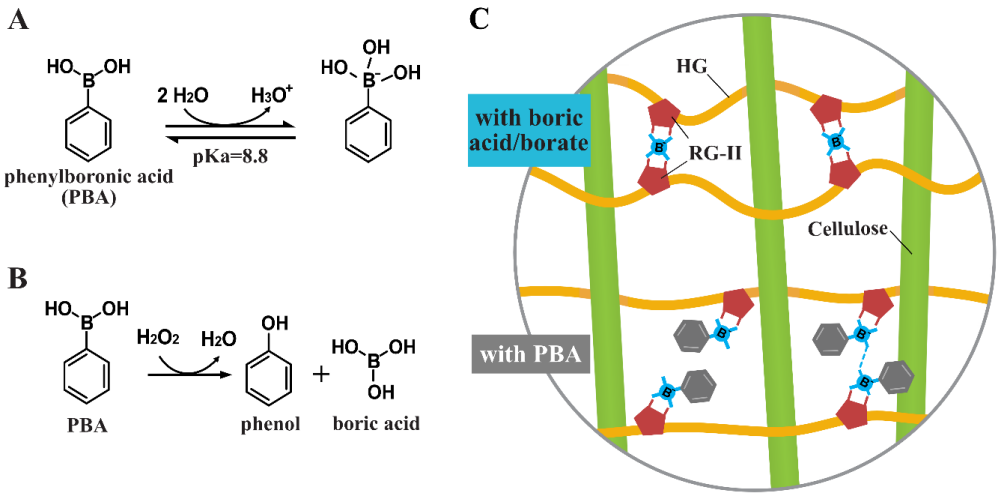

Figure 1.4. Hypotheses of the effects of phenylboronic acid (PBA) on rhamnogalacturonan II (RG-II) dimerization. A, The uncharged and anion forms of PBA, adapted from (Yan et al., 2004). B, PBA deboronation induced by H_2O_2, adapted from (Graham et al., 2021). C, Proposed effects of PBA on RG-II dimerization, modified from (Matthes et al., 2020; Hays et al., 2024). With adequate boron, the RG-II in cell walls is crosslinked by borate through the *cis*-diols on the side chains. With PBA treatment, RG-II dimerization is proposed to either be inhibited through PBA-mediated blockage of boron binding sites, or promoted through PBA-mediated RG-II dimerization (Bassil et al., 2004; Hays et al., 2024). HG: homogalacturonan, B: boron.

1.5 Regulation of boron homeostasis

To adapt to variable boron levels in the environment, plants have developed many strategies to regulate the balance of boron uptake, distribution, and utilization. Boron transport plays a central role in the regulation of boron homeostasis, yet other regulatory mechanisms exist and warrant exploration.

Boron uptake and distribution are regulated through both passive diffusion and boron transporters. The passive diffusion across plasma membranes is determined by the boron

gradient from high boron concentration to low boron concentration, and is affected by the chemical speciation of boron, as boric acid permeates the phospholipid bilayer more easily than the borate anion (Stangoulis et al., 2001). The passive transport is also affected by transpiration and diffusion barriers. In maize, enhanced transpiration can fully rescue the tassel phenotypes and partially rescue the ear phenotypes in *tls1* (Matthes et al., 2018). In Arabidopsis and citrus, Casparian strips inhibit the boron apoplastic diffusion under boron toxicity (Ruiz et al., 2016; Muro et al., 2023).

The boron channels/transporters are regulated in response to boron levels, in aspects of abundance, localization, and activity. The regulation happens at transcriptional level or post-transcriptional levels, and the regulation is species-specific. For example, in Arabidopsis under boron deficiency, messenger ribonucleic acid (mRNA) levels of *NIP5;1* are induced and that of *BOR1* are unaffected (Takano et al., 2002; Takano et al., 2006). Under excess boron, NIP5;1 is post-transcriptionally repressed (Tanaka et al., 2011) and BOR1 is translationally repressed and degraded through endocytosis (Takano et al., 2005; Kasai et al., 2011; Aibara et al., 2018). In rice, the *NIP3;1* analog *Low silicon rice 1* (*Lsi1*) does not respond to boron deficiency, while OsBOR1 is degraded in response to high boron (Huang et al., 2022). Boron transport is also indirectly affected by some transcription factors modulating the mRNA levels of boron transporter genes, in boron-dependent manners (Feng et al., 2020; 2021; Tsednee et al., 2022; Zhang et al., 2024a). Some of the boron transporters contribute to both boron uptake and distribution, for example, AtBOR1, OsNIP3;1, TLS1 (Noguchi et al., 1997; Takano et al., 2002; Hanaoka et al., 2014; Durbak et al., 2014; Matthes et al., 2018; Muro et al., 2025; Wang et al., 2025); while others are specifically responsible for refining the distribution, such as Arabidopsis NIP6;1 and NIP4;1/4;2 (Tanaka et al., 2008; Perez Di Giorgio et al., 2016).

Apart from uptake and distribution, boron transporters can also contribute directly to boron utilization. For example, BOR2 delivers boron into vesicles for RG-II crosslinking (Miwa et al., 2013). Variation of boron utilization efficiency is caused by genetic factors linked to transporter genes or to loci of unknown function (Xu et al., 2002; Jamjod et al., 2004; Zeng et al., 2008; Zhang Q et al., 2014; Zhang Z et al; 2024). Mutagenesis studies have indicated additional genetic factors of boron utilization, such as *Low Boron Tolerance 1*, *Transmembrane Nine 1*, and *Vacuolar Type ATPase 2;1*, which are unrelated to boron transporters (Huai et al., 2018; Hiroguchi et al., 2021; Onuh and Miwa, 2023). Phytohormones also play important roles in boron homeostasis (Chu et al., 2025a). The responses of the auxin cascade to boron deficiency are well documented. For example, auxin levels or signaling are up-regulated in Arabidopsis roots and *Brassica napus* under boron deficiency (Martin-Rejano et al., 2011; Li et al., 2015;

Camacho-Cristobal et al., 2015; Zhou et al., 2016; Eggert and von Wirén, 2017; Herrera-Rodriguez et al., 2022; Tao et al., 2023). In addition, ABA induces *NIP5;1* expression (Gomez-Soto et al., 2019). Gibberellins induce expression of the vacuole boron channel gene *Tonoplast Intrinsic Protein 5;1* and alleviate boron toxicity (Pang et al., 2010; 2017). Brassinosteroid signaling negatively affects boron absorption and translocation (Zhang et al., 2021). And treatment of exogenous brassinosteroid enhances RG-II dimerization in the *mur1* mutant (Jewaria et al., 2025).

Genomic approaches have been applied to identify molecular candidates regulating the homeostasis of mineral elements in many species. Variation in seed boron levels has been investigated in for example barley, rice, maize, and peanut (Zhang et al., 2019; Wang et al., 2020; Jia et al., 2021; Wu et al., 2021), and variation of boron levels in leaves or whole shoots had been investigated in rice (Yang et al., 2018). Using grain boron levels as input, the boric acid channel gene *NIP2;2/Lsi6* (barley) and the borate transporter gene *rte2* (maize) were detected respectively (Jia et al., 2021; Wu et al., 2021). Notably, these approaches also detected various other genes unrelated to boron transport, with no functional validation. Genomic studies of tolerance to high-boron stress have yielded similar findings. Some of them identified transporter genes (Sutton et al., 2007), whereas others found no correlation between boron tolerance and either shoot boron concentration or transporter genes (de Abreu Neto et al., 2017). These findings suggest that boron homeostasis is a polygenic trait, and there are additional regulators that warrant identification.

1.6 Aims

The molecular mechanisms impacted by boron deficiency and those regulating boron homeostasis in maize remain elusive. The elucidation of such mechanisms will advance our understanding of the molecular functions of boron, and provide knowledge to improve maize resilience to impaired boron conditions.

This thesis tested the usability of phenylboronic acid (PBA) as a boron deficiency mimic in maize and used the ear leaf boron levels as input trait for a GWAS to identify novel molecular players involved in boron homeostasis in maize. The following hypotheses were tested:

1. The PBA-induced maize root defects mimic those induced by boron deficiency, and are caused by interference of PBA with boron-mediated RG-II crosslinking.
2. The underlying molecular causes of the boron deficiency/PBA-induced root defects are tissue specific.
3. The auxin cascade is involved in the boron deficiency/PBA-induced root defects.
4. Boron homeostasis is a polygenic trait in maize.

2 Phenylboronic acid-induced defects in maize roots are independent of rhamnogalacturonan-II dimerization

Liuyang Chu[1], Deepak Sharma[2], Alexa Brox[1], Cay Christin Schäfer[1], Norman B. Best[3], Ha Ngoc Duong[4], Yen On Chan[5], Jutta Baldauf[1], Beatrice Klammer[1], Julia Brück[1], Felix Plotecki[1], Gabriel Schaaf[6], Ruthie Angelovici[4], Frank Hochholdinger[1], Breanna Urbanowicz[2], and Michaela S. Matthes[1,*]

[1] University of Bonn, Institute of Crop Science and Resource Conservation, Crop Functional Genomics, Römerstraße 164, 53117 Bonn, Germany

[2] University of Georgia, Complex Carbohydrate Research Center, 315 Riverbend Rd, Athens, Georgia, 30602, USA

[3] Plant Genetics Research Unit, USDA-ARS, Columbia, MO 65211, USA

[4] Division of Biological Sciences, Christopher S. Bond Life Sciences Center, Interdisciplinary Plant Group, and Missouri Maize Center, University of Missouri, Columbia, MO 65211-7310, USA

[5] Institute for Data Science and Informatics, Christopher S. Bond Life Sciences Center, University of Missouri-Columbia, Columbia, MO 65211-7310, USA

[6] University of Bonn; Institute of Crop Science and Resource Conservation, Plant Nutrition, Karl Robert Kreiten Str. 13, 53115 Bonn, Germany

*To whom correspondence should be addressed: mmatthes@uni-bonn.de

Manuscript in revision at *Plant Physiology*

Abstract

Soil boron deficiency is a global abiotic stress, negatively impacting on crop yield. In the dicot model species Arabidopsis thaliana, inhibition of root elongation is one of the earliest symptoms of boron deficiency. In the monocot model maize (*Zea mays* L.), boron deficiency-induced root defects are widely unexplored. In this study, we assessed boron deficiency-induced defects in the primary root system of maize and tested the suitability of phenylboronic acid (PBA) as boron deficiency mimic by performing phenotypic, histological, molecular, and biochemical analyses. Our analyses showed that boron deficiency and PBA resulted in similar defects in primary root elongation and lateral root density. The PBA-induced defects, however, were much stronger than those induced by boron deficiency, particularly regarding lateral root development. We provide evidence that the PBA-induced defects were caused by the boric acid moiety and show that both boron deficiency and PBA altered the levels of auxin and reactive oxygen species. Strikingly, PBA did not affect rhamnogalacturonan-II (RG-II) dimerization. Interference of boron-mediated RG-II crosslinking, however, was previously proposed to be the mode of action of PBA in planta. Our study shows that PBA is particularly suited for the molecular dissection of lateral root development in maize and suggests that PBA can reveal boron-related, yet RG-II-independent molecular targets.

Introduction

The micronutrient boron is needed for proper growth and activity of meristematic tissues (Chu et al., 2025). Therefore, limited boron availability can drastically impact on plant development. In crop plants, reproductive development is severely affected, which leads to major yield declines under boron deficiency. The first organ that senses boron deficiency is the root. In Arabidopsis (*Arabidopsis thaliana*), the boron-deficient root is short and stunted with an accumulation of root hairs and an increased root diameter (Bolaños et al., 2023; Chu et al., 2025). In the monocot cereal maize (*Zea mays* L.), only few studies investigated boron deficiency-induced root defects. In these studies, maize root systems either did not respond to boron deficiency (Lordkaew et al., 2011; Bienert et al., 2023) or showed reductions in primary root length, lateral root number, and lateral root density (Eltinge, 1936; Wilder et al., 2022). These discrepancies likely reflect genotype- and tissue-specific differences of boron sensitivity in maize. Assessing the impact of boron deficiency on crop roots is hampered by the difficulty in accessing root systems grown in soil, but also by the difficulty in creating boron-deficient growing conditions.

Boron uptake and distribution within plants is regulated by boron transporters (Miwa and Fujiwara, 2010) and the primary function of boron is considered to be the stabilization of the pectin subunits rhamnogalacturonan-II (RG-II) in the primary cell wall (Kobayashi et al., 1996; O'Neill et al., 1996; Matoh, 1997). Approaches to experimentally induce boron deficiency on the plant level include the characterization of boron transporter mutants or mimicking boron deficiency by competitively inhibiting crosslinking of RG-II (Matthes et al., 2020). The maize boron transporter mutants *tassel-less1* (*tls1*), *rotten ear* (*rte*), and *rte2* are inherently boron-deficient and were employed to characterize boron-related processes in maize (Leonard et al., 2014; Chatterjee et al., 2014; Durbak et al., 2014; Chatterjee et al., 2017; Matthes et al., 2022; Matthes et al., 2023). Due to their chemical structures, boronic acids, including phenylboronic acid (PBA), were hypothesized to be boron deficiency mimics in plants and were used to study plant developmental processes (Bassil et al., 2004; Fang et al., 2016; Matthes and Torres-Ruiz, 2016; Matthes and Torres-Ruiz, 2017; Duran et al., 2018; Housh et al., 2020).

Germination of maize kernels in PBA solution led to root defects similar to defects in boron-deficient citrus roots (Li et al., 2016), including shorter primary roots and reductions in lateral root density (Housh et al., 2020). Notably, some of the induced defects were partially rescued by boric acid (Housh et al., 2020). Specifically, the PBA-induced lateral root defects were intriguing and were also reported in Arabidopsis and beans (Odhnoff et al., 1961; Hays et al.,

2024). Lateral root development is tightly controlled by pathways mediated by the phytohormone auxin (Du and Scheres, 2018; Hochholdinger et al., 2018; Vanneste et al., 2025), implying potential crosstalk between boron and auxin. Whether the PBA-induced defects resemble boron deficiency-induced defects in the maize primary root and whether the phenotypes are causally connected to altered auxin pathways is not known.

The use of PBA as a boron deficiency mimic was recently challenged by the hypothesis that PBA might stabilize RG-II crosslinks instead of inhibiting them (Hays et al., 2024). Furthermore, PBA can be oxidatively deboronated (Graham et al., 2021), implying that in planta PBA might not be present as PBA, but in the form of its oxidation products, which include phenol and/or additional oxidation products, and strikingly boric acid.

To address these outstanding questions, we characterized boron deficiency- and PBA-induced defects in the maize primary root using the B73 inbred line and mutants related to auxin biosynthesis. We additionally assessed whether PBA affects RG-II dimerization in vitro and evaluated the impacts of the potential oxidation of PBA in planta. Our study showed that both boron deficiency and PBA led to shorter primary roots and to a strong reduction of lateral root density. PBA, however, did not interfere with RG-II dimerization. Whereas primary root reductions were also observed with excessive H_2O_2, particularly the lateral root density defects were specific to both oxidative stable and unstable boronic acids, suggesting boron-related, yet RG-II dimerization-independent targets of PBA. Applying a genome-wide association approach, we highlight hormone- and oxidative stress-related genes as putative candidates aiding in addressing the molecular mechanisms underlying the PBA-induced lateral root density defects.

Material and Methods

Seedling assays

The maize B73 inbred line, the maize auxin biosynthesis mutants *vanishing tassel2* (*vt2*) and *sparse inflorescence1* (*spi1*; Gallavotti et al., 2008b; Phillips et al., 2011), the auxin transporter marker line PINFORMED1a-YFP (PIN1-a-YFP; Gallavotti et al., 2008a; Krishnakumar et al., 2015), 241 inbred lines from the 282 Goodman-Buckler association panel (Flint-Garcia et al., 2005) and celery (*Apium graveolens;* RG-II analyses) were used.

All seedling assays were done in germination paper with 10 kernels per paper roll and incubation in the dark at 28°C in the indicated culture solution.

Seedling assays (B73) in the PBA gradient were done with full Hoagland media with different PBA concentrations (0 mM, 0.1 mM, 0.2 mM, 0.4 mM, 0.8 mM, 1.0 mM and 2 mM). The Hoagland media (3.5 mM $Ca(NO_3)_2$, 2.5 mM KNO_3, 1 mM $MgSO_4$, 1 mM KH_2PO_4, 4.55 µM $MnCl_2$, 0.2 µM $CuSO_4$, 0.3475 µM $ZnSO_4$, 0.0605 µM Na_2MoO_4, 14 µM Fe-EDTA, 50 µM $B(OH)_3$) was prepared in ultrapure water. The assays were done with three replicates (with seeds from three B73 plants) for six days.

Time series (B73) were done with four treatments: +B, 50 µM boric acid; -B, 0 µM boric acid; +B+PBA, 50 µM boric acid and 0.4 mM PBA (Sigma-Aldrich, USA); -B+PBA, 0 µM boric acid and 0.4 mM PBA. The treatments were based on boron-free Hoagland media prepared with ultrapure water and treated with boron chelating resin AmberLite® IRA 743 (Sigma-Aldrich, USA, 5 g/L, 24 h). All solutions were prepared in plastic. For every treatment, eight rolls (with 10 kernels per roll) were incubated for 4 - 6 days. The experiment was repeated eight times (biological replicates).

Seedling assays with the auxin biosynthesis inhibitor L-kynurenine (Kyn), the auxin transport inhibitor naphtylphtalamic acid (NPA), *spi1* or *vt2* mutants, and PIN1a-YFP lines were based on the same treatments (+B, -B, +B+PBA, -B+PBA) with 0.4 mM PBA. In the assays with 2,4-dichlorophenoxyacetic acid (2,4-D) the PBA-concentration was 1 mM. We used the synthetic auxin 2,4-D and not indole-3-acetic acid (IAA), because the solvent of 2,4-D is H_2O, whereas that for IAA is ethanol. 2,4-D induces the same maize seedling root phenotypes as IAA (Draves et al., 2022).

Assays with H_2O_2, phenol, boric acid, 2-carboxyphenylboronic acid (2-CPBA) and 1-butylboronic acid (BBA) were based on full Hoagland media. The sample number and biological replicates are given in the respective figures.

For genome-wide association studies (GWAS), 241 inbred lines were treated with H_2O or 1 mM PBA in the dark at 28 °C for six days. The seedling assay was repeated twice.

Root phenotyping

For the time series, pictures of the seedlings were taken 4 to 6 days after treatment (DAT). Primary root length and lateral root density were determined using ImageJ (Schneider et al., 2012). Lateral root density was calculated by the total amount of lateral roots divided by the branching zone (Fig. S1A).

For GWAS, primary root length and lateral root density for the PBA-treatment and the water control were phenotyped accordingly. Ratios between the PBA-treatment and the water control were calculated and used as input data for the GWAS (primary root length-, lateral root density-ratio).

Histology

Root samples (1 cm of the primary root tip and 2 cm root pieces from the maturation zone; Fig. S1C) were collected, fixed, dehydrated, embedded in paraffin wax, and sectioned (8 µm) using a microtome (Leica RM2125 RTS). Sections were stained with toluidine blue according to Wu and McSteen (2007). See Supplementary Material and Methods.

Microscopy

Toluidine blue-stained sections were imaged using AxioCam MRc Microscope (Carl Zeiss, Germany). Root meristem length and root diameter were analyzed using PALM Microbeam Plattform (Carl Zeiss, Germany). Medial sections of the primary roots were used and meristem length was defined according to Ioio et al., 2007 (Fig. S1F). Root diameter was measured from cross sections of the 2 cm maturation zone samples (Fig. S1C, G). For each sample the root diameter was averaged over all sections.

Overviews of individual slides containing longitudinal sections of the 2 cm maturation zone samples (Fig. S1C) were imaged using an automatic fluorescent microscope (BX63) with a 2x objective (PLAPON 2x/0.08), the bright field detector (UC50), and the cellSens Dimension software (Olympus Corporation, Japan). From these images (512x512), all visible lateral root bulges in all sections (*ca.* 20) of a sample (n = 4 biological replicates per treatment) were counted. From the obtained number the maximum number of lateral root bulges of all slides for one sample was determined.

Phytohormone quantification

IAA, 1-amino-cyclopropane-1-carboxylic acid (ACC), and abscisic acid (ABA) were

quantified from 1 cm root tips and the maturation zone (Fig. S1D). Samples were ground in liquid nitrogen and 100 mg of each sample was lyophilized. High-performance liquid chromatography-mass spectrometry (HPLC) was applied (Dilkes and Best, 2025).

RG-II dimerization assays

Monomeric RG-II (mRG-II) from celery was used as a substrate for *in vitro* dimerization assays and prepared according to Barnes et al., (2021). Standard RG-II dimerization reactions contained 50 mM NaOAc buffer (pH 3.8), 200 µM mRG-II, 1 mM boric acid, and 0.5 mM $Pb(NO_3)_2$, unless otherwise indicated. Assays involving boronic acids contained 1 mM PBA or 0.4 mM PBA in place of boric acid under standard conditions. All reactions were performed at room temperature (RT)for 16 h, stopped by flash-freezing, then analyzed by size exclusion chromatography (SEC) using a Superdex-75 10-300GL Increase column with refractive index (RI) detection (Barnes et al., 2021).

Preparation of cell walls and pectin isolation

B73 was cultivated in Hoagland media ± 1 mM PBA. Whole roots were harvested 6 DAT. To prepare cell wall material as alcohol insoluble residue (AIR), roots were lyophilized and homogenized in liquid nitrogen, then resuspended in 70% (v/v) ethanol at RT for 8 h. The suspensions were centrifuged (2000 *g*, 10 min) and the pellet was washed with 80% (v/v) ethanol, 90% (v/v) ethanol, absolute ethanol, then filtered and resuspended in methanol:chloroform (1:1, v/v). After 8 h, the material was centrifuged, washed twice with acetone, then vacuum dried. AIRs were de-starched by α-amylase (*Bacillus licheniformis*, Sigma-Aldrich, USA) in MES/Tris buffer (20 mM, pH 6.5). The insoluble material was subsequently washed with ultra-pure H_2O and acetone and freeze dried. The dry material was then suspended in NaOAc (50 mM, pH 5.2) for 24 h at 45°C and purified again with glucoamylase (Spirizyme®; 60 µL/g; Novozymes A/S, Denmark) and α-amylase (Liquozyme®; 300 µL/g; Novozymes A/S, Denmark). The de-starched AIR was collected by filtration through nylon mesh (100 µm pore size) and washed with deionized H_2O. In order to isolate pectin domains, 1 g de-starched AIR was treated with endo-polygalacturonanase M2 (EPG) (*Aspergillus aculeatus*, 5 U/g, Megazyme, Ireland) in 100 mL NaOAc (50 mM, pH 5.2) for 24 h (30 °C, 250 rpm). The EPG-treated AIR was collected by filtration through nylon mesh (100 µm pore size) and then retreated with EPG. The combined EPG-solubilized fractions were concentrated by rotary evaporation at 37 °C, dialyzed (Spectrum™ Spectra/Por™, 3500 Dalton MWCO) against deionized water, and freeze dried. Solutions of the EPG-soluble material from maize AIR (6-8 mg) in NH_4HCO_2 (50 mM, pH 5), with an injection volume of 200 µL were applied to Agilent 1100 series HPLC using a Superdex-75 Increase column (30 x 1 cm, Cytiva,

USA) eluted at 0.5 mL/min with NH_4HCO_2 (50 mM, pH 5), with RI detection (Barnes et al., 2021).

NMR spectroscopy

^{1}H-NMR spectra were recorded with a Varian Inova NMR spectrometer (Agilent Technologies, USA) operating at 600 MHz using a 5 mm cold probe and a sample temperature of 25 ºC. A onetime D_2O exchange was performed on pectin samples by dissolving (5-6 mg) in D_2O (1 ml, 99.9%; Cambridge Isotope Laboratories, USA) and freeze drying. Freeze-dried samples were dissolved in 0.6 mL D_2O and transferred to 5 mM NMR tubes before spectral data acquisition. Data were processed using MestReNova software (Mestrelab Research S.L., Spain).

Boron quantification

Boron concentration was quantified from roots and shoots of 50 seedlings per biological replicate (n = 3) with the curcumin method using an Infinite M200 Pro NanoQuant plate reader (TECAN, Switzerland) according to (Wimmer and Goldbach, 1999). Samples were collected 6 DAT, dried at 60 °C and ground in an agate mortar. 500 mg per sample was digested with nitric acid in a CEM Mars 5 microwave digestion system (CEM Corporation, USA).

Reactive oxygen species detection

Hydrogen peroxide (H_2O_2) production in the roots was visualized by 3,3′-diaminobenzidine staining (DAB; Ugalde et al., 2021). Staining intensity was represented by average optical density (AOD) and quantified from the 1 cm root tip and from 1 cm below the branching zone (Fig. S1) using ImageJ (Schneider et al., 2012). AOD of root minus AOD of background was used for analyses.

Genome-wide association study

For each trait (primary root length-, lateral root density-ratio), the best linear unbiased estimates (BLUEs) were computed using the BLUE script from the HAPPI_GWAS pipeline (https://github.com/Angelovici-Lab/HAPPI_GWAS_2; Slaten et al., 2020). Outliers were removed by fitting a linear mixed-effects model with the 'lmer' function in the 'lme4' package in R (Bates et al., 2015) using raw trait values as the response variable, replicate as a random effect, and accession as a fixed effect. Afterwards, the Box-Cox transformation (Box and Cox, 1964) was applied to each trait. To account for environmental variations, the BLUE results of each accession were obtained from the fitted model across both replicates. The BLUE results were used as the response variables in downstream GWAS.

The broad-sense heritability (H^2) was estimated for each trait using a linear mixed-effects model,

with genotypes as random effects using the lmer function in the lme4 R package (Bates et al., 2015). Genetic and residual variance components were extracted, and H^2 was calculated as the proportion of total phenotypic variance attributed to genetic variance.

Variant filtering was carried out using VCFtools (Danecek et al., 2011) by retaining only single nucleotide polymorphisms (SNPs) with a minor allele frequency > 0.05 and present in at least 95% of the population. After filtering, 4,704,048 SNPs remained for analysis. GWAS were conducted using the GAPIT (version 3; Wang and Zhang, 2021), with underlying BLINK (Huang et al., 2019), FarmCPU (Liu et al., 2016) and MLMM (Segura et al., 2012) models. Multiple testing correction was performed using the false discovery rate (Benjamini and Hochberg, 1995) at a 5% threshold and the Bonferroni method (Dunn, 1961). Candidate genes were identified within a 100-kb window on both sides surrounding each significant SNP. Gene annotations and physical positions were based on the *Zea mays* B73 reference genome, version 5 (https://www.maizegdb.org/genome/assembly/Zm-B73-REFERENCE-NAM-5.0). Manhattan and quantile-quantile (QQ) plots were visualized using the gwaspr R package (Wright, 2025).

Statistics

Statistical analyses were done in R v. 4.5.1 (R Core Team, 2025). For analyses of the traits in the time serial, the primary root length and the log-transformed lateral root density were fitted into a linear mixed-effect model with treatment and replicates as fixed effects, roll number as random effect, and a random error effect using the lme4 package v. 1.1 (Bates et al., 2015) to meet normal distribution. Multiple comparisons based on the estimated means calculated with the fitted model were done with the multcompView v. 0.1-10 (Hothorn et al., 2008; Graves et al., 2024) and the emmeans v. 1.11.1 (Lenth, 2024) packages. For chemical seedling assays, comparisons were done based on means estimated with general linear models with biological replicates and treatments as fixed effects. For lateral root density, log-transformation was applied to meet normal distribution. Boron concentration, lateral root primordia numbers, meristem length, and root diameter were compared between treatments by one-way analysis of variance (ANOVA) followed by Fisher's exact test ($p \leq 0.05$). Phytohormone concentrations were compared by one-way ANOVA followed by Tukey's test ($p \leq 0.05$), using agricolae package v. 1.3-7 (de Mendiburu, 2023). DAB-staining intensity was compared by Tukey´s test following a general linear model with treatment and genotype as fixed effects. Statistical significance was detected at $p \leq 0.05$. For all the boxplots and bar plots, the raw data were used for plotting with ggplot2 package v.3.5.2 (Wickham, 2016). For each boxplot, the whiskers extend from the box to the highest and lowest values within 1.5 times the interquartile range

from the upper and lower quartiles. The black line within each boxplot represents the median. Points outside of this range are considered outliers.

.

Results

To address functions of PBA *in planta*, we tested the impact of PBA on maize root development. Germination of maize kernels in paper rolls soaked in Hoagland media containing PBA led to the development of seedlings with reduced primary root length and reduced lateral root density compared to the control. The severity of these defects was dose-dependent (Fig. 1A). Increasing concentrations of PBA led to a visible thickening of the primary root and to the development of more root hairs (Fig. 1B). These phenotypes are reported boron deficiency-related phenotypes (Chu et al., 2025), corroborating that PBA induced similar phenotypes as boron deficiency. The lowest concentration of PBA that significantly reduced primary root length was 0.4 mM, whereas the lowest concentration reducing lateral root density was 0.1 mM (Fig. 1C-D). These results showed that the PBA-induced root defects are trait-specific, causing strong defects particularly in lateral root density.

PBA- and boron deficiency treatments induce similar phenotypes in the maize primary root with different severities

To assess the similarities of PBA- (+PBA) and boron deficiency (-B)-induced defects, time trial experiments from 4 days after treatment (DAT) until 6 DAT were performed. Boron-free Hoagland media with 0.4 mM PBA was used, which was the lowest concentration leading to significant defects in both primary root elongation and lateral root density (Fig. 1C-D).

From 5 DAT, the primary roots of +PBA and -B treatments were significantly shorter than that of the control treatment (+B), indicating that PBA can reduce primary root growth similarly to boron deficiency (Fig. 2A; Fig. S2B). However, both -B and +PBA had only subtle effects on primary root elongation in maize. In addition, the severity of PBA-induced defects was independent of the addition of boric acid (Fig. 2A; Fig. S2B), showing that the amount of boron in Hoagland media (50 µM) was insufficient to suppress the PBA-induced root elongation defects. The PBA treatments led to significant increases in primary root elongation compared to the +B control treatment 4 DAT (Fig. S2A).

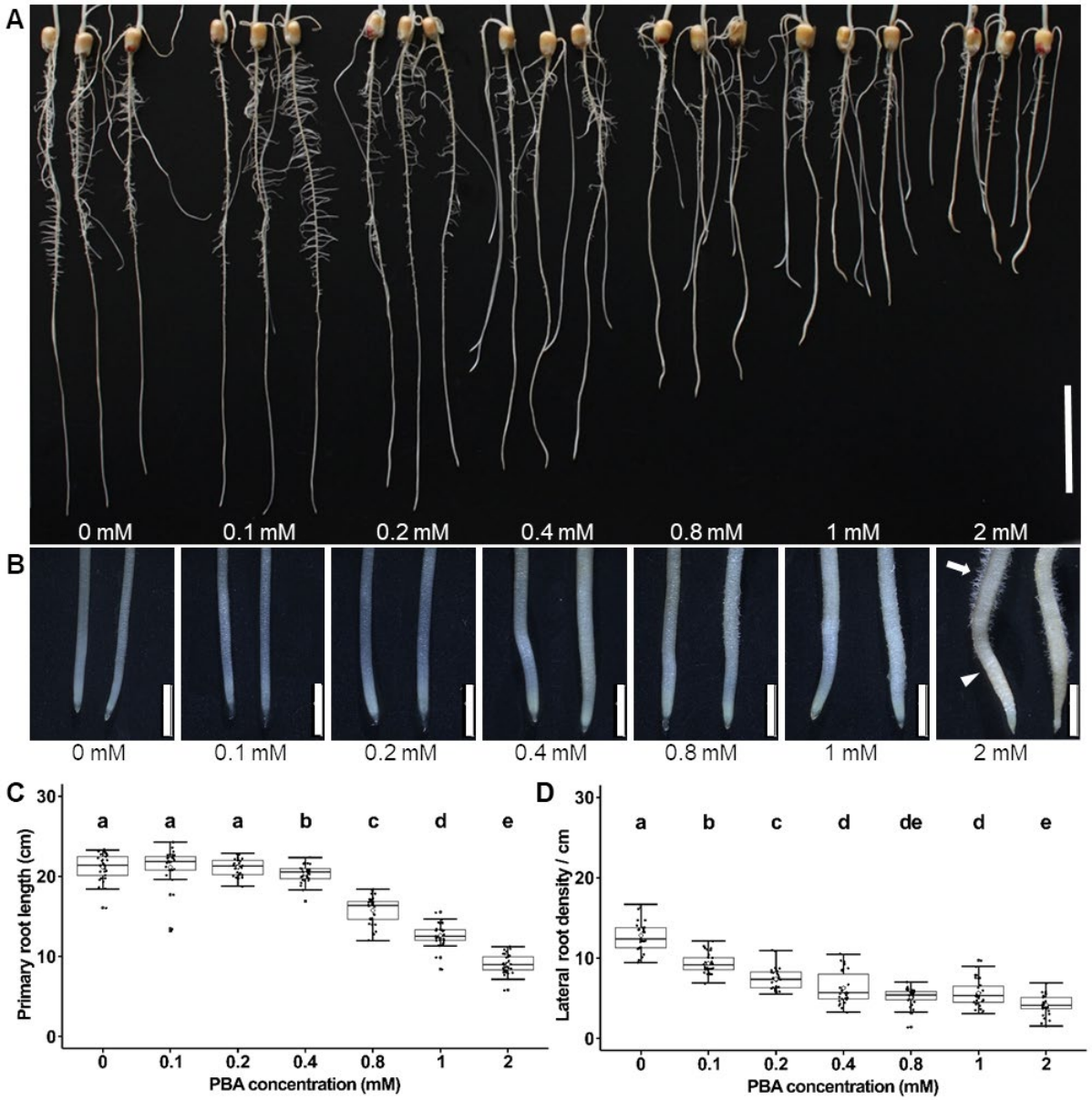

Figure 1 Phenylboronic acid (PBA) leads to defects in maize primary roots in a concentration-dependent manner. A, Representative image of primary roots 6 days after treatment (DAT) with the indicated PBA concentrations. B, Representative images of the primary root tips as shown in A, the concentrations of the respective PBA-treatments are indicated. The white arrow in the 2 mM PBA image points to the development of root hairs and the white arrowhead pinpoints a thickened root tip. C-D, Boxplots of primary root length (C) and lateral root density (D) of seedlings grown in the indicated PBA-treatments 6 DAT. The white-filled diamond within each boxplot represents the mean of 3 biological replicates ($n \geq 9$ per replicate per treatment). The compared means were estimated by a general linear model with treatments and replicates as categorial factors. Black dots represent the individual data points. The different letters indicate statistically significant differences ($p \leq 0.05$) as determined by the Benjamini Hochberg (C) or Tukey's test (D). The scale bar in A = 5 cm and in B = 3 mm.

Lateral roots were visible starting from 5 DAT. Boron deficiency led to a significant reduction in lateral root density compared to the +B control treatment. The PBA treatments, however, led to a strong reduction in lateral root density compared to both the +B control treatment and the -B treatment (Fig. 2B; Fig. S2C).

On a cellular level, meristem length under PBA conditions was significantly longer 6 DAT (Fig. 2C), whereas root diameter was significantly increased in the PBA-treatments 4 DAT and 5 DAT (Fig. 2D, Fig. S2F). Meristem length and root diameter under boron deficiency 6 DAT were not significantly different from both the +B control and the PBA-treatments (Fig. 2C).

To address the cause of lateral root density reduction, we quantified the number of lateral root primordia in the root maturation zone (Fig. S1C). The PBA treatments led to severe reductions in the number of lateral root primordia (Fig. 2E), suggesting that lateral root initiation is inhibited in PBA-treated maize seedlings. The number of lateral root primordia in the -B treatment was in between the control and the +PBA-treatments, suggesting that boron deficiency also led to defects in lateral root initiation, yet not as strong as the PBA treatments.

Our phenotypic analyses, therefore, showed that PBA induced similar defects to boron deficiency, yet more severely, particularly in lateral root development. Boron deficiency only slightly impacts on primary root development in maize.

Boron concentration analyses revealed that our setup induced boron deficiency conditions in both root and shoot tissues, whereas the PBA treatments led to enhanced boron levels (Fig. 2F; Table S1), as previously reported (Housh et al., 2020).

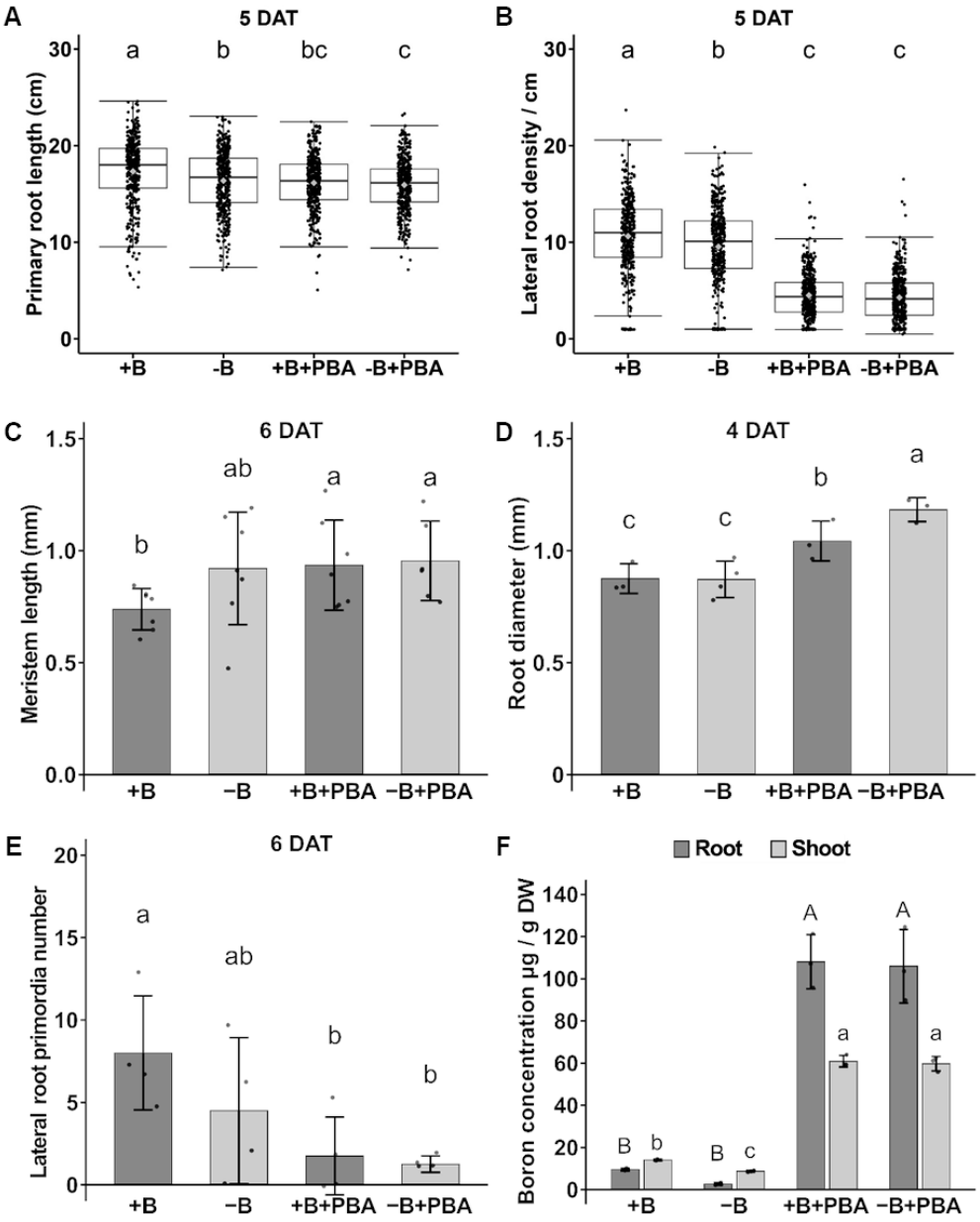

Figure 2 Phenylboronic acid- (PBA) and boron deficiency treatments induce primary root defects in maize. A, Boxplots of primary root length 5 days after treatment (DAT) of: 50 µM boric acid (+B), no boric acid (-B; 0 µM boric acid), 50 µM boric acid + 0.4 mM PBA (+B+PBA), or without boric acid + 0.4 mM PBA (-B+PBA). All treatments were made in Hoagland media. The grey diamond within each boxplot represents the mean of 8 biological replicates (n > 40 per replicate per treatment). B, Boxplots of lateral root density of seedlings germinated in the same boron and PBA treatments as in A 5 DAT. The grey diamond within each boxplot represents the mean of 8 biological replicates (n > 40 per replicate per treatment). Log-transformation was performed before modelling. For the boxplots in A-B: Different letters indicate statistically significant differences as determined by Tukey´s test ($p \leq 0.05$). C, Bar plots of meristem length in the primary root tip 6 DAT. D, Bar plots of root diameter 4 DAT. E, Bar plots of lateral root primordia number 6 DAT. F, Bar plots of boron concentration in root- and shoot tissue 6 DAT. Data in C - F represent the mean ± standard deviation of 3 (C, D, F) or 4 (E) biological replicates. Different letters indicate significant differences as determined by Fisher's test ($p \leq 0.05$) following analysis of variance. DW = dry weight. See also Figs. S1-2.

The PBA-induced primary root elongation defects are sensitive to auxin levels and auxin transport processes

Due to the importance of auxin for root development in maize (Cowling et al., 2023), we assessed an involvement of the auxin cascade in the observed boron deficiency- and PBA-induced defects. In primary root tips, concentrations of the active auxin IAA were significantly reduced in both the -B and the +PBA treatments 4 and 5 DAT (Fig. 3A-B). Adding exogenous auxin in the form of 2,4-D led to a strong reduction in primary root elongation and to root curvature in the +B condition (Fig. 3E-F). The PBA treatment, but not boron deficiency, partially suppressed the 2,4-D-induced primary root length and curvature defects (Fig. 3E-F), suggesting an interaction between auxin levels and PBA during primary root elongation in maize.

In the maturation zone, where lateral roots are formed, IAA levels were also significantly reduced in both the -B and the +PBA conditions 4 and 5 DAT (Fig. 3C-D). No 2,4-D-induced defect was observed in the +B condition or with PBA-treatments (Fig. 3G). In contrast, the addition of 2,4-D in the boron deficiency treatment led to significant reductions in lateral root density compared to the non-2,4-D control (-B; Fig. 3G), suggesting that lateral root density under boron deficiency is sensitive to auxin levels.

Boron deficiency can also lead to alterations of ABA and ethylene pathways (Martin-Rejano et al., 2011; Eggert and von Wirén, 2017; Herrera-Rodriguez et al., 2022). Levels of both ABA and the ethylene precursor ACC were unaltered in primary root tips 5 DAT in any of the tested conditions (Fig. S3A-D). In the maturation zone, ACC-levels were significantly enhanced 5 days after -B or +PBA treatment (Fig. S3G) and ABA-levels remained unaltered (Fig. S3F, H). ABA- and ACC-levels were generally not significantly different 4 DAT (Fig. S3E-F). One exception was the ACC-levels in the -B+PBA treatment, which were significantly higher than the +B control 4 DAT (Fig. S3E). The phytohormone quantifications suggest that the detected tissue-specific differences in ABA- or ACC-levels were consequential to the observed phenotypes, whereas the reductions of IAA might mediate the observed phenotypic defects since they were already observed 4 DAT prior phenotypic differences.

We, therefore, additionally germinated B73 seeds with low kernel boron concentrations in Kyn, a chemical that interferes with auxin biosynthesis by competitively inhibiting TRYPTOPHANE AMINOTRANSFERASE 1 (TAA1) activity (He et al., 2011). The addition of Kyn to the +B condition led to a significant increase in primary root length, but did not differentially affect primary root length in the -B or +PBA treatments (Fig. S4A). Regarding lateral root density,

however, the addition of Kyn in the boron deficiency treatments (-B; -B+PBA) led to significant reductions compared to the controls (Fig. S4B), similar to results with 2,4-D, corroborating that lateral root density under boron deficiency is sensitive to altered auxin levels. Applying a genetics approach with the *TAA1*-ortholog *vt2* (Phillips et al., 2011), which is expressed during primary root development in maize (Winter et al., 2007; Stelpflug et al., 2016; Hoopes et al., 2018), showed that *vt2* mutants and wild-type siblings were not significantly different regarding primary root length and lateral root density under boron-deficient or PBA-conditions (Fig. S4C-D). Lateral root density in the *vt2* mutants, however, was significantly reduced in the +B condition (Fig. S4D).

In Arabidopsis, different boronic acids were suggested to be specific auxin biosynthesis inhibitors targeting YUCCA (YUC) proteins (Kakei et al., 2015). The *spi1* mutant (Gallavotti et al., 2008b) is a maize *yuc*-mutant and *spi1* gene expression is low in the root (Zheng et al., 2023). Mutants and wild-type siblings were not significantly different regarding primary root length and lateral root density in the tested treatments (Fig. S4E-F).

We next assessed, whether auxin transport contributes to the observed defects using the auxin transport blocker, NPA (Teale and Palme, 2018). Similar to the 2,4-D treatment, NPA led to significant reductions in primary root length in the +B and in the -B treatment. These NPA-mediated primary root length reductions were partially suppressed by PBA (Fig. S5A). Whereas NPA treatment led to significant reductions of lateral root density in the +B and the -B treatment, no further reduction of lateral root density was observed in the NPA + PBA treatments (Fig. S5B). NPA particularly affects PIN-mediated auxin transport (Abas et al., 2021). Therefore, PIN1a-YFP localization (Gallavotti et al., 2008a) in the boron deficiency- and PBA-treatments was assessed. Whereas in +B, PIN1a-YFP was mainly localized apolarly at the plasma membrane, -B and +PBA treatments led to visible reductions of plasma membrane localization and increased cytosolic accumulation of PIN1a-YFP. Quantification of the YFP-fluorescence ratios between the plasma membrane and the cytosol, however, did not detect significant differences (Fig. S5C-D).

This set of experiments suggested that boron deficiency and PBA treatments show interactions with auxin during primary root development, yet altered auxin biosynthesis or auxin export appear not causal to the observed phenotypic defects.

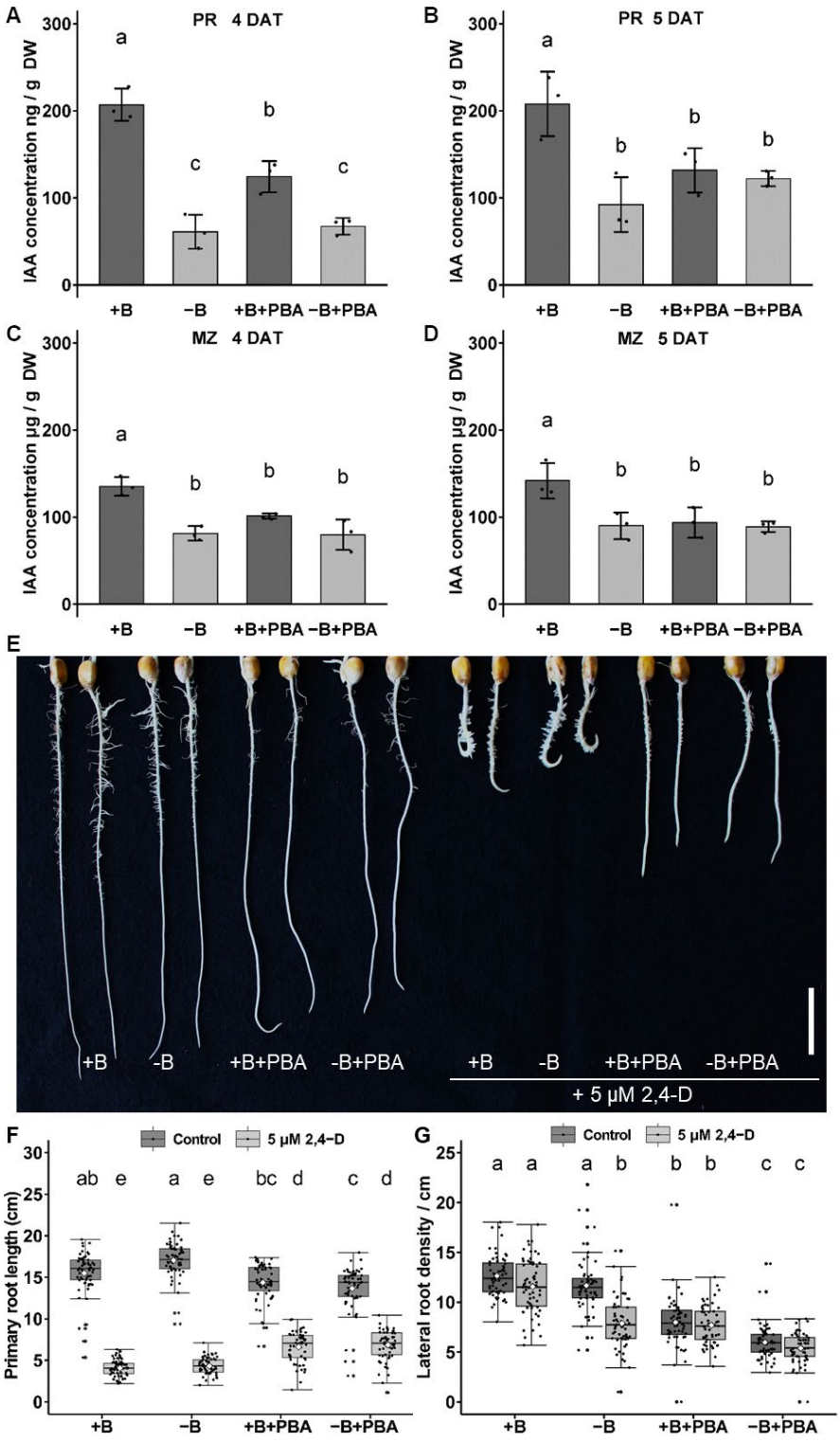

Figure 3 Alterations of auxin-levels are not causal to the boron deficiency- and phenylboronic acid (PBA)-induced defects in maize primary roots. A-D, Bar plots of indole-3-acetic acid concentrations in seedling roots 4 (A, C) or 5 (B, D) days after treatment (DAT) of: 50 µM boric acid (+B), without boric acid (-B; 0 µM boric acid), 50 µM boric acid + 1 mM PBA (+B+PBA), or without boric acid + 1 mM PBA (-B+PBA). All treatments were made in Hoagland media. Samples were collected from 1 cm root tips (A, B) and the maturation zone (C, D). Data are shown as the mean ± standard deviations (n = 3 biological replicates). Different letters indicate significant differences as determined by Tukey's test ($p \leq 0.05$) following analysis of variance. E, Representative image of seedlings 6 DAT of: +B, -B, +B+PBA, -B+PBA, +B+2,4-D (50 µM boric acid + 2.5 µM 2,4-D), -B+2,4-D (2.5 µM 2,4-D), +B+PBA+2,4-D (50 µM boric acid + 1 mM PBA + 2.5 µM 2,4-D), -B+PBA+2,4-

D (1 mM PBA + 2.5 μM 2,4-D). All treatments were made in Hoagland media. F-G, Boxplots of primary root length (F) and lateral root density (G) of seedlings 6 DAT, as shown in E. The white diamond within each boxplot represents the mean of 3 biological replicates (n ≥ 17 per replicate per treatment). Different letters indicate statistically significant differences as determined by Tukey's test ($p \leq 0.05$). The scale bar in E = 3 cm. 2,4-D = 2,4-dichlorophenoxyacetic acid, DW = dry weight, IAA = indole-3-acetic acid, MZ = maturation zone, PR = primary root tip.

PBA cannot interfere with RG-II dimerization

To test whether PBA treatment leads to RG-II dimerization defects in planta, we investigated the impact of PBA on individual pectic domains in maize cells walls. Pectins are multi-domain macromolecules and endopolygalacturonase (EPG) was used to hydrolyze the homogalacturonan (HG) fragments tethering pectic domains, releasing them from the wall. EPG-solubilized material was analyzed by size-exclusion chromatography (SEC) to investigate the profile of RG-I, dimeric RG-II (dRG-II), mRG-II and oligogalacturonic acids (OGAs; Fig. 4A; Fig. S6A; Barnes et al., 2021. The pectin fractions released from maize cell walls by EPG, however, did not yield a typical profile, and contained contaminating saccharides in the region where RG-II would typically elute (Fig 4A; Fig. S6A), hampering quantitative conclusions.

We, therefore, evaluated boron-mediated RG-II dimerization *in vitro* using celery RG-II as a model glycoform (O'Neill et al.,2020; Barnes et al., 2021). We incubated purified celery mRG-II with either 1 mM boric acid (control) or PBA in the presence of 0.5 mM $Pb(NO_3)_2$ as a catalyst for 16 h at RT. SEC profiles of the formed products indicated that addition of boric acid to mRG-II resulted in almost complete borate cross-linked dRG-II (Fig 4B). In contrast, the addition of PBA did not show formation of dRG-II, indicating that PBA is not capable of dimerizing mRG-II *in vitro* (Fig. 4B). To test whether PBA can inhibit RG-II dimerization, mRG-II was pretreated with 1 mM PBA for 16 h before incubation with 1 mM boric acid for 1 h. SEC profiles of the products showed that ~90% mRG-II was converted to dRG-II, confirming that PBA cannot competitively inhibit boric acid-mediated RG-II dimerization in vitro (Table S2).

We further assessed whether PBA can be covalently linked to pectin in maize primary root cell walls grown in the presence of PBA (6 DAT). Since we were unable to purify RG-II from maize roots, we analyzed the total EPG solubilized pectin fraction by 1D ^1H nuclear magnetic resonance (NMR). No signals corresponding to the PBA benzene ring (signals at 6.5 - 8 ppm) were detected in either control or PBA-treated samples, indicating PBA is not covalently linked to any pectic domain (Fig. 4C). Some background signals were observed in this region, which are likely due to small amounts of protein contamination from EPG extraction.

PBA, with the empty p orbital of boron prone to attack by nucleophilic species, can be

deboronated by reactive oxygen species (ROS), like H_2O_2 (Graham et al., 2021). In this case, PBA is oxidized to phenol and to boric acid, suggesting that oxidation of PBA in the presence of H_2O_2 might provide boric acid accessible for RG-II dimerization. To investigate whether PBA is oxidized in the germination media, ultraviolet (UV) spectroscopy was employed. Over the time span of our time trial experiments, Hoagland media containing PBA exhibited a UV absorbance peak at 267 nm. Meanwhile, the signal of phenol (an absorbance peak at 270 nm) was not detected (Fig. S7). This suggests that PBA is not oxidized in the media but might be oxidized *in planta*.

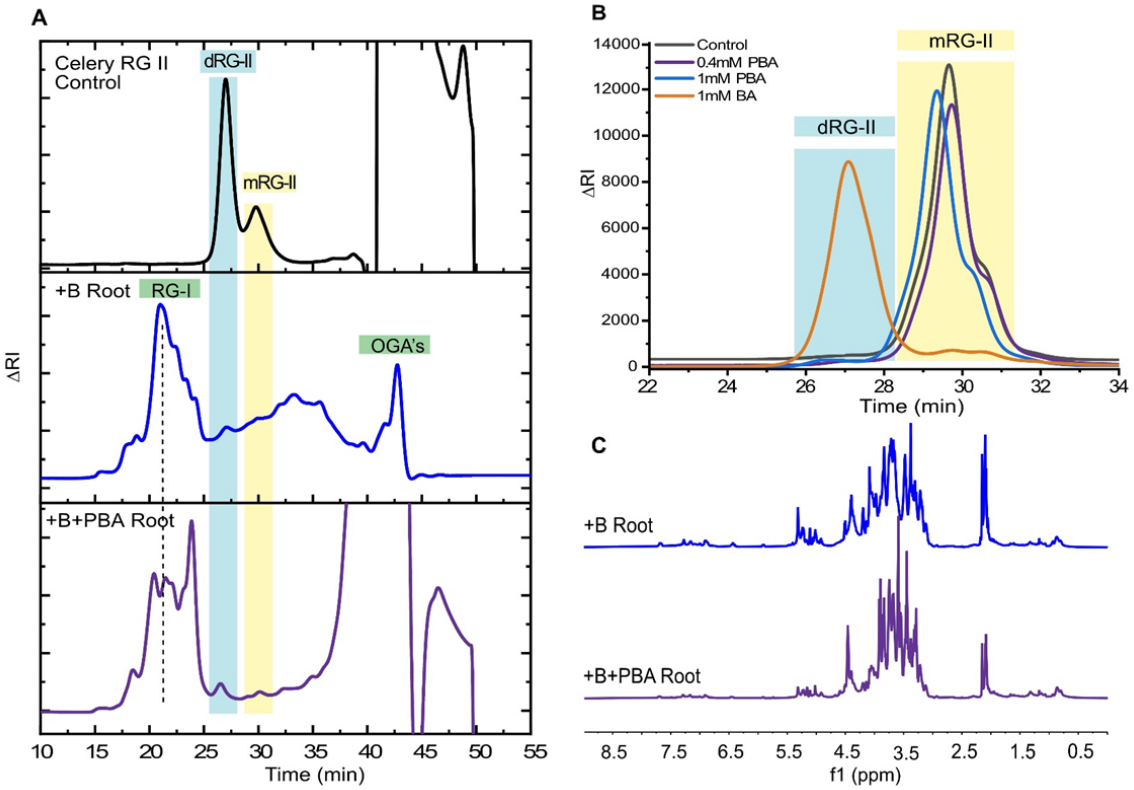

Figure 4 Phenylboronic acid (PBA) does not dimerize monomeric rhamnogalacturonan-II (mRG-II) *in vitro* and does not interfere with boron-mediated mRG-II dimerization. A, A typical size-exclusion chromatography (SEC) profile of celery RG-II (top panel: Celery RG II Control) and SEC profiles of endopolygalacturonase (EPG) extracts from maize roots cultivated in Hoagland media with 50 µM boric acid (middle panel: +B Root) or with 50 µM boric acid and 1 mM PBA (buttom panel: +B+PBA Root) for 6 days. B, SEC profiles of celery mRG-II after an overnight incubation with 0.4 mM PBA + lead (Pb^{2+}) as catalyst, 1 mM PBA + Pb^{2+}, 1 mM boric acid (BA) +/- Pb^{2+}, or without PBA/BA (negative control). C, 1D proton nuclear magnetic resonance of the EPG extracts of maize roots, as indicated in A. RI = refractive index, RG = rhamnogalacturonan, OGA's = oligogalacturonic acids. See also Fig. S6A.

The PBA-induced root defects are related to the boric acid moiety

To assess PBA oxidation *in planta*, we visualized H_2O_2 levels in primary roots using DAB 6 days after PBA treatment. Visual inspection suggested that PBA treatment leads to an accumulation of H_2O_2 in the primary root tip in a dose-dependent manner (Fig. 5A). Quantification of the DAB-staining corroborated that +PBA and -B led to an accumulation of H_2O_2 in the primary root tips compared to the +B control (Fig. 5B; Fig. S8A-B). Interestingly, the -B+PBA treatment led to a significantly higher H_2O_2 accumulation compared to the +B+PBA treatment. Likewise, only the -B+PBA treatment led to a significant increase in the DAB-staining in the maturation zone (Fig. 5C).

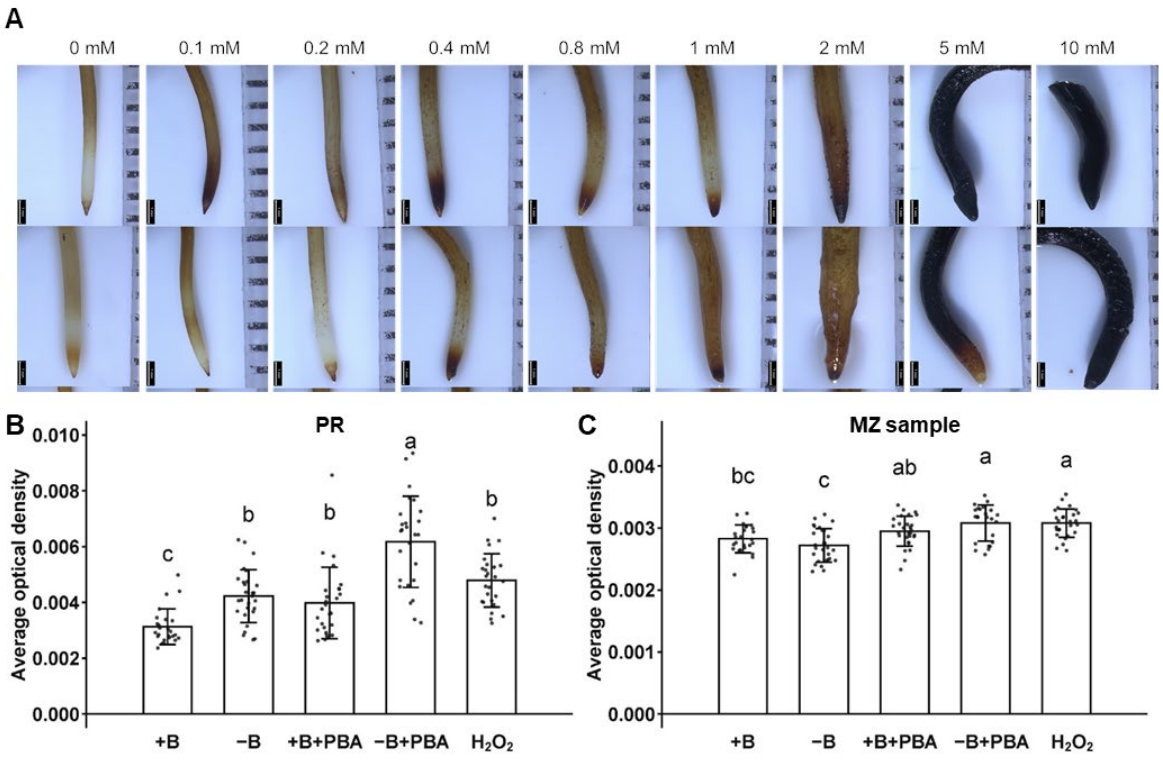

Figure 5 Phenylboronic acid (PBA) alters the accumulation pattern of reactive oxygen species (ROS) in maize primary roots. A, Representative images of 3,3′-diaminobenzidine (DAB)-stained root tips 6 days after treatment (DAT) with the indicated PBA-concentrations (0 mM, 0.1 mM, 0.2 mM, 0.4 mM, 0.8 mM, 1 mM, 2 mM, 5 mM, 10 mM). All treatments were made in Hoagland media. B-C, Bar plots of the DAB-intensity within a 1 cm region of the primary root tip (B) and 1 cm below the branching zone = maturation zone sample (C) 6 DAT of: 50 µM boric acid (+B), without boric acid (-B; 0 µM boric acid), 50 µM boric acid + 1 mM PBA (+B+PBA), without boric acid + 1 mM PBA (-B+PBA), or with 1 mM H_2O_2. The DAB-stain intensity was evaluated with average optical density using ImageJ (Schneider et al., 2012). Data depict the mean ± standard deviation of 3 biological replicates ($n \geq 7$ per treatment per replicate). Different letters indicate statistically significant differences as determined by Tukey's test ($p \leq 0.05$). MZ = maturation zone, PR = primary root tip. See also Figs. S1, S8.

These results suggested that due to an increase of H_2O_2, PBA might be oxidized *in planta*. We, therefore, addressed the impact of exogenous H_2O_2 and of exogenously applied phenol and boric acid on maize root development (Fig. 6; Figs. S6, S8). Primary root length and lateral root density defects were specific to the PBA treatment, as these defects were not detected with exogenous H_2O_2 nor PBA oxidation products (Fig. 6B-C). Noteworthy, the H_2O_2+PBA treatment did not lead to reductions of primary root length or lateral root density (Fig. 6; Fig. S6), which corroborates that H_2O_2 reacts with PBA directly (as confirmed by UV spectroscopy; Fig. S7) leading to oxidation of PBA and further confirming it is not the oxidation products that cause the observed root phenotypes. Exogenous H_2O_2 in concentrations $\leq$ 2 mM showed an increase in primary root length and no effect on lateral root density, whereas concentrations > 2 mM led to a reduction in primary root length and to an increase in lateral root density (Fig. S8).

To further assess whether the PBA-induced defects are mediated by PBA oxidation, we applied 2-CPBA, an oxidatively stable analog of PBA (Graham et al., 2021; Figs. S6-S7). 2-CPBA did not induce primary root length defects (Fig. S9C), but significantly reduced lateral root density with high concentrations (Fig. 6D). In addition, BBA, a non-aromatic boronic acid (Fig. S6C), induced lateral root density defects, but also reduced primary root length with high concentrations (Fig. 6E, Fig. S9D). These results suggest that particularly the PBA-induced lateral root density defects are mediated by the boric acid moiety, yet likely not via disturbance of RG-II dimerization. The severity of the induced defects might be affected by other functional groups of the boronic acids or their acid dissociation constants (Fig. S6C).

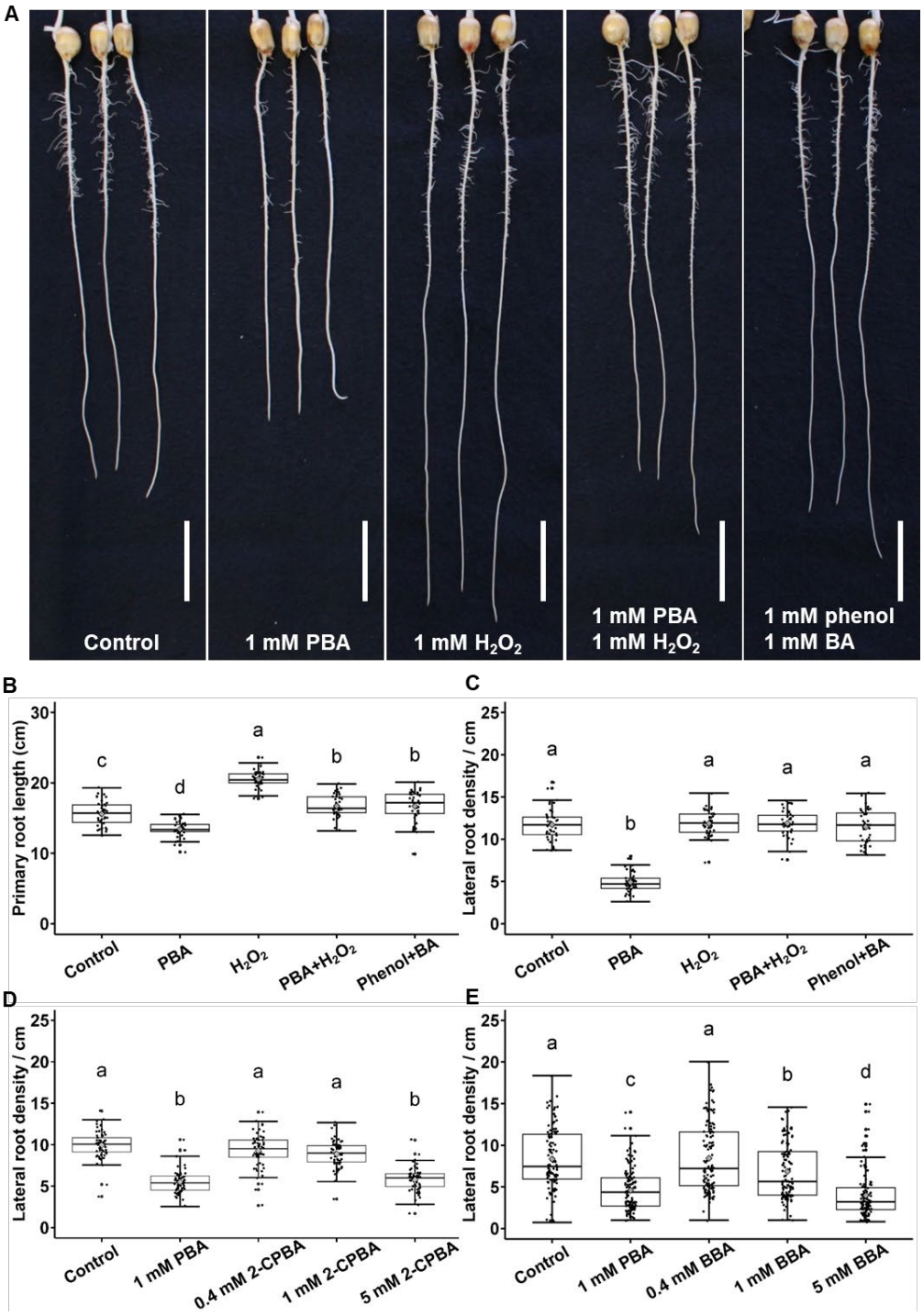

Figure 6 The phenylboronic acid (PBA)-induced root defects are not caused by excessive H_2O_2 or the PBA oxidation products. A, Representative image of roots 6 days after treatment (DAT) of: Control (Hoagland media), 1 mM PBA, 1 mM H_2O_2, 1 mM PBA + 1 mM H_2O_2, or 1 mM phenol + 1 mM boric acid (BA). B-C, Boxplots of primary root length (B) and lateral root density (C) 6 days after the indicated treatments as shown in A. The grey diamond in each boxplot represents the mean of 4 biological replicates ($n \geq 9$ per replicate per treatment). D-E, Box plots of lateral root density of seedlings germinated in Hoagland media with different concentrations of 2-carboxyphenylboronic acid (2-CPBA in D) or 1-butylboronic acid (BBA in E). Roots were phenotyped 6 DAT, where Hoagland media = Control. The grey diamond in each boxplot represents the mean of 3 biological replicates (D) or 6 biological replicates (E) with $n \geq 17$ per replicate per treatment. For the boxplots in B – E: Different letters indicate statistically significant differences as determined by Tukey's test ($p \leq 0.05$). The scale bars in A = 3 cm. See also Figs. S6, S9.

PBA-induced primary root defects underlie genetic variation

To identify targets of PBA, primary root length and lateral root density upon PBA treatment and without PBA (H_2O) were phenotyped in 241 lines of the Goodman-Buckler association panel (Flint-Garcia et al., 2005; Table S3). Phenotypic variation compared to B73 was observed with lines showing for example no differences in the root traits between treatments (Fig. 7A, 4722), lines showing enhanced root defects upon PBA-treatment (Fig. 7A, A641) or additional phenotypes like an enhanced root curvature (Fig. 7A, SC312R). Ratios of primary root length and lateral root density between the PBA- and the control-treatment were calculated (Table S3) and broad sense heritabilities of 0.37 (primary root length ratio) and 0.30 (lateral root density ratio) were determined. This statistically indicated genetic variation of these traits and we employed a genome-wide association approach (GWAS) using these traits.

From the GWAS of the lateral root density ratio data, 65 SNPs (267 genes on chromosomes 1 - 10) were identified from two statistical models (FarmCPU, BLINK; Table S4; Fig. S10). Using the primary root length ratio data, 8 SNPs (28 genes on chromosomes 2 and 5) were detected (Table S4). Three overlapping (between models) SNPs for lateral root density ratio were detected on chromosome 1, 2 and 10 (S1_24194798, S2_369889, S10_65000157; Fig. 7B; Table S4) and one overlapping SNP for the primary root ratio data was detected on chromosome 2 (S2_108751891; Table S4). Genes underlying the primary root length ratio GWAS were related to endocytosis (clathrin assembly proteins), ubiquitination (E3-ubiquitin ligase), stress responses (*CCAAT-HETEROMERIC COMPLEX2*, NAC transcription factor), root development (*GLUCURONOXYLAN4-O-METHYLTRANSFERASE 3*, member of the transmembrane 9 superfamily), polar cell elongation (*LONGIFOLIA*), and jasmonic acid-related processes (*LUMAZINE SYNTHASE*, *JASMONATE METHYLESTERASE*). With respect to the lateral root density ratio GWAS, genes underlying the detected SNPs were related to various hormone cascades, including auxin (*AUXIN RESPONSE FACTOR25*, *IAA19*, *WALLS ARE THIN1*, *SMALL AUXIN UP RNAs22*), ethylene (EREB transcription factors), cytokinin (*CYTOKININ HYDROXYLASE*), brassinosteroids (*CATASTERONE C-26 HYDROXYLASE*) and peptide signal phytosulfokine (*PHYTOSULFOKINE PEPTIDE PRECURSOR3*). Moreover, genes involved in lateral root development (*ROOTLESS CONCERNING CROWN AND SEMINAL ROOTS1, LATERAL ORGAN BOUNDARIES DOMAIN-CONTAINING TRANSCRIPTION FACTOR1*), ROS homeostasis (peroxidases, NADH-dehydrogenase, flavin-containing monooxygenases), endocytosis, and cell wall modification (*PECTIN METHYLESTERASE35*, xyloglucan endotransglucosylase/hydrolase, *LACCASE16*) were detected (Table S4). These results suggest that potential PBA targets are tissue-specific

representing many different cellular pathways.

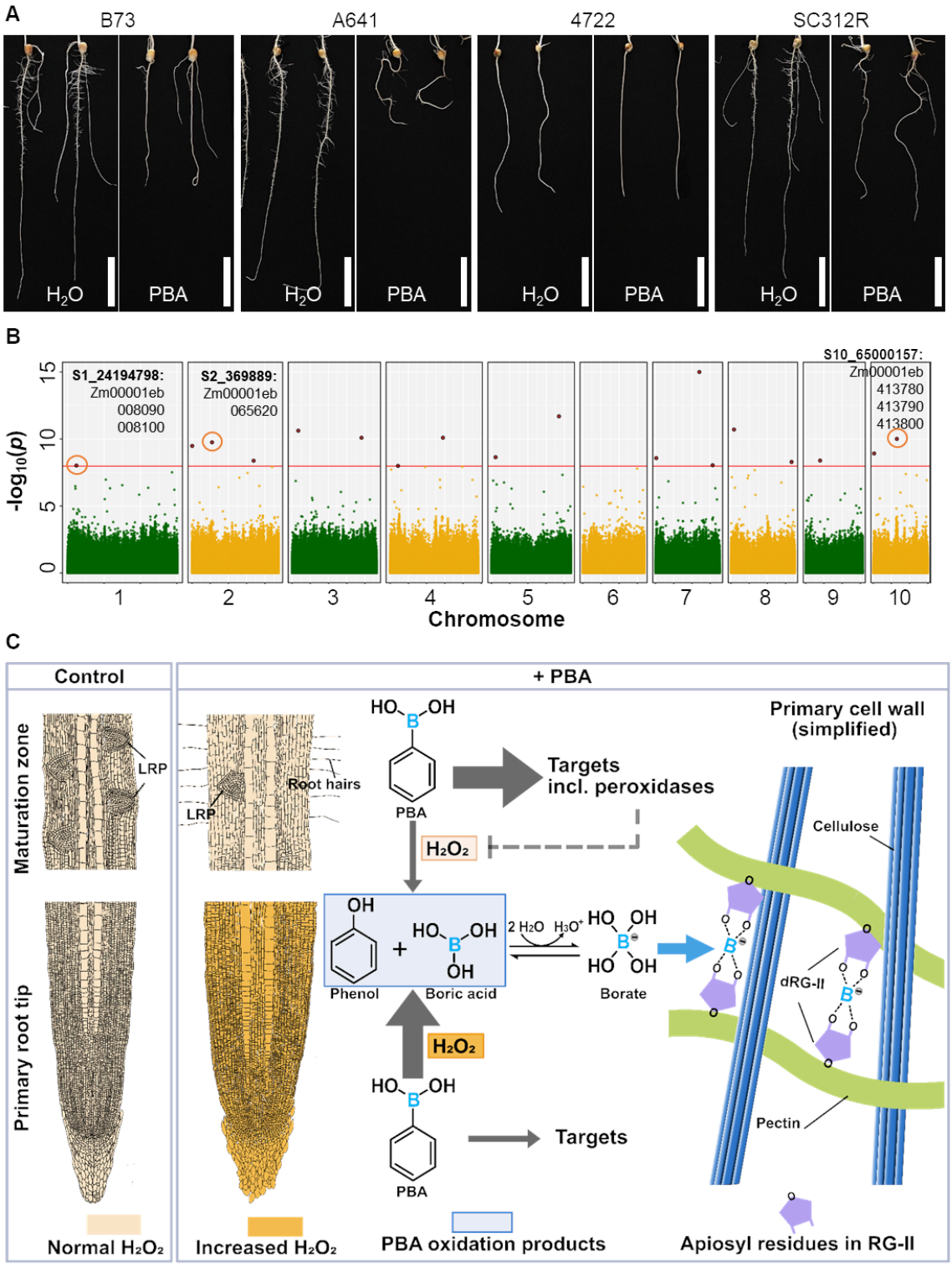

Figure 7 The phenylboronic acid (PBA)-induced primary root defects show genetic variation and imply tissue-specific regulation. A, Representative images of seedling roots from selected inbred lines of the 282 Goodman-Buckler association panel (Flint-Garcia et al., 2005) germinated in H_2O or 1 mM PBA and analyzed 6 days after treatment. B, Manhattan plot depicting genomic regions associated with variation in lateral root density ratios (1 mM PBA / H_2O) in a subset of the 282 Goodman-Buckler association panel using the FarmCPU model. Highlighted are the overlapping SNPs detected between FarmCPU and BLINK models. The genes underlying the overlapping SNPs (in a 200 kb window) are indicated. C, Hypothetical

model of the effects of PBA in the maize primary root: Control conditions (+B) lead to the normal development of the primary root tip and to the initiation of multiple lateral root primordia (LRP) at the maturation zone (for simplicity only a portion of the maturation zone is depicted). Furthermore, tissue-specific levels of various phytohormones, including auxin, and of reactive oxygen species, including H_2O_2 are observed (denoted as normal in the model). PBA-treatment leads to tissue-specific defects in the maize primary root. These defects include shorter and thicker primary roots, reduced lateral root density, reduced LRP numbers, and an increased occurrence of root hairs. In the root tip, increased levels of H_2O_2 and reduced levels of auxin are observed. The increased H_2O_2 levels likely cause (full or partial) oxidation of PBA, yielding phenol (and/or additional oxidation products) and boric acid. Additionally, unoxidized PBA might still interact with (uncharacterized) targets. Due to the increased H_2O_2 compared to control conditions, most of the PBA is likely oxidized (as indicated by the big grey arrow pointing towards PBA's oxidation products) and therefore that the primary root tip elongation defects are caused by an interaction of multiple factors (the oxidation products of PBA, H_2O_2, hormone alterations, unoxidized PBA and its targets). In the maturation zone where lateral roots are formed, auxin levels are reduced, but H_2O_2-levels are not altered. PBA, therefore, might primarily be unoxidized (as indicated by the big grey arrow pointing towards PBA targets). Therefore, the observed phenotypes might be correlated with the interaction of PBA and its targets, most notably with potentially peroxidases, which in turn might feedback on H_2O_2-homeostasis (as indicated by the dashed line). Some of the PBA might be oxidized and therefore the PBA oxidation products (phenol and/or additional oxidation products and boric acid) might additionally be present in the maturation zone. The resulting boric acid (as borate), can be incorporated into the cell wall and crosslink rhamnogalacturonan-II (RG-II). The scale bars in A = 5 cm. LRP = lateral root primordia, SNP = single nucleotide polymorphism. See also Fig. S10.

Discussion

Reported boron deficiency-induced defects include a reduction of root length, swelling of the primary root tip, an alteration of lateral root density and an accumulation of root hairs (Bolanos et al., 2023; Chu et al., 2025).

In our study, boron deficiency led to a reduction in primary root length and a reduction of lateral root density in maize (Fig. 2A-B). Notably, the boron deficiency-induced defects were marginal, which is striking given that auxin- and H_2O_2 levels, both factors known to affect root development, were significantly altered under boron deficiency (Figs. 3, 5). These results indicate so far unidentified mechanisms regulating maize root development under boron deficiency, that act downstream of or parallel to auxin and ROS. Our results corroborate previous studies reporting that boron deficiency does not affect the maize root (Bienert et al., 2023). The observed boron deficiency-induced defects, however, varied between experimental repetitions and between the different mutant assays (Figs. 2-3, Figs. S2-S5), suggesting genotypic and/or additional environmental impacts influencing the severity of the induced defects.

The PBA-induced defects were similar to the observed boron deficiency-induced defects, yet more severe (Figs. 1-3, Figs. S2-S5). This observation suggested either enhanced boron deficiency defects or additional boron-unrelated defects. PBA, furthermore, reduced primary root length and lateral root density in a dose-dependent manner (Fig. 1), similar to other studies (Housh et al., 2020; Hays et al., 2024). Concentrations of PBA ≥ 0.4 mM increased the thickness of primary root tips (Figs. 1-2), comparable to observations in apple, where 0.5 mM PBA induced swollen tips at pollen tubes (Fang et al., 2016) and comparable to enlarged citrus root tips under boron deficiency (Li et al., 2016). In Arabidopsis 50 - 200 µM PBA inhibited primary root elongation, reduced lateral root density, and induced root curvature (Hays et al., 2024). In the B73 maize genotype, 200 µM PBA only had strong negative effects on lateral root density, but not on primary root length and did not induce root curvature (Fig. 1). The latter was consistently not observed even with higher PBA concentrations (Fig. 1). Different inbred lines, however, showed varying degrees of root curvature with 1 mM PBA (Fig. 7A). These findings corroborate that the PBA-induced defects are species- and tissue-specific, but also concentration-dependent, and underly genetic variation. Moreover, PBA negatively affects development across species most strikingly lateral root development.

Lateral root development is regulated by multiple phytohormones (Zhang et al., 2023; Yalamanchili et al., 2024), but also by ROS (Pasternak et al., 2023), and their crosstalk with

particularly auxin (Tsukagoshi, 2016). Both boron deficiency- and PBA-treatment led to a reduction of IAA levels in both the primary root and the lateral root formation zone (Fig. 3A-D). These findings were contrary to studies in Arabidopsis, where boron deficiency leads to an accumulation of auxin levels in the primary root tip (Martin-Rejano et al., 2011; Tao et al., 2023) and highlighted species-specificities in the boron-deficiency response of plants. Despite the significant reductions in IAA levels under both boron deficiency and PBA treatment, overproduction of auxin, simulated with 2,4-D, did not suppress the induced phenotypes (Fig. 3E-G). Unlike Arabidopsis, where IAA partially restored the PBA-induced root defects (Hays et al., 2024), in maize, the reduction of IAA is likely not causative to the observed root phenotypes under these treatments. 2,4-D, however, led to severe reductions in primary root length in maize and strikingly induced root curvature (Fig. 3E-F). Noteworthy, these auxin-induced defects were partially suppressed by PBA, but not by boron deficiency (Fig. 3E-F). These findings suggest interaction between PBA and auxin levels during primary root elongation. In Arabidopsis, different boronic acids might inhibit auxin biosynthesis by targeting YUC-proteins (Kakei et al., 2015), which remains to be elucidated in maize. In our study, *spi1* (*yuc*) mutants did not respond differently to PBA treatment compared to the wild-type controls (Fig. S4E-F). Given that *spi1* is only weakly expressed in roots (Zheng et al., 2023) and that there are 14 *YUC*s in maize (Cowling et al., 2023; Matthes et al., 2019), PBA might target additional members of the YUC-family in maize roots.

In the maturation zone where lateral roots are formed, altered auxin levels or transport appear consequential to lateral root density defects following PBA- and boron deficiency treatments (Fig. 3, Fig. S5D). The enhancement of the boron deficiency-induced lateral root density defects with 2,4-D or Kyn application (Fig. 3G; Fig. S4B), however, suggests that lateral root development under boron deficiency is sensitive to altered auxin levels. Similar parallels between boron and auxin levels were drawn in the boron-deficient *tls1* mutant, where altered auxin levels enhanced the boron deficiency-induced vegetative defects (Matthes et al., 2023). Given that IAA-levels under boron deficiency in the maturation zone were reduced (Fig. 3C- D), it is surprising that the addition of 2,4-D enhanced the lateral root density defects under boron deficiency, but might indicate a tissue- or cell type-specific regulation of auxin homeostasis in lateral roots that might be affected by boron nutrition.

In addition, PBA-treatment and boron deficiency increased H_2O_2 levels, particularly at the maize primary root tip (Fig. 5A-B). ROS homeostasis, including H_2O_2 levels, is important for root development (Pasternak et al., 2023). Excessive H_2O_2 reduced primary root length in Arabidopsis linearly (Su et al., 2016). In maize, excessive H_2O_2 (1 - 2 mM) increased primary

root length and reduced it with concentrations > 2 mM (Fig. S8). In the primary root tip, the dose-dependence of H_2O_2-induced defects might contribute to the dose-dependence of PBA- induced defects and might explain the observation that low PBA concentrations lead to only marginal defects. In addition, exogenous H_2O_2 increased the diameter of rice root tips (Xiong et al., 2015), potentially explaining the PBA-induced increase in root diameter (Fig. 2D; Fig. S2F-G).

The similarities in phenotypes between boron deficiency and PBA-treatment (Figs. 2,5; Figs. S2-S4) support that the PBA-induced defects are boron-related. This is further corroborated by observations that the severity of individual PBA-induced defects varied depending on the boron treatment (Figs. 2-3, 5; Figs. S2-S3). Unlike boron deficiency, the primary defect induced by PBA *in planta* is likely independent of RG-II dimerization: The amounts of dRG-II in maize pectin were similar independent of the addition of PBA to the growth media (Fig. 4A), PBA was not covalently linked to RG-II or any other pectic domain (Fig. 4C), and PBA could not inhibit borate-mediated RG-II dimerization nor replace borate to form dRG-II *in vitro* (Table S2). Although peaks corresponding to dRG-II were clearly identified, pectin domains hydrolyzed from maize cell walls by EPG did not yield the expected profile of RG-I, dRG-II, mRG-II, and OGAs. This was likely related to the presence of highly esterified or glycosylated HG (Zhang et al., 2025). Optimization of pectin isolation or characterization from maize root samples should be addressed in future studies to understand the variations across pectin domains.

Our study, in combination with reports that PBA is oxidatively unstable (Graham et al., 2021), suggests oxidation of PBA *in planta* resulting in boric acid (as borate) available for dRG-II formation (Figs. 4, 7C). Indeed, PBA-treatment increased H_2O_2 at the maize primary root tip (Fig. 5A-B). This increase might be a consequence of PBA oxidation products, since both, phenol treatment and excessive boron, were shown to induce ROS production or oxidative stress in plants (Xu et al., 2012; Zhao et al., 2024). It can be speculated, that the PBA-induced increase of H_2O_2 in turn will oxidize PBA, suggesting that PBA at the maize root tip is mostly present in the form of its oxidation products (Fig. 7C). The PBA-induced primary root length reduction, therefore, is likely mediated by a complex interaction of the oxidation products of PBA, potentially unoxidized PBA, ROS, reduced auxin levels, and likely additional, uncharacterized targets of PBA (Fig. 7C).

In the maturation zone, the increase of H_2O_2 was less obvious (Fig. 5C), suggesting tissue-specificity of the mechanisms underlying the PBA-induced defects. Oxidation of PBA might

be less prevalent and therefore PBA might contribute more significantly to the observed phenotypic defects (Fig. 7C). This speculation is substantiated by observations that oxidatively stable boronic acids and non-aromatic boronic acids led to similar lateral root defects as PBA (Fig. 6D-E; Fig. S9), whereas excessive H_2O_2 or phenol and boric acid did not (Fig. 6; Figs. S6B, S8). The PBA-induced lateral root defects might be primarily mediated by interactions of PBA with its targets, which might be boron-related, but independent of RG-II-dimerization. We most notably detected ROS-related candidate genes (Fig. 7B; Table S4), highlighting that PBA might directly interact with oxidative stress-related targets. Such interactions might contribute to the PBA-induced alterations of ROS-levels in the maize root (Figs. 5, 7C). Interestingly, two class III peroxidase genes were detected (Table S4). Peroxidases commonly function in quenching of H_2O_2 (Smirnoff and Arnaud, 2019). Class III peroxidases are typically highly glycosylated and located in vacuoles or cells walls (Almagro et al., 2009; Freitas et al., 2024). Furthermore, Arabidopsis PEROXIDASE39, involved in root growth (Tsukagoshi et al., 2010), can bind to PBA through the boric acid moiety (Wimmer et al., 2009) and a horseradish peroxidase can bind to PBA-monolayers (Liu et al., 2005). It is tempting to speculate that during maize lateral root development, PBA might bind to one (or more) peroxidases *in vivo* and might influence the degradation of peroxides, thereby affecting lateral root development. Since a need for boron in facilitating the attachment of peroxidases to the plant cell wall and an increase in peroxidase activity under boron-deficiency were reported (Shive and Barnett, 1973), peroxidases might be affected by altered boron levels in maize, which remains to be tested.

Conclusion

Our study shows that boron deficiency significantly altered auxin- and ROS levels, but induced only mild phenotypic defects in the maize primary root. Strikingly, PBA also significantly altered auxin- and ROS levels, but induced severe phenotypic defects. We show, that PBA's mode of action is boron-related, but independent of RG-II dimerization.

Acknowledgements

We thank Julian Waters for student support, Marion Pitz for valuable input regarding statistical analysis, Nur Gömec and Ira Kurth for assistance with boron measurements. We are grateful for plant care by Helmut Rehkopf, Christa Schulz, and the field crew of the Dienstleistungsplattform für Pflanzenversuche (University of Bonn). We also thank Prof. Dr. Felix Bock and his team (University Hospital of Cologne) for support with automated microscopy. This work was supported by the German Research Foundation (DFG) grant MA

9520/1-1 to M.S.M.

Mention of trade names or commercial products in this publication is solely for the purpose of providing specific information and does not imply recommendation or endorsement by the U.S. Department of Agriculture. The U.S. Department of Agriculture is an equal opportunity provider and employer.

Competing Interests

None declared.

Author contributions

LC: Experimental design, performed the majority of the experiments, all statistical analyses (except GWAS), interpretation of results, and writing of the manuscript. DS: RG-II analysis, NMR. AB, CS, JBr, BK, FP: Seedling assays. NBB: Hormone quantification. HND, YOC: GWAS. JB: Statistical analysis (time trial). GS: Boron analytics. RA, FH, BU: Experimental design and student supervision. MSM: Study and experimental design, data analysis, student supervision, interpretation of results, writing of the manuscript.

All authors agreed on the final version of the manuscript.

Data availability

All data supporting the findings are included in the article and/or supporting information. Material will be made accessible upon reasonable request.

References

Abas, L., Kolb, M., Stadlmann, J., Janacek, D. P., Lukic, K., Schwechheimer, C., Sazanov, L. A., Mach, L., Friml, J., and Hammes, U. Z. (2021). Naphthylphthalamic acid associates with and inhibits PIN auxin transporters. Proc. Natl. Acad. Sci. **118**:e2020857118.

Almagro, L., Gómez Ros, L. V., Belchi-Navarro, S., Bru, R., Ros Barceló, A., and Pedreño, M. A. (2009). Class III peroxidases in plant defence reactions. J. Exp. Bot. **60**:377–390.

Barnes, W. J., Koj, S., Black, I. M., Archer-Hartmann, S. A., Azadi, P., Urbanowicz, B. R., Peña, M. J., and O'Neill, M. A. (2021). Protocols for isolating and characterizing polysaccharides from plant cell walls: a case study using rhamnogalacturonan-II. Biotechnol. Biofuels Bioprod. **14**:142.

Bassil, E., Hu, H., and Brown, P. H. (2004). Use of phenylboronic acids to investigate boron function in plants. Possible role of boron in transvacuolar cytoplasmic strands and cell-to-wall adhesion. Plant Physiol. **136**:3383–3395.

Bates, D., Mächler, M., Bolker, B., and Walker, S. (2015). Fitting linear mixed-effects models using lme4. J. Stat. Softw. **67**:1–48.

Benjamini, Y., and Hochberg, Y. (1995). Controlling the false discovery rate: a practical and powerful approach to multiple testing. J. R. Stat. Soc. Ser. B Stat. Methodol. **57**:289–300.

Bienert, M. D., Junker, A., Melzer, M., Altmann, T., von Wirén, N., and Bienert, G. P. (2023). Boron deficiency responses in maize (*Zea mays* L.) roots. J. Plant Nutr. Soil Sci. online ahead of print. https://doi.org/10.1002/jpln.202300173.

Bolanos, L., Abreu, I., Bonilla, I., Camacho-Cristobal, J. J., and Reguera, M. (2023). What can boron deficiency symptoms tell us about its function and regulation? Plants **12**:777.

Box, G. E. P., and Cox, D. R. (1964). An analysis of transformations. J. R. Stat. Soc. Ser. B Stat. Methodol. **26**:211–243.

Chatterjee, M., Tabi, Z., Galli, M., Malcomber, S., Buck, A., Muszynski, M., and Gallavotti, A. (2014). The boron efflux transporter *rotten ear* is required for maize inflorescence development and fertility. Plant Cell **26**:2962–2977.

Chatterjee, M., Liu, Q., Menello, C., Galli, M., and Gallavotti, A. (2017). The combined action of duplicated boron transporters is required for maize growth in boron-deficient conditions. Genetics **206**:2041–2051.

Chu, L., Schäfer, C. C., and Matthes, M. S. (2025). Molecular mechanisms affected by boron deficiency in root and shoot meristems of plants. J. Exp. Bot. **76**:1866–1878.

Cowling, C. L., Dash, L., and Kelley, D. R. (2023). Roles of auxin pathways in maize biology. J. Exp. Bot. **74**:6989–6999.

Danecek, P., Auton, A., Abecasis, G., Albers, C. A., Banks, E., DePristo, M. A., Handsaker, R. E., Lunter, G., Marth, G. T., Sherry, S. T., et al. (2011). The variant call format and VCFtools. Bioinformatics **27**:2156–2158.

de Mendiburu, F. (2023). agricolae: Statistical procedures for agricultural research. R package version 1.3-7. 2023, https://cran.r-project.org/package=agricolae.

De Paola, C. C., Bennett, B., Holz, R. C., Ringe, D., and Petsko, G. A. (1999). 1-Butaneboronic acid binding to *Aeromonas proteolytica* aminopeptidase: A case of arrested development. Biochemistry **38**:9048–9053.

Dilkes, B. P., and Best, N. B. (2025). Analysis of polar and nonpolar small plant growth hormones and quantification by LC/MS. Cold Spring Harb. Protoc. online ahead of print. https://doi:10.1101/pdb.prot108647.

Draves, M. A., Muench, R. L., Lang, M. G., and Kelley, D. R. (2022). Maize seedling growth and hormone response assays using the rolled towel method. Curr. Protoc. **2**:e562.

Du, Y., and Scheres, B. (2018). Lateral root formation and the multiple roles of auxin. J. Exp. Bot. **69**:155–167.

Dunn, O. J. (1961). Multiple comparisons among means. J. Am. Stat. Assoc. **56**:52–64.

Duran, C., Arce-Johnson, P., and Aquea, F. (2018). Methylboronic acid fertilization alleviates boron deficiency symptoms in *Arabidopsis thaliana*. Planta **248**:221–229.

Durbak, A. R., Phillips, K. A., Pike, S., O'Neill, M., Mares, J., Gallavotti, A., Malcomber, S. T., Gassmann, W., and McSteen, P. (2014). Transport of boron by the *tassel-less1* aquaporin is critical for vegetative and reproductive development in maize. Plant Cell **26**:2978–2995.

Eggert, K., and von Wirén, N. (2017). Response of the plant hormone network to boron deficiency. New Phytol. **216**:868–881.

Eltinge, E. T. (1936). Effect of boron deficiency upon the structure of *Zea mays*. Plant Physiol. **11**:765–778.

Fang, K., Gao, S., Zhang, W., Xing, Y., Cao, Q., and Qin, L. (2016). Addition of phenylboronic acid to *Malus domestica* pollen tubes alters calcium dynamics, disrupts actin filaments and affects cell wall architecture. PLOS ONE **11**:e0149232.

Flint-Garcia, S. A., Thuillet, A.-C. eline, Yu, J., Pressoir, G., Romero, S. M., Mitchell, S. E., Doebley, J., Kresovich, S., Goodman, M. M., and Buckler, E. S. (2005). Maize association population: a high-resolution platform for quantitative trait locus dissection. Plant J. **44**:1054–1064.

Freitas, C. D. T., Costa, J. H., Germano, T. A., De O. Rocha, R., Ramos, M. V., and Bezerra, L. P. (2024). Class III plant peroxidases: From classification to physiological functions. Int. J. Biol. Macromol. **263**:130306.

Gallavotti, A., Yang, Y., Schmidt, R. J., and Jackson, D. (2008a). The relationship between auxin transport and maize branching. Plant Physiol. **147**:1913–1923.

Gallavotti, A., Barazesh, S., Malcomber, S., Hall, D., Jackson, D., Schmidt, R. J., and McSteen, P. (2008b). *sparse inflorescence1* encodes a monocot-specific YUCCA-like gene required for vegetative and reproductive development in maize. Proc. Natl. Acad. Sci. USA **105**:15196–15201.

Graham, B. J., Windsor, I. W., Gold, B., and Raines, R. T. (2021). Boronic acid with high oxidative stability and utility in biological contexts. Proc. Natl. Acad. Sci. **118**:e2013691118.

Graves, S., Piepho, H.-P., and Dorai-Raj, L. S. with help from S. (2024). multcompView: Visualizations of Paired Comparisons. R package version 0.1-10. 2024, https://cran.r-project.org/package=multcompview

Hays, Q., Ropitaux, M., Gügi, B., Vallois, A., Baron, A., Vauzeilles, B., Lerouge, P., Anderson, C. T., and Lehner, A. (2024). Phenylboronic acid interacts with pectic rhamnogalacturonan-II and displays anti-auxinic effects during *Arabidopsis thaliana* root growth and development. J. Exp. Bot. erae315.

He, W., Brumos, J., Li, H., Ji, Y., Ke, M., Gong, X., Zeng, Q., Li, W., Zhang, X., An, F., et al. (2011). A small-molecule screen identifies L-kynurenine as a competitive inhibitor of TAA1/TAR activity in ethylene-directed auxin biosynthesis and root growth in *Arabidopsis*. Plant Cell **23**:3944–3960.

Herrera-Rodriguez, M. B., Camacho-Cristobal, J. J., Barrero-Rodriguez, R., Rexach, J., Navarro-Gochicoa, M. T., and Gonzalez-Fontes, A. (2022). Crosstalk of cytokinin with ethylene and auxin for cell elongation inhibition and boron transport in Arabidopsis primary root under boron deficiency. Plants **11**:2344.

Hochholdinger, F., Yu, P., and Marcon, C. (2018). Genetic control of root system development in maize. Trends Plant Sci. **23**:79–88.

Hothorn, T., Bretz, F., and Westfall, P. (2008). Simultaneous inference in general parametric models. Biom. J. **50**:346–363.

Housh, A. B., Matthes, M. S., Gerheart, A., Wilder, S. L., Kil, K.-E., Schueller, M., Guthrie, J. M., McSteen, P., and Ferrieri, R. (2020). Assessment of a ^{18}F-phenylboronic acid radiotracer for imaging boron in maize. Int. J. Mol. Sci. **21**:976.

Huang, M., Liu, X., Zhou, Y., Summers, R. M., and Zhang, Z. (2019). BLINK: a package for the next level of genome-wide association studies with both individuals and markers in the millions. GigaScience **8**:giy154.

Ioio, R. D., Linhares, F. S., Scacchi, E., Casamitjana-Martinez, E., Heidstra, R., Costantino, P., and Sabatini, S. (2007). Cytokinins determine *Arabidopsis* root-meristem size by controlling cell differentiation. Curr. Biol. **17**:678–682.

Kakei, Y., Yamazaki, C., Suzuki, M., Nakamura, A., Sato, A., Ishida, Y., Kikuchi, R., Higashi, S., Kokudo, Y., Ishii, T., et al. (2015). Small-molecule auxin inhibitors that target YUCCA are powerful tools for studying auxin function. Plant J. **84**:827–837.

Kobayashi, M., Matoh, T., and Azuma, J. (1996). Two chains of rhamnogalacturonan ii are cross-linked by borate-diol ester bonds in higher plant cell walls. Plant Physiol. **110**:1017–1020.

Krishnakumar, V., Choi, Y., Beck, E., Wu, Q., Luo, A., Sylvester, A., Jackson, D., and Chan, A. P. (2015). A maize database resource that captures tissue-specific and subcellular-localized gene expression, via fluorescent tags and confocal imaging (Maize Cell Genomics Database). Plant Cell Physiol. **56**:e12–e12.

Lenth, R. V., Banfai, B., Bolker, B., Buerkner, P., Giné-Vázquez, I., Herve, M., Jung, M., Love, J., Miguez, F., Piaskowski, J., et al. (2025). emmeans: Estimated Marginal Means, aka Least-Squares Means. R package version 1.11.1. 2025, https://cran.r-project.org/package=emmeans.

Leonard, A., Holloway, B., Guo, M., Rupe, M., Yu, G., Beatty, M., Zastrow-Hayes, G., Meeley, R., Llaca, V., Butler, K., et al. (2014). *Tassel-less1* encodes a boron channel protein required for inflorescence development in maize. Plant Cell Physiol. **55**:1044–1054.

Li, Q., Liu, Y., Pan, Z., Xie, S., and Peng, S. (2016). Boron deficiency alters root growth and development and interacts with auxin metabolism by influencing the expression of auxin synthesis and transport genes. Biotechnol. Biotechnol. Equip. **30**:661–668.

Liu, S., Wollenberger, U., Halámek, J., Leupold, E., Stöcklein, W., Warsinke, A., and Scheller, F. W. (2005). Affinity interactions between phenylboronic acid-carrying self-assembled monolayers and flavin adenine dinucleotide or horseradish peroxidase. Chem. Eur. J. **11**:4239–4246.

Liu, X., Huang, M., Fan, B., Buckler, E. S., and Zhang, Z. (2016). Iterative usage of fixed and random effect models for powerful and efficient genome-wide association studies. PLOS Genet. **12**:e1005767.

Lordkaew, S., Dell, B., Jamjod, S., and Rerkasem, B. (2011). Boron deficiency in maize. Plant Soil **342**:207–220.

Martin-Rejano, E. M., Camacho-Cristobal, J. J., Herrera-Rodriguez, M. B., Rexach, J., Navarro-Gochicoa, M. T., and Gonzalez-Fontes, A. (2011). Auxin and ethylene are involved in the responses of root system architecture to low boron supply in Arabidopsis seedlings. Physiol. Plant. **142**:170–8.

Matoh, T. (1997). Boron in plant cell walls. Plant Soil, **193**:59–70.

Matthes, M., and Torres-Ruiz, R. A. (2016). Boronic acid treatment phenocopies monopteros by affecting PIN1 membrane stability and polar auxin transport in *Arabidopsis thaliana* embryos. Development **143**:4053–4062.

Matthes, M., and Torres-Ruiz, R. A. (2017). Boronic acids as tools to study (plant) developmental processes? Plant Signal. Behav. **12**:e1321190.

Matthes, M. S., Best, N. B., Robil, J. M., Malcomber, S., Gallavotti, A., and McSteen, P. (2019). Auxin EvoDevo: Conservation and diversification of genes regulating auxin biosynthesis, transport, and signaling. Mol. Plant **12**:298–320.

Matthes, M. S., Robil, J. M., and McSteen, P. (2020). From element to development: The power of the essential micronutrient boron to shape morphological processes in plants. J. Exp. Bot. **71**:1681–1693.

Matthes, M. S., Darnell, Z., Best, N. B., Guthrie, K., Robil, J. M., Amstutz, J., Durbak, A., and McSteen, P. (2022). Defects in meristem maintenance, cell division, and cytokinin signaling are early responses in the boron deficient maize mutant *tassel-less1*. Physiol. Plant. **174**:e13670.

Matthes, M. S., Best, N. B., Robil, J. M., and McSteen, P. (2023). Enhancement of developmental defects in the boron-deficient maize mutant *tassel-less1* by reduced auxin levels. J. Plant Nutr. Soil Sci. online ahead of print. https://doi.org/10.1002/jpln.202300155.

McSteen, P., Malcomber, S., Skirpan, A., Lunde, C., Wu, X., Kellogg, E., and Hake, S. (2007). *barren inflorescence2* encodes a co-ortholog of the pinoid serine/threonine kinase and is required for organogenesis during inflorescence and vegetative development in maize. Plant Physiol. **144**:1000–1011.

Miwa, K., and Fujiwara, T. (2010). Boron transport in plants: Co-ordinated regulation of transporters. Ann. Bot. **105**:1103–1108.

Odhnoff, C. (1961). The influence of boric acid and phenylborie acid on the root growth of bean (*Phaseolus vutgaris*). Physiol. Plant. **14**:187–220

O'Neill, M. A., Black, I., Urbanowicz, B., Bharadwaj, V., Crowley, M., Koj, S., and Peña, M. J. (2020). Locating methyl-etherified and methyl-esterified uronic acids in the plant cell wall pectic polysaccharide rhamnogalacturonan II. SLAS Technol. **25**:329–344

O'Neill, M. A., Warrenfeltz, D., Kates, K., Pellerin, P., Doco, T., Darvill, A. G., Albersheim, P., De, P., and Viala, P. (1996). Rhamnogalacturonan-II, a pectic polysaccharide in the walls of growing plant cell, forms a dimer that is covalently cross-linked by a borate ester. J. Biol. Chem. **271**:22923–22930.

Pasternak, T., Palme, K., and Pérez-Pérez, J. M. (2023). Role of reactive oxygen species in the modulation of auxin flux and root development in *Arabidopsis thaliana*. Plant J. **114**:83–95.

Phillips, K. A., Skirpan, A. L., Liu, X., Christensen, A., Slewinski, T. L., Hudson, C., Barazesh, S., Cohen, J. D., Malcomber, S., and McSteen, P. (2011). *vanishing tassel2* encodes a grass-specific tryptophan aminotransferase required for vegetative and reproductive development in maize. Plant Cell **23**:550–566.

Schneider, C. A., Rasband, W. S., and Eliceiri, K. W. (2012). NIH Image to ImageJ: 25 years of image analysis. Nat. Methods **9**:671–675.

Segura, V., Vilhjálmsson, B. J., Platt, A., Korte, A., Seren, Ü., Long, Q., and Nordborg, M. (2012). An efficient multi-locus mixed-model approach for genome-wide association studies in structured populations. Nat. Genet. **44**:825–830.

Shive, J. B., and Barnett, N. M. (1973). Boron deficiency effects on peroxidase, hydroxyproline, and boron in cell walls and cytoplasm of *Helianthus annuus* L. hypocotyls. Plant Cell Physiol. **14**:573–583.

Slaten, M. L., Chan, Y. O., Shrestha, V., Lipka, A. E., and Angelovici, R. (2020). HAPPI GWAS: Holistic Analysis with Pre- and Post-Integration GWAS. Bioinformatics **36**:4655–4657.

Smirnoff, N., and Arnaud, D. (2019). Hydrogen peroxide metabolism and functions in plants. New Phytol. **221**:1197–1214.

Sporzyński, A., Adamczyk-Woźniak, A., Zarzeczańska, D., Gozdalik, J. T., Ramotowska, P., and Abramczyk, W. (2024). Acidity constants of boronic acids as simply as possible: Experimental, correlations, and prediction. Molecules **29**:2713.

Su, C., Liu, L., Liu, H., Ferguson, B. J., Zou, Y., Zhao, Y., Wang, T., Wang, Y., and Li, X. (2016). H_2O_2 regulates root system architecture by modulating the polar transport and redistribution of auxin. J. Plant Biol. **59**:260–270.

Tao, L., Zhu, H., Huang, Q., Xiao, X., Luo, Y., Wang, H., Li, Y., Li, X., Liu, J., Jásik, J., et al. (2023). PIN2/3/4 auxin carriers mediate root growth inhibition under conditions of boron deprivation in Arabidopsis. Plant J. **115**:1357–1376.

Teale, W., and Palme, K. (2018). Naphthylphthalamic acid and the mechanism of polar auxin transport. J. Exp. Bot. **69**:303–312.

Tsukagoshi, H. (2016). Control of root growth and development by reactive oxygen species. Curr. Opin. Plant Biol. **29**:57–63.

Tsukagoshi, H., Busch, W., and Benfey, P. N. (2010). Transcriptional regulation of ROS controls transition from proliferation to differentiation in the root. Cell **143**:606–616.

Vanneste, S., Pei, Y., and Friml, J. (2025). Mechanisms of auxin action in plant growth and development. Nat. Rev. Mol. Cell Biol. http://doi.org/10.1038/s41580-025-00851-2.

Wang, J., and Zhang, Z. (2021). GAPIT Version 3: Boosting power and accuracy for genomic association and prediction. Genom. Proteom. Bioinform. **19**:629–640.

Wickham, H. (2016). ggplot2: Elegant graphics for data analysis.R package version 3.5.2, 2016. https://ggplot2.tidyverse.org.

Wilder, S. L., Scott, S., Waller, S., Powell, A., Benoit, M., Guthrie, J. M., Schueller, M. J., Awale, P., McSteen, P., Matthes, M. S., et al. (2022). Carbon-11 radiotracing reveals physiological and metabolic responses of maize grown under different regimes of boron treatment. Plants **11**:241.

Wimmer, M. A., Lochnit, G., Bassil, E., Muhling, K. H., and Goldbach, H. E. (2009). Membrane-associated, boron-interacting proteins isolated by boronate affinity chromatography. Plant Cell Physiol. **50**:1292–304.

Wright, D. (2025). gwaspr: GWAS plotting in R. R package version 1, 2025. https://derekmichaelwright.github.Io/gwaspr/.

Wu X, McSteen P. (2007) The role of auxin transport during inflorescence development in maize (*Zea mays*, Poaceae). Am J Bot. **94**:1745-55.

Xiong, J., Yang, Y., Fu, G., and Tao, L. (2015). Novel roles of hydrogen peroxide (H_2O_2) in regulating pectin synthesis and demethylesterification in the cell wall of rice (*Oryza sativa*) root tips. New Phytol. **206**:118–126.

Xu, J., Su, Z.-H., Chen, C., Han, H.-J., Zhu, B., Fu, X.-Y., Zhao, W., Jin, X.-F., Wu, A.-Z., and Yao, Q.-H. (2012). Stress responses to phenol in *Arabidopsis* and transcriptional changes revealed by microarray analysis. Planta **235**:399–410.

Yalamanchili, K., Vermeer, J. E. M., Scheres, B., and Willemsen, V. (2024). Shaping root architecture: towards understanding the mechanisms involved in lateral root development. Biol. Direct **19**:87.

Zhang, W., Fang, D., Dong, K., Hu, F., Ye, Z., and Cao, J. (2023). Insights into the environmental factors shaping lateral root development. Physiol. Plant. **175**:e13878.

Zhang, L., Vlach, J., Black, I. M., Archer-Hartmann, S., Heiss, C., Azadi, P., and Urbanowicz, B. R. (2025). The pectin puzzle: Decoding the fine structure of rhamnogalacturonan-I (RG-I) in *Arabidopsis thaliana* uncovers new pectin features. Carbohydr. Polym. **368**:124161.

Zhao, S., Huq, Md. E., Fahad, S., Kamran, M., and Riaz, M. (2024). Boron toxicity in plants: understanding mechanisms and developing coping strategies; a review. Plant Cell Rep. **43**:238.

3 Association of the benzoxazinoid pathway with boron homeostasis in maize

3.1 The benzoxazinoid biosynthesis in maize

Benzoxazinoids are a class of specialized secondary metabolites associated with various antifeedant, insecticidal and antimicrobial processes (Wouters et al., 2016). Aside from defense, benzoxazinoids also serve as regulation signals, influence the performance of neighboring plants and shape the rhizosphere microbiome (Hu et al., 2018a; Cotton et al., 2019; Gfeller et al., 2024; Richter et al., 2024). Some benzoxazinoids can modify the bioavailability of iron, aluminum, and arsenic (Poschenrieder et al., 2005; Hu et al., 2018b; Hu et al., 2021; Caggìa et al., 2024).

In maize, the benzoxazinoid biosynthesis pathway is well characterized (Fig. 4.1). The biosynthesis starts in plastids, where indole-3-glycerolphosphate (IGP) is transformed to indole by BENZOXAZINLESS1 (BX1), and then indole is converted to indolin-2-one (ION) by BX2 in the endoplasmic reticulum. ION undergoes hydroxylation catalyzed by BX3 to yield 3-hydroxy-indolin-2-one (HION). HION is catalyzed by BX4 to produce 2-hydroxy-1,4-benzoxazin-3-one (HBOA) and subsequently to 4-dihydroxy-2H-1,4-benzoxazin-3(4H)-one (DIBOA) by BX5 (Frey et al., 2009). DIBOA is further glucosylated to DIBOA glucoside (DIBOA-Glc) by BX8/BX9, and DIBOA-Glc is hydroxylated by BX6 to form 2,4,7-trihydroxy-1,4-benzoxazin-3-one glucoside (TRIBOA-Glc; Von Rad et al., 2001). Afterwards, BX7 catalyzes the methoxylation of TRIBOA-Glc to yield 2,4-dihydroxy-7-methoxy-1,4-benzoxazin-3-one-glucoside (DIMBOA-Glc; (Jonczyk et al., 2008). In maize B73, DIMBOA-Glc is the predominant benzoxazinoid (Frey et al., 2009).

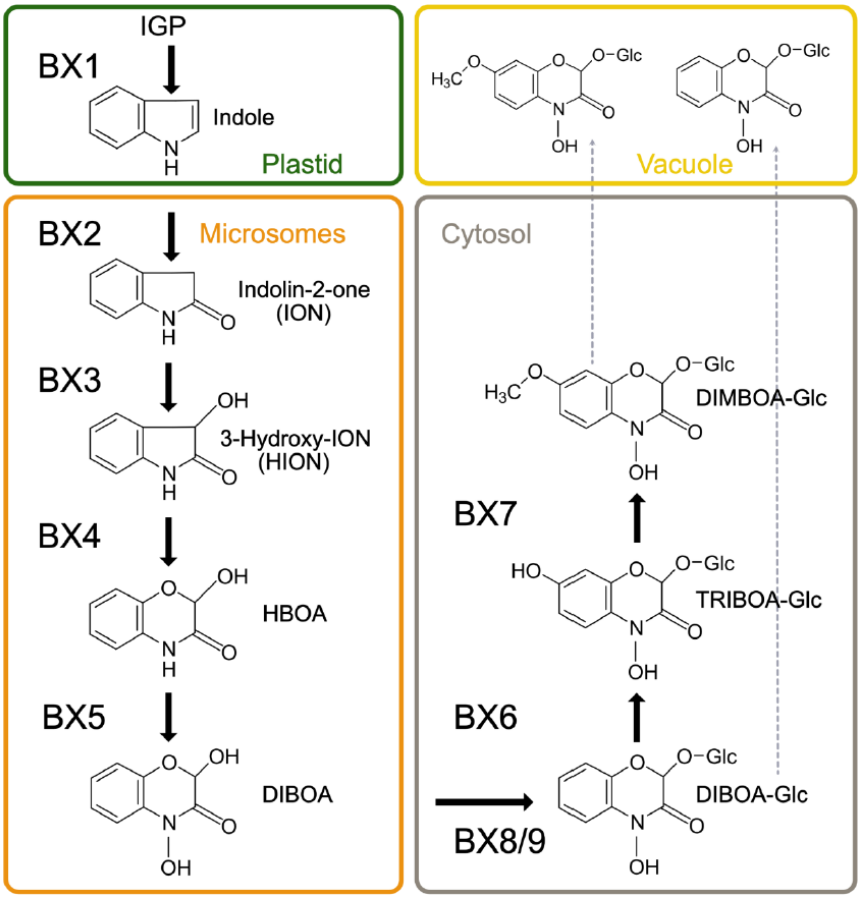

Figure 3.1. Benzoxazinoid biosynthesis pathway in maize. BX = BENZOXAZINLESS, DIBOA=2,4-dihydroxy-1,4-benzoxazin-3-one, DIMBOA=2,4-dihydroxy-7-methoxy-1,4-benzoxazin-3-one, Glc = glucoside, IGP= indole-3-glycerol phosphate, TRIBOA=2,4,7-trihydroxy-2H-1,4-benzoxazin-3-(4 H)-one-Glc. DIMBOA-Glc and DIBOA-Glc are stored in the vacuole as indicated by the dashed line and are activated to aglucones upon cell disruption, taken from (Chu et al., 2025a).

3.2 Association of the benzoxazinoid pathway with boron homeostasis in maize

Plant Physiology®

Plant Physiology, 2025, **197**, kiae611
https://doi.org/10.1093/plphys/kiae611
Advance access publication 8 November 2024
Research Article

Association of the benzoxazinoid pathway with boron homeostasis in maize

Liuyang Chu,[1,†] Vivek Shrestha,[2,†] Cay Christin Schäfer,[1] Jan Niedens,[3] George W. Meyer,[2] Zoe Darnell,[2] Tyler Kling,[2] Tobias Dürr-Mayer,[4] Aleksej Abramov,[5] Monika Frey,[5] Henning Jessen,[4] Gabriel Schaaf,[6] Frank Hochholdinger,[1] Agnieszka Nowak-Król,[3] Paula McSteen,[2] Ruthie Angelovici,[2] Michaela S. Matthes[1,*]

[1]Institute of Crop Science and Resource Conservation, Crop Functional Genomics, University of Bonn, Friedrich-Ebert-Allee 144, Bonn 53113, Germany
[2]Division of Biological Sciences, Bond Life Sciences Center, Interdisciplinary Plant Group, and Missouri Maize Center, University of Missouri, Columbia, MO 65211-7310, USA
[3]Boron-Containing Functional Materials, Institute of Inorganic Chemistry and Institute for Sustainable Chemistry & Catalysis with Boron, University of Würzburg, Am Hubland, Würzburg 97074, Germany
[4]Institute of Organic Chemistry, University of Freiburg, Albertstr. 21, Freiburg im Breisgau 79104, Germany
[5]Chair of Plant Breeding, Technical University of Munich, Liesel-Beckman Str. 2, Freising 85354, Germany
[6]Institute of Crop Science and Resource Conservation, Plant Nutrition, University of Bonn, Karl-Robert-Kreiten Straße 13, Bonn 53115, Germany
*Author for correspondence: mmatthes@uni-bonn.de
†These authors contributed equally to the work.
The author responsible for distribution of materials integral to the findings presented in this article in accordance with the policy described in the Instructions for Authors (https://academic.oup.com/plphys/pages/General-Instructions) is M. Matthes.

Abstract
Both deficiency and toxicity of the micronutrient boron lead to severe reductions in crop yield. Despite this agricultural importance, the molecular basis underlying boron homeostasis in plants remains unclear. To identify molecular players involved in boron homeostasis in maize (*Zea mays* L.), we measured boron levels in the Goodman-Buckler association panel and performed genome-wide association studies. These analyses identified a *benzoxazinless* (*bx*) gene, *bx3*, involved in the biosynthesis of benzoxazinoids, such as 2,4-dihydroxy-7-methoxy-1,4-benzoxazin-3-one (DIMBOA), which are major defense compounds in maize. Genes involved in DIMBOA biosynthesis are all located in close proximity in the genome, and benzoxazinoid biosynthesis mutants, including *bx3*, are all DIMBOA deficient. We determined that leaves of the *bx3* mutant have a greater boron concentration than those of B73 control plants, which corresponded with enhanced leaf tip necrosis, a phenotype associated with boron toxicity. By contrast, other DIMBOA-deficient maize mutants did not show altered boron levels or the leaf tip necrosis phenotype, suggesting that boron is not associated with DIMBOA. Instead, our analyses suggest that the accumulation of boron is linked to the benzoxazinoid intermediates indolin-2-one (ION) and 3-hydroxy-ION. Therefore, our results connect boron homeostasis to the benzoxazinoid plant defense pathway through *bx3* and specific intermediates, rendering the benzoxazinoid biosynthesis pathway a potential target for crop improvement under inadequate boron conditions.

Introduction

The micronutrient boron is essential for proper plant growth (Warington 1923) and both deficiencies and toxicities of boron in the soil lead to severe yield reductions in many major crops, including maize (*Zea mays* L.) (Brdar-Jokanović 2020). Soils with either low or toxic boron levels are widespread in the world (Landi et al. 2019; Brdar-Jokanović 2020; and references therein), making the study of the effects of boron supply on plant development an important topic for agriculture. After uptake from the soil, boron moves along the transpiration stream and accumulates at its end. Consequently, excess boron accumulates at the leaf blade tips and extends into the margins (Brown and Shelp 1997; Marschner 2012), which causes leaf necrosis when boron supply is too high (Eaton 1944; Reid et al. 2004). Boron toxicity leads to reduced chlorophyll content, stomatal conductance, and photosynthesis (as reviewed in Landi et al. (2019)). Boron deficiency primarily affects meristematic tissues (Sommer and Sorokin 1928), leading to reductions in leaf blade width and length, sterility, and in severe cases to seedling lethality. In the root, both boron deficiency and toxicity lead to a reduction in primary root length (Reid et al. 2004; Choi et al. 2007; Aquea et al. 2012; Esim et al. 2013; Poza-Viejo et al. 2018; Zhang et al. 2021) and to a reduction in lateral root density (Housh et al. 2020; Wilder et al. 2022). Understanding the molecular mechanisms that allow for efficiently using low levels or tolerating toxic levels of boron will help in developing efficient and tolerant varieties providing a sustainable solution to overcome yield reductions due to suboptimal or toxic boron supply.

The main characterized function of boron is in crosslinking of the pectin subunits rhamnogalacturonan-II (RG-II) in the cell wall (Kobayashi et al. 1996; Matoh et al. 1996; O'Neill et al. 1996) and boron efficiency processes include boron uptake, boron trans- and retranslocation, and boron utilization. From these processes, genetic components involved in boron uptake are currently best understood in the model organism *Arabidopsis thaliana* (Arabidopsis). Boron is taken up by plants in the form of boric acid and transported within plants in the form of the borate anion (for a recent review, see Onuh and Miwa (2021)). While passive uptake prevails in boron adequate soil conditions, facilitated

Received September 5, 2024. Accepted October 25, 2024.

and active boron transport is needed in low and excess soil boron conditions. Boron transporters belong to the nodulin 26-like intrinsic protein (NIP) subfamily of the major intrinsic protein (MIP) family of boric acid importers and the high boron requiring family of borate exporters. In Arabidopsis, the 3 NIPs, involved in boron import, and the 7 BORs, involved in boron export, have tissue and functional specificities (as reviewed in Onuh and Miwa (2021)). The major players are AtNIP5;1 (Takano et al. 2006) and AtBOR1 (Noguchi et al. 1997). Orthologs of these genes have been characterized in many plant species, including maize (Chatterjee et al. 2014, 2017; Durbak et al. 2014; Leonard et al. 2014; Chatterjee et al. 2017). *Zmtassel-less1* (*Zmtls1*) is the *AtNIP5;1* co-ortholog in maize and shows seedling lethality, when grown in low boron conditions. When grown in adequate boron conditions, only reproductive defects are prominent (Durbak et al. 2014; Leonard et al. 2014). Due to impaired boron uptake, this mutant is inherently boron deficient in meristem tissues and all defects can be rescued by boron fertilization (Durbak et al. 2014; Matthes et al. 2018), making it a good tool to study boron deficiency responses in maize (Matthes et al. 2022, 2023). Boron transporters additionally were shown to provide molecular targets for engineering plants adapted to altered soil boron concentrations (Miwa et al. 2006; Sutton et al. 2007; Kato et al. 2009; Schnurbusch et al. 2010; Uraguchi et al. 2014; Hayes et al. 2015; He et al. 2021).

Several lines of evidence indicate that additional molecular candidates exist that either regulate intracellular levels of boron or adapt cellular metabolism to changing boron levels. For example, various classes of genes are differentially regulated in boron deficient and toxic conditions (Peng et al. 2012) and there are striking differences between phenotypes of boron transporter mutants and phenotypes of plants grown in boron-deficient conditions (as reviewed in Matthes et al. (2020)). Numerous studies additionally highlight the importance of meristem genes and phytohormone cascades in the adaptation of plants to low boron levels (Abreu et al. 2014; Eggert and von Wirén 2017; Poza-Viejo et al. 2018; Gómez-Soto et al. 2019; Matthes et al. 2022, 2023; Pommerrenig et al. 2022). Recently, the boron deficiency response was additionally shown to reflect a wounding response in *Brassica napus* (Verwaaijen et al. 2023). These examples suggest that there are additional pathways that regulate either plant boron levels or susceptibilities and therefore might be harnessed for developing high yielding crops in boron-deficient conditions.

In Arabidopsis, few non-boron transporter genes potentially involved in boron homeostasis were identified. Of those, specific transcription factors were identified that regulate boron import by directly binding to the promoter of the boron transporter gene *NIP5;1* (Kasajima and Fujiwara 2007; Kasajima et al. 2010; Feng et al. 2020; Zhang et al. 2024). For others, a link to boron transport remains elusive and they might therefore act independent of it. These include the *low boron tolerance 1* mutant (Huai et al. 2018), for which the underlying gene remains to be identified, and the *sensitive to high-level of boron 1* mutant, which is defective in AtHEME OXYGENASE1, involved in photomorphogenesis (Lv et al. 2017), genes encoding specific subunits of condensin II (Sakamoto et al. 2011), affecting RG-II biosynthesis or dimer formation (O'Neill et al. 2001; Sechet et al. 2018) or genes influencing the deposition of pectin in the cell wall (Hiroguchi et al. 2021). More recently evidence from Arabidopsis and *Rosa* cell suspension cultures emphasized the importance of a properly functioning Golgi apparatus for boron-related processes (Chormova et al. 2014; Chormova and Fry 2016; Begum and Fry 2022; Onuh and Miwa 2023).

Efforts to elucidate molecular mechanisms underlying boron homeostasis in crops are ongoing and include the assessment of genetic variation (Pommerrenig et al. 2018; He et al. 2021), quantitative trait locus (QTL) analyses (Paull et al. 1991; Jefferies et al. 1999, 2000; Xu et al. 2001; Sutton et al. 2007; Schnurbusch et al. 2010; Zhao et al. 2012; Pallotta et al. 2014), or genome-wide association studies (GWAS) (de Abreu Neto et al. 2017; Jia et al. 2021). Furthermore, transcriptome studies identified genes that respond to varying boron levels in the soil or growing media (Zeng et al. 2008). While such efforts detected various genomic regions and a multitude of genes affected by altered soil boron levels, the elucidation of molecular players instrumental for boron homeostasis, and therefore, deficiency or toxicity tolerance, is not resolved.

Here, we report the detection of the benzoxazinoid biosynthesis gene *benzoxazinless3* (*bx3*) as a molecular candidate associated with boron homeostasis in the major crop maize. Our study links altered boron levels with *bx3* and the benzoxazinoid pathway intermediates indolin-2-one (ION) and 3-hydroxy-indolin-2-one (HION). Benzoxazinoids are indole-derived secondary defense metabolites, which have best been studied in grasses (Poacea) and additionally independently evolved in some eudicot species (Florean et al. 2023). They not only regulate below and aboveground biotic interactions but are also known as signaling molecules and as iron chelators supporting iron uptake (Hu et al. 2018). Our study, therefore, adds another layer to the multifunctionality of benzoxazinoids and suggests the benzoxazinoid pathway as target for engineering plants adapted to altered soil boron concentrations.

Results

Goodman-Buckler association panel shows extensive variation in boron concentration in maize ear leaves

To investigate the extent of phenotypic variability of leaf boron concentrations, boron concentrations from 277 inbred lines (Supplementary Table S1) of the 282 maize Goodman-Buckler association panel (Flint-Garcia et al. 2005) were quantified. The diversity panel was grown in replicates in the summers of 2017 and 2018 at Genetics Farm of the University of Missouri, Columbia, USA, where soil boron concentrations of 0.39 mg/kg are considered low (Durbak et al. 2014; Matthes et al. 2018). This can be seen by the occurrence of the strong boron-deficient leaf phenotype of the maize *Zmtassel-less1* (*Zmtls1*) mutant, which is defective in active boron transport (Durbak et al. 2014; Matthes et al. 2022).

After flowering, the boron concentration of ear leaves (the leaf subtending the ear shoot) was analyzed. In the analyzed back-transformed best linear unbiased predictors (BLUPs) from the diversity panel, the boron concentration varied between 8.6 μg/g (line CMV3) and 17.8 μg/g (line IL14H) (Supplementary Table S1) with a mean of 11.9 μg/g (Supplementary Table S2). The broad sense heritability calculated on a line-mean basis was 0.31 (Supplementary Table S2), indicating that the boron concentration in maize ear leaves is a complex trait and warrants genetic dissection to unravel this complexity.

GWAS uncovers 2 significant loci associated with the natural variation in boron concentration

To associate the observed variation in ear leaf boron concentration with the diverse inbred lines in the Goodman-Buckler association panel, we performed a GWAS using BLUPs from the analyzed 277 inbred lines. Using the publicly available single nucleotide polymorphism (SNP) data from the 282 Goodman-Buckler association,

2 significant SNP-trait associations (Fig. 1A) were identified. One SNP was on chromosome 4 (chr4) and 1 on chr7 (Fig. 1A; Table 1), suggesting that the genomic regions that are in linkage disequilibrium (LD) with them were significantly associated with the ear leaf boron concentration in maize. A quantile-quantile plot from the GWAS showed that our GWAS model is not inflated and depicts that few *P*-values of the performed association tests between SNP data and boron concentration data were more significant than expected (Fig. 1B).

We identified 6 candidate genes from the 200 kb intervals (100 kb upstream and downstream) centered around the significant SNP on chr4 and 8 candidate genes centered around the SNP on chr7 (Table 1). Two of the 6 chr4 genes were annotated as *benzoxazinless3* (*bx3*) and *bx4* (Table 1), involved in benzoxazinoid biosynthesis. The annotated genes underlying the peak on chr7 encoded an alcohol dehydrogenase, a DNAJ domain-containing protein, and the gibberellin receptor GID1L2 (Table 1).

Correlation analysis of gene expression of GWAS hits and boron concentration in the Goodman-Buckler association panel

To assess a potential connection between the identified GWAS candidate genes' transcript expression and boron concentration in the maize ear leaf, a correlation analysis was performed using publicly available gene expression data of the GWAS candidate genes in leaf tissues of the 282 Goodman-Buckler association panel (Kremling dataset, Kremling et al. 2018; Supplementary Table S3). Of the 14 detected GWAS hits, data for 6 genes were available from the Kremling dataset. We detected significant

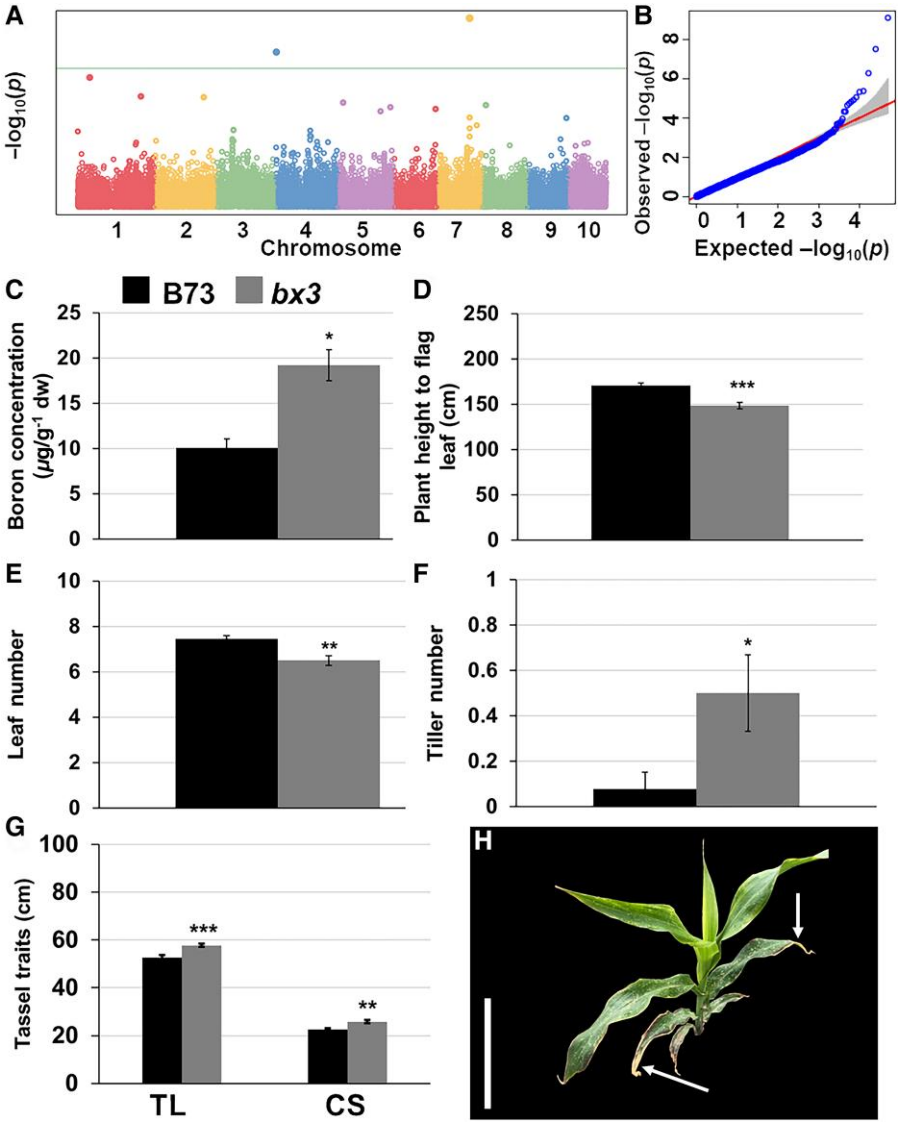

Figure 1. Phenotypes of the *bx3* mutant grown in the field (Bonn-Endenich 2020). **A)** Manhattan plot depicting genomic regions associated with variations of boron concentrations in a subset of the 282 Goodman-Buckler association panel. **B)** A quantile-quantile (qq) plot depicting the expected (*x*-axis) and observed (*y*-axis) −log(10) *P*-values. **C)** Boron concentration in ear leaves of the *bx3* mutant and B73 siblings. **D)** Plant height to flag leaf at maturity of the *bx3* mutant and B73 siblings. **E)** Leaf number between the leaf subtending the ear and the flag leaf of the *bx3* mutant and B73 siblings. **F)** Tiller number of the *bx3* mutant and B73 siblings. **G)** Tassel traits of the *bx3* mutant and B73 siblings. **H)** *bx3* plant image at 42 days after planting. The image was digitally extracted. Note that arrows in **H)** depicting leaf senescence at the leaf blade tip and the margins of *bx3*. Statistical analyses in **C)** through **G)** depict means and the error bars represent standard error of means. Sample numbers in **C to F)** were 13 (B73) and 14 (*bx3*) and in **G)** 10 (B73) and 11 (*bx3*). Statistical significance was calculated using Student's *t*-test (*$P < 0.05$, ***$P < 0.005$). Scale bar in **H)** = 15 cm. TL, tassel length; CS, length of central spike.

Table 1. GWAS of the boron concentration in ear leaves of the 282 Goodman-Buckler association panel and the candidate genes from 200 kb interval centered on the significant SNP (100 kb upstream/downstream) are summarized

Chr:SNP	Position	P-value	MAF	Effect size	Gene (B73_v2)	Gene (B73_v4) Zm00001d	Gene (B73_v5) Zm00001eb	Gene_description (v2)
4:ss196451184	3002213	3.34×10^{-08}	0.381	−0.011	GRMZM2G422877	48699	165520	Conserved gene of unknown function
					GRMZM5G896369	48701	165530, 165540	Hypothetical protein LOC100383896
					GRMZM5G830888, GRMZM2G469483	NA	NA	No description
					GRMZM2G167549	48702	165550	Cytochrome P450 71C2 (EC 1.14) (Protein benzoxazineless 3)
					GRMZM2G172491	48703	165560, 165570	Cytochrome P450 71C1 (EC 1.14) (Protein benzoxazineless 4)
7:ss196479729	126000000	7.81×10^{-10}	0.392	0.0124	GRMZM2G147191	20727	315020	Alcohol dehydrogenase
					GRMZM2G179045	20728	315030	Hypothetical protein LOC100381799
					GRMZM2G368058	20728	315030	No description
					GRMZM2G479068	20728	315030	No description
					GRMZM2G076802	NA	315040	DNAJ domain-containing protein
					GRMZM2G076778	20731	315050	Conserved gene of unknown function
					GRMZM2G003246	20732	315060	Gibberellin receptor GID1L2
					GRMZM2G518756	NA	NA	No description

Chromosome (Chr.), SNP ID, position, *P*-value, minor allele frequency (MAF), effect size, gene ID based on V2, V4, and V5 assembly, and gene description are summarized.

correlations between gene expression and boron concentration for 5 of the GWAS hits (*bx3* on chr4; alcohol dehydrogenase, DNAJ domain-containing protein, GRMZM2G076778 [which is a gene with unknown function], and Gibberellin Receptor on chr7) in one or multiple leaf tissues, suggesting that the variation of boron concentration in the Goodman-Buckler association panel might be correlated with expression level changes of these candidate genes. While *bx3* and the alcohol dehydrogenase gene showed a negative correlation in the third leaf, the DNAJ domain-containing protein and the Gibberellin Receptor genes showed positive correlations in various leaf tissues. GRMZM2G076778 depicted a negative correlation in adult leaf tissue (Supplementary Table S3).

The GWAS candidate genes *bx3* and *bx4* are differentially expressed in the maize boron transporter mutant *Zmtls1*

To further assess a connection between the identified genes and boron concentration in maize leaves, we tested, whether the identified GWAS candidate genes are differentially expressed in the maize boron transporter mutant *Zmtls1*, for which RNA-seq data of developing tassel meristems (~1 mm) are publicly available (Matthes et al. 2022). In *Zmtls1* tassel meristems, boron levels were found to be reduced compared with wild-type siblings (Durbak et al. 2014). We found that the chr4 candidate genes *bx3* and *bx4* were significantly upregulated in *Zmtls1* in that dataset, with $\log_2$ fold changes of 1.56 for *bx3* (*P-adj* = 0.0013) and 1.42 for *bx4* (*P-adj* = 0.0025) (Matthes et al. 2022; Table 2). Notably, none of the other candidate genes on chr4 or chr7 appeared as differentially expressed in the *Zmtls1* RNA-seq dataset (Table 2).

Taken together, the chr4 candidate gene *bx3* was the only GWAS candidate, whose expression in leaf tissue (Kremling et al. 2018) showed a significant correlation with the measured leaf boron concentration in the 282 Goodman-Buckler association panel (negative correlation) and which was also differentially expressed in the boron-deficient tassel meristem of the *Zmtls1* mutant.

Mature plants of maize *bx3* mutants have a boron concentration phenotype

The previous GWAS and expression analyses linked the *bx3* gene with variation in boron concentration in maize. To test if there was a boron-associated phenotype in *bx3* mutants, we analyzed

Table 2. Differential expression of GWAS candidate genes and benzoxazinoid biosynthesis genes in developing meristems of Zmtls1 compared with wild-type controls

Gene ID	tls1 vs WT ($\log_2$FC)	P-adj
Zm00001d048702 (*bx3*)	1.56	0.001288
Zm00001d048703 (*bx4*)	1.42	0.002502
Zm00001d48699 (unknown)	ns	
Zm00001d48701 (hypothetical)	ns	
Zm00001d20727 (alcohol dehydrogenase)	ns	
Zm00001d20728 (hypothetical)	ns	
Zm00001d20731 (unknown)	ns	
Zm00001d20732 (gibberellin receptor GID1L2)	ns	
Zm00001d048709 (*bx1*)	ns	
Zm00001d048710 (*bx2*)	ns	
Zm00001d048705 (*bx5*)	ns	
Zm00001d048634 (*bx6*)	1.66	1.66×10^{-16}
Zm00001d049179 (*bx7*)	ns	
Zm00001d048707 (*bx8*)	ns	

ns, not statistically significantly different.

boron concentration in ear leaves of mature *bx3* mutants (Frey et al. 1997) and in the B73 inbred line grown at the field site in Bonn, where soil boron levels averaged 0.27 mg/kg. Soil boron concentrations in combination with the appearance of the strong seedling phenotype of the boron-deficient maize mutant *Zmtls1* in Bonn-Endenich (Supplementary Fig. S1) showed that these field site conditions are comparable to those at the Genetics Farm in Columbia, Missouri (Durbak et al. 2014), the field site used for the GWAS.

Analyses from field grown plants in 2020 and 2021 showed that boron concentration was significantly elevated in the ear leaves of *bx3* mutants compared with B73 (Fig. 1C; Supplementary Tables S2 and S3), substantiating a correlation between *bx3* and boron levels in maize. This increase was nutrient specific as the concentrations of the other tested micro- and macronutrients were either unchanged (magnesium, calcium, phosphorus, sulfur, iron, zinc) or even decreased (manganese, copper) in the *bx3* mutant. Only potassium also showed a mild increase in *bx3* ear leaves (Supplementary Table S4). During the 2023 field season, however, no elevated boron concentrations were detected in *bx3* ear leaves compared with B73 (Supplementary Fig. S1). Similar observations were made in the greenhouse, when *bx3* mutants were grown in boron-rich soil (ED73 soil boron = 1.97 mg/kg) (Supplementary Fig. S2). In addition, the *Zmtls1* phenotype was also less severe with enhanced boron concentrations in ear leaves under the 2023 field conditions and under greenhouse conditions (Supplementary Fig. S1). It, therefore, seems likely that either variation in soil boron concentration or additional, not yet identified environmental factors influenced the boron-related phenotype in *bx3* and *tls1*.

Elevated boron concentrations in *bx3* ear leaves compared with B73 siblings did not lead to striking differences in reported boron toxicity phenotypes, like leaf tip necrosis in mature leaves (Supplementary Figs. S2 and S3), suggesting that the elevated boron concentrations in *bx3* ear leaves were not toxic. However, earlier during vegetative development (42 days after planting [DAP] in the field), *bx3* mutants showed severe leaf senescence at the leaf blade tip of particularly older leaves, extending into the leaf blade margins, which was not observed in B73 (arrowed in Fig. 1H; Supplementary Fig. S3B), suggesting a developmental factor influencing the phenotypes observed in *bx3* mutants.

In addition, the *bx3* mutants showed minor alterations of other potentially boron-related phenotypes: Plant height (up to the flag leaf) was significantly reduced in *bx3* mutants compared with B73 (Fig. 1D), and *bx3* mutants had significantly fewer leaves between the ear and the tassel compared with B73 siblings (Fig. 1E). In addition, tiller number, tassel length (TL), and the length of central spike (CS) were significantly increased in *bx3* mutants compared with B73 siblings (Fig. 1, F and G; Supplementary Table S5). While kernel row number was slightly, but significantly reduced in *bx3* mutants compared with B73 control plants, ear length was significantly longer (Supplementary Table S5). These morphological data suggested that enhanced boron levels in the *bx3* mutants did not lead to striking boron toxicity symptoms in field grown plants at maturity.

Bx3 mutants show a leaf tip necrosis phenotype during seedling development and its severity correlates with boron levels

In order to characterize the impact of boron levels on the observed leaf tip necrosis phenotype that we observed 6 weeks after planting (Fig. 1H), we analyzed the phenotype of *bx3* mutants earlier in development grown with different levels of boron. We first grew *bx3* mutants and B73 siblings in the growth chamber in boron sufficient soil (boron concentration of ED73 soil = 1.97 mg/kg) and phenotypically characterized seedling development over time (Fig. 2; Supplementary Table S6). We evaluated plant height, V-stage, leaf tip necrosis, and leaf number at 14 (developmental stage: V1/2 with 3 to 4 leaves emerged) and 25 DAP (developmental stage: V3/4, with 5 to 6 leaves emerged) (Fig. 2; Supplementary Fig. 4G and Table S6). At both time points, the *bx3* mutant was phenotypically not distinguishable from B73 with respect to plant height, leaf number, and V-Stage (Supplementary Table S6). However, at 14 DAP (developmental stage: V1/2), when both B73 and *bx3* had 3 to 4 leaves, the leaf tips of leaves 1 and 2 showed a distinct leaf tip necrosis phenotype in *bx3* mutants, but not in the B73 control (Fig. 2, A to C). In addition, we detected statistically significantly higher boron concentrations in pooled first and second leaves of *bx3* mutants compared with those of B73 14 DAP (Fig. 2D). This showed that boron levels are also enhanced in seedling leaves of the *bx3* mutant and suggested that these elevated boron levels correlated with the observed leaf tip necrosis phenotype.

Since the *Zmtls1* mutant showed enhanced boron levels in ear leaves under field conditions in 2023 (Supplementary Fig. S1), we did not use a genetics approach using double mutant analysis to determine the effects of lowered boron levels on *bx3* mutants. Instead, we grew the *bx3* mutants and B73 control plants in boron-free media (HGoTech GmbH, Bonn, Germany), where boron concentration = 0.03 mg/kg.

The leaf tip necrosis phenotype remained present in the *bx3* mutant, when grown in the boron-free media, whereas boron concentration in seedling leaves of *bx3* (leaves 1 and 2 pooled) were not statistically significantly different from the B73 control (Fig. 2, E to H). Therefore, we tested whether adding extra boron could influence the severity of the leaf tip necrosis phenotype by subjecting *bx3* mutants and B73 control plants (grown in ED73 soil) to the following watering regimes: Ultra-pure water (Merck Millipore, Burlington, USA), Peter's fertilizer (ICL specialty fertilizers, Tel-Aviv, Israel), Peter's fertilizer +0.5 mM boric acid, and Peter's fertilizer +1 mM boric acid. The ultra-pure water and Peter's fertilizer treatments showed the leaf tip necrosis phenotype in *bx3* plants, but not in B73 plants 14 DAP. In contrast, the treatments with Peter's fertilizer and additional boric acid caused the occurrence of the leaf tip necrosis phenotype also in B73 seedlings (Fig. 3, A to C; Supplementary Table S7), suggesting that the additional boric acid treatment caused this phenotype even in B73. In the *bx3* mutant, no enhancement of the leaf tip necrosis score was detected between the different watering regimes; however, the senesced leaf area in *bx3* mutants was significantly larger in the additional boric acid treatments compared with the ultra-pure water and Peter's fertilizer treatments (Fig. 3D).

Taken together, these analyses showed that the severity of the leaf tip necrosis phenotype in *bx3* mutants is correlated with enhanced boron levels. However, the variability of the results indicated that there are also additional, so far unidentified factors, contributing to the leaf tip necrosis phenotype in *bx3* mutants.

Investigation of a correlation between additional benzoxazinoid pathway genes and boron homeostasis

To determine if the link between boron levels and *bx3* was specific to *bx3*, we investigated other genes in the benzoxazinoid pathway. *bx3* encodes a cytochrome P450 monooxygenase that is involved in the biosynthesis of benzoxazinoids, a group of specialized secondary metabolites (Frey et al. 1997; Supplementary Fig. S5). The

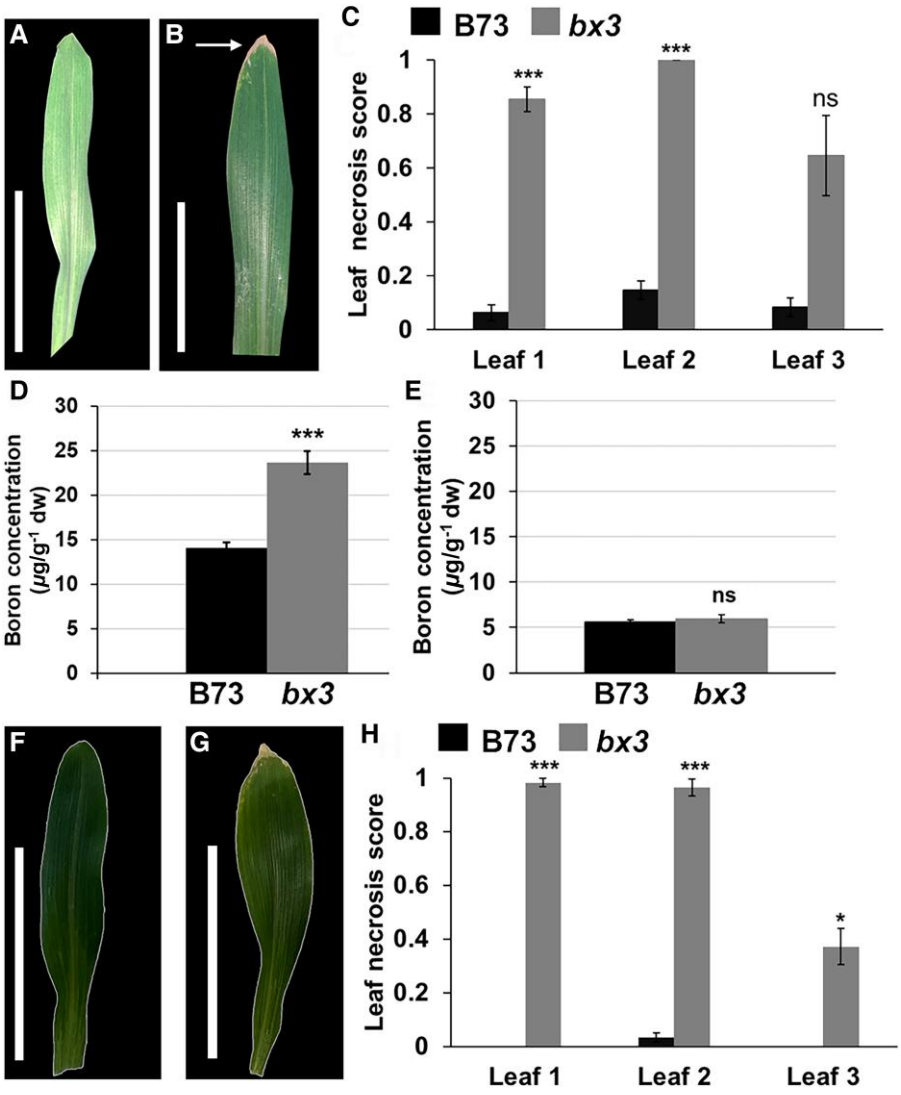

Figure 2. Leaf phenotypes of B73 and *bx3* seedlings. Images of the first leaves of **A)** B73 and **B)** *bx3* 14 days after planting (DAP) grown in the growth chamber in ED73 soil (boron concentration = 1.97 mg/kg). Arrows indicate leaf tip senescence. The images were digitally extracted for comparison. **C)** Statistical analysis of leaf tip necrosis in all emerged leaves of ED73-grown B73 and *bx3* 14 DAP. Depicted are means of 3 biological replicates, where $n = 16$ per genotype and biological replicate. Error bars show standard error of means. Statistical analysis of boron concentration (µg/g dw) in leaves 1 and 2 (pooled) of B73 and *bx3* 14 DAP, when **D)** seedlings grew in ED73 soil and **E)** seedlings grew in HGoTech substrate (boron concentration 0.03 mg/kg). Given are means over 4 biological replicates. The error bars represent standard error of means. Images of the first leaves of **F)** B73 and **G)** *bx3* 14 DAP grown in the growth chamber in HGoTech substrate. Images are digitally extracted for comparison. **H)** Statistical analysis of leaf tip necrosis in all emerged leaves of HGoTech-grown B73 and *bx3* 14 DAP. Depicted are means of 4 biological replicates, where $n = 15$ per genotype and biological replicate. Error bars show standard error of means. Statistical significance in **C)**, **D)**, and **H)** at $^{*}P < 0.05$, $^{**}P < 0.01$, $^{***}P < 0.005$ according to Student's *t*-test. Scale bars in **A, B, and F)**, **G)** = 5 cm. ns, not statistically significantly different.

predominant benzoxazinoids are 2,4-dihydroxy-1,4-benzoxazin-3-one (DIBOA) and 2,4-dihydroxy-7-methoxy-1,4-benzoxazin-3-one (DIMBOA), the latter being the major benzoxazinoid in B73 maize. There are 14 characterized *bx* genes in maize (as reviewed in de Bruijn et al. (2018)) with *bx1* to *bx9* involved in the synthesis of DIMBOA and *bx1* to *bx8* being located in proximity on chr4 (as reviewed in Frey et al. (2009)). We, therefore, assessed the possibility that the GWAS detected a significant correlation with the *bx* gene cluster on chr4, rather than individual *bx* genes, which was also reasoned by the detection of both *bx3* and *bx4* in the GWAS (Table 1). We performed correlation analyses with publicly available expression data in leaf tissue (Kremling et al. 2018) for all *bx* genes located on chr4 and the boron concentration data obtained from 277 lines of the 282 Goodman-Buckler association panel (Supplementary Table S1), similar to the correlation analyses with the detected GWAS candidates (Supplementary Table S3). These analyses showed that, in addition to gene expression of *bx3*, that of *bx2* also showed a negative correlation in the base of third leaf tissue, and that of *bx5* showed a positive correlation in the tip of third leaf tissue with boron concentration (Supplementary Table S8).

Furthermore, we examined *bx* gene expression of the chr4 cluster in the developing tassel meristem dataset of the *Zmtls1* mutant, which has reduced boron levels in that tissue. We found that in addition to *bx3* and *bx4*, also expression of *bx6* is significantly upregulated in *Zmtls1* mutants compared with normal siblings (Table 2). These results indicated that a potential correlation between *bx* genes and boron concentration in maize might not be restricted to *bx3* and that benzoxazinoid biosynthesis could be altered in *Zmtls1*. Therefore, we quantified levels of DIMBOA in *Zmtls1* leaves and found that the levels were significantly reduced

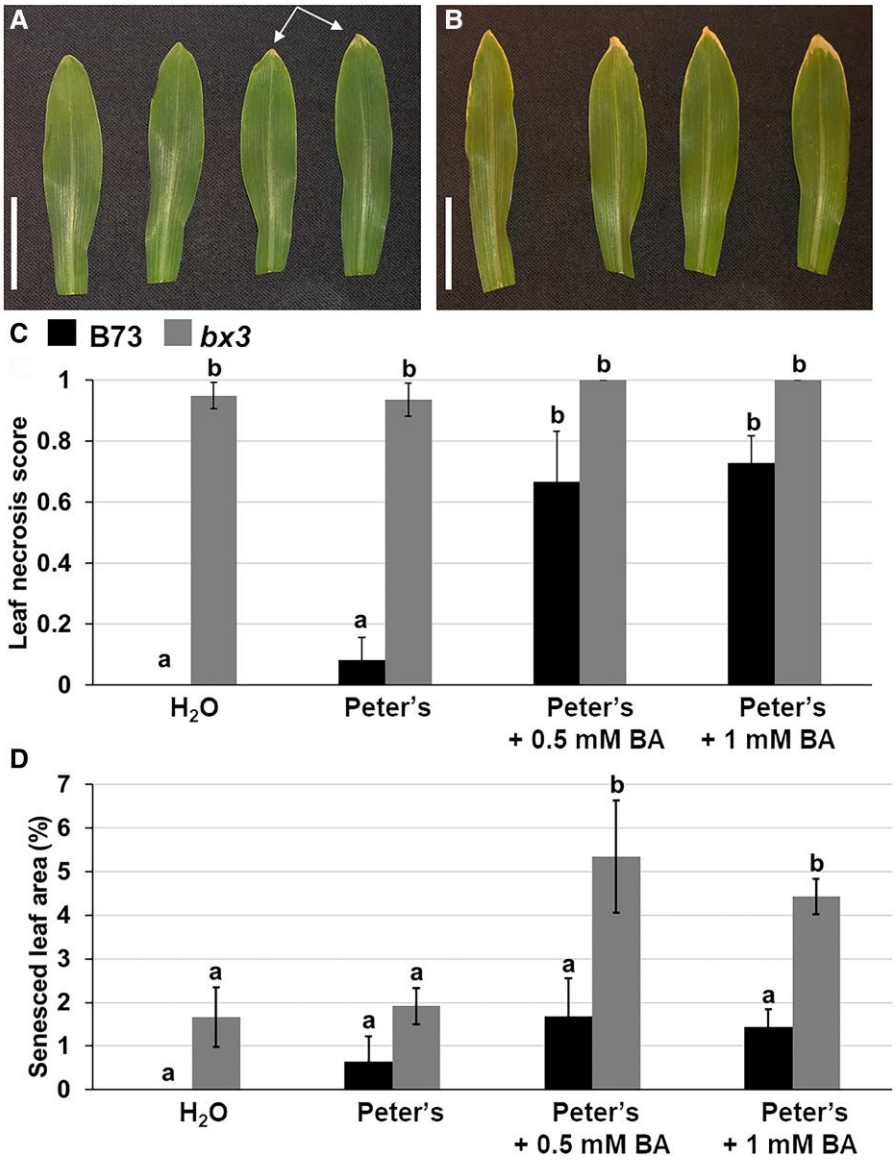

Figure 3. Senesced leaf area is enhanced by boron fertilization. Images of first leaves of **A)** B73 and **B)** *bx3* grown in ED73 soil. The images were taken 14 days after planting (DAP) with different watering regimes (from left to right: H_2O, Peter's fertilizer, Peter's fertilizer +0.5 mM boric acid (BA), Peter's fertilizer +1 mM BA). Arrows in **A)** point to leaf tip necrosis in B73. **C)** Statistical analysis of leaf necrosis score 14 DAP in B73 and *bx3* seedlings. **D)** Statistical analysis of senesced leaf area 14 DAP in B73 and *bx3* seedlings. **C and D)** show means of 4 biological replicates with 4–6 individuals per genotype and replicate. Error bars represent standard error of means. Different letters indicate statistical significance at $P < 0.05$ according to an analysis of variance with post hoc multiple comparison correction using the Tukey algorithm.

compared with wild-type controls (WT = 462.01 ± 71.01 ng/g, *Zmtls1* = 229.41 ± 59.99 ng/g, $P < 0.05$).

Boron homeostasis appears to be linked to *bx3* rather than DIMBOA

To test potential correlations between boron levels and benzoxazinoid biosynthesis, we analyzed boron concentration and assessed the leaf tip necrosis phenotype in *bx1* and *bx2* mutants, which were reported to have reduced DIMBOA levels (Hamilton 1964; Frey et al. 1997; Tzin et al. 2015).

We found that boron levels in ear leaves of *bx1* or *bx2* mutants were not statistically significantly different compared with their respective inbred control (Fig. 4A), when grown in Bonn-Endenich (soil boron concentration: 0.27 mg/kg in 2021). Likewise, *bx1* (developmental stage: V1/2) and *bx2* mutants (VE/1) did not show the striking leaf tip necrosis phenotype observed in *bx3* mutants (developmental stage: V1/2) at 14 DAP (Fig. 4, B to E, Supplementary Table S9). While the *bx2* mutant (introgressed in W22 and not B73) was not at the same developmental stage (VE/1) as *bx1* or *bx3* at 14 DAP, it did not show a statistically significant difference in leaf tip necrosis compared with its inbred control (W22) in any of the analyzed timepoints (Supplementary Table S9). In contrast, *bx1* showed a similar leaf tip necrosis phenotype to *bx3* at 18 DAP (developmental stage of both mutants: V2) and at 25 DAP (developmental stage of both mutants: V3). This phenotype, however, was restricted to the first leaf (18 DAP) or the first 2 leaves (25 DAP) (Fig. 4; Supplementary Table S9), which was in contrast to *bx3*, where the leaf necrosis phenotype was present in all developed leaves (Supplementary Table S9).

Taken together, our analyses therefore suggested a link between boron and *bx3* rather than boron and DIMBOA and raised

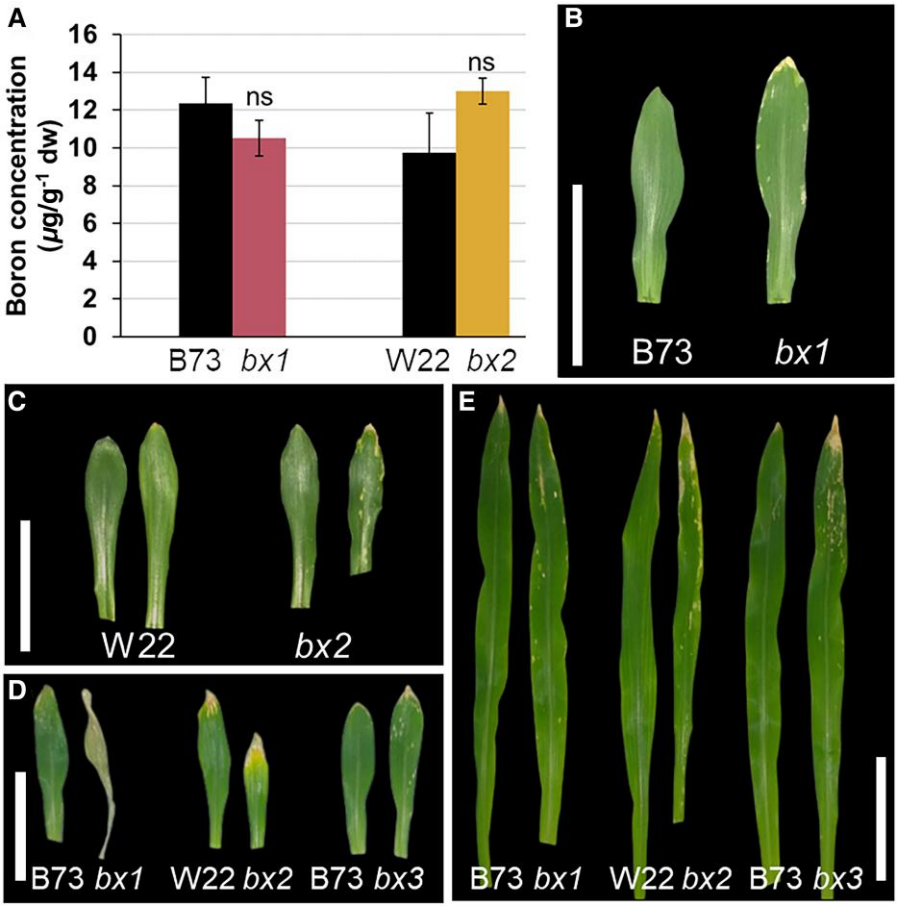

Figure 4. Boron-related phenotypes observed in the *bx3* mutant are not found in *bx1* or *bx2*. **A)** Statistical analysis of boron concentration (µg/g) in ear leaves of *bx1* and *bx2* mutants compared with the respective inbred control (grown in the field, Bonn-Endenich). Depicted are means ± standard error of means and statistical significance was calculated using Student's *t*-test ($P < 0.05$) ($n = 3$, where each replicate is a pool of four individual leaves). Leaf phenotypes of B73, W22, and mutants of *bx1*, *bx2*, *bx3* at 14, 18, and 25 days after planting (DAP), where **B)** Leaf 1 at 18 DAP, **C)** Leaf 1 at 18 DAP, **D)** Leaf 1 at 25 DAP, **E)** Leaf 2 at 25 DAP. The images in **B to E)** were digitally extracted. Scale bars in **B to E)** = 5 cm.

the question whether the lack of a functional BX3 enzyme or the accumulation of the BX3 substrate (Supplementary Fig. S5A) is connected with the observed boron accumulation.

Boron concentration is elevated in transgenic Arabidopsis lines expressing *BX1* and *BX2*

Although all 3 maize *bx* mutants we investigated are DIMBOA deficient (Frey et al. 1997; Tzin et al. 2017), *bx3* unlike *bx1* and likely *bx2* also accumulates the intermediate ION, which is the substrate of the BX3 enzyme (Abramov et al. 2021; Supplementary Fig. S5A). In order to test, whether elevated ION levels correlate with the observed boron concentration elevation in the *bx3* mutant, we made use of Arabidopsis lines, where parts of the benzoxazinoid biosynthesis pathway were transgenically introduced (Abramov et al. 2021). Arabidopsis does not endogenously express this pathway, allowing an assessment of a potential boron–benzoxazinoid correlation in a "clean" background. We found that boron concentration in rosette leaves at bolting stage of *pSUR2::Bx1Bx2*, which accumulate ION, was significantly higher compared with the *Col-0* control. On the other hand, functional expression of BX3 (*p35S::*Bx3 lines, which do not accumulate ION) did not influence the boron concentration. Therefore, a direct effect of the enzyme seems to be unlikely (Fig. 5). In addition, *pSUR2::Bx1Bx2* overexpressing lines showed a subtle leaf tip necrosis phenotype, compared with *Col-0* and *p35S::Bx3* lines (Fig. 5). Since *pSUR2::BX1BX2* lines were reported to additionally show elevated salicylic acid (SA) levels, we additionally assessed the impact of SA accumulation on the boron-related phenotypes of *pSUR2::Bx1Bx2* lines, by analyzing *pSUR2::Bx1Bx2* crossed to *NahG* lines (*pSUR2::Bx1Bx2* x *NahG*), where the SA hydroxlase *NahG* was introduced (Abramov et al. 2021). Our results showed that boron concentration is also significantly elevated in *pSUR2::Bx1Bx2xNahG* rosette leaves compared with *Col-0* controls and that the leaf tip necrosis phenotype in these lines is enhanced (Fig. 5, E and F; Supplementary Table S10). Therefore, these results suggested that a correlation between boron levels and the benzoxazinoid pathway is linked to an accumulation of the intermediate ION.

Boric acid forms a complex with the benzoxazinoid intermediate 3-hydroxy-ION (HION)

The benzoxazinoid DIMBOA was reported to chelate iron thus making it bioavailable (Hu et al. 2018), but also complex formation between DIMBOA and other nutrients, including zinc, copper, and manganese was reported (as reviewed in Wouters et al. (2016)). We therefore reasoned that elevated boron levels in the *bx3* mutant could be related to a benzoxazinoid-mediated alteration of boron transport or mobility. The correlation between boron levels and an accumulation of ION led us to test the hypothesis that boric acid and ION might form a complex, which in turn might

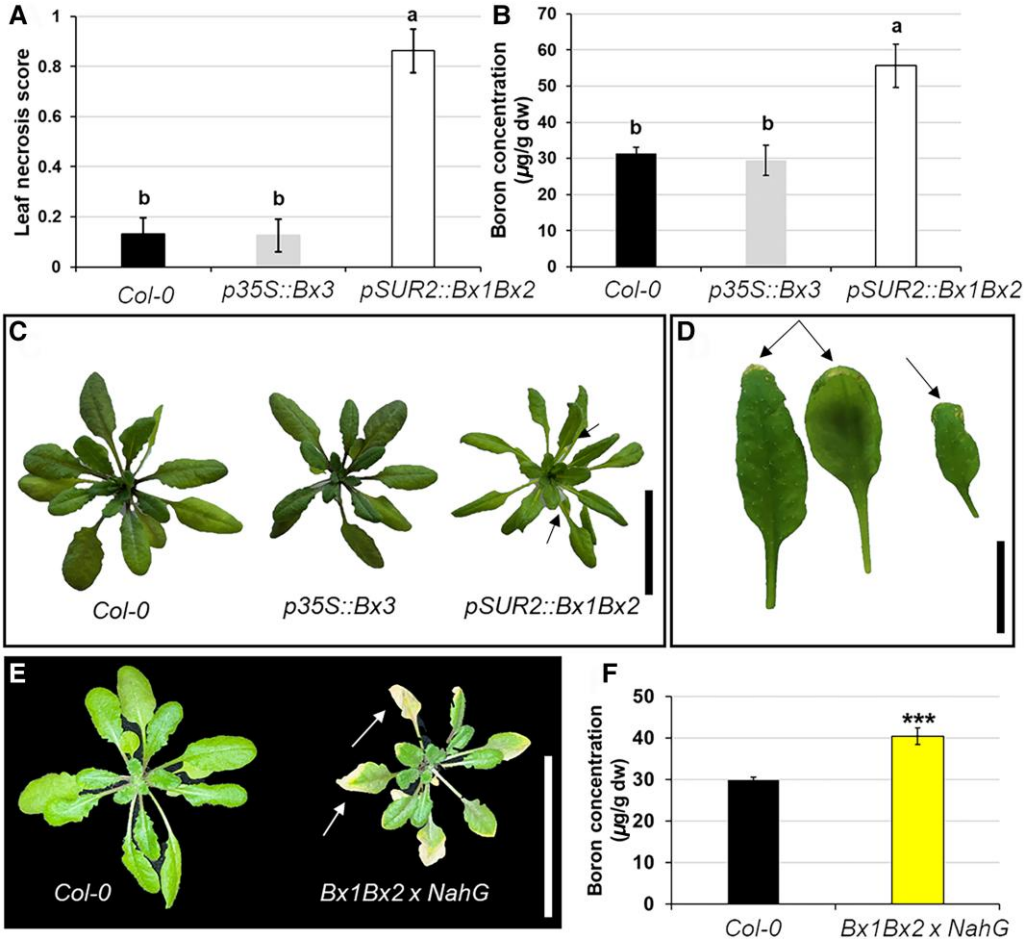

Figure 5. Analysis of boron–benzoxazinoid relations in transgenic Arabidopsis. **A)** Statistical analysis of leaf tip necrosis in *Col-0*, *p35S::Bx3*, and *pSUR2::Bx1Bx2* Arabidopsis lines. **B)** Statistical analysis of boron concentration (µg/g dw) in *Col-0*, *p35S::Bx3*, and *pSUR2::Bx1Bx2* Arabidopsis lines. **C)** Rosette leaf phenotypes of *Col-0*, *p35S::Bx3*, and *pSUR2::Bx1Bx2*. Note that arrows in *pSUR2::Bx1Bx2* pointing to a leaf tip necrosis phenotype in older leaves. **D)** Images of different leaves showing a subtle leaf tip necrosis phenotype in *pSUR2::Bx1Bx2* transgenic Arabidopsis. Note arrows that point to the leaf tip necrosis phenotype. **E)** Rosette leaf phenotypes of *Col-0* and *pSUR2::Bx1Bx2* in the *NahG* mutant background (*pSUR2::Bx1Bx2xNahG*). Note arrows in *pSUR2::Bx1Bx2xNahG* pointing to severely senesced rosette leaves. The images in **C to E)** were digitally extracted for comparison. **F)** Statistical analysis of boron concentration (µg/g dw) in *Col-0* and *pSUR2::Bx1Bx2xNahG* Arabidopsis lines. Statistical analyses in **A, B, and F)** depict means over 3 to 4 biological replicates ($n = 13–15$ individuals per biological replicate) ± standard error of means. Different letters indicate statistically significant differences according to an analysis of variance and post hoc Tukey test ($P < 0.05$). *** indicates statistical significance at $P < 0.005$ according to Student's *t*-test. Scale bars in **C)** = 4.5 cm, in **D)** = 1 cm, and in **E)** = 5 cm.

influence boron transport or mobility in maize. The reaction between ION and boric acid, however, did not lead to any boric acid–ION complex (Supplementary Fig. S6). As boron is known to specifically interact with *cis*-diol groups, which are not present in the benzoxazinoid intermediate ION, we also tested the next intermediate in the benzoxazinoid pathway, 3-hydroxy-ION (HION). HION is the product of the enzymatic function of BX3 (Supplementary Fig. S5A) that may tautomerize to the lactim species bearing 2 *cis*-diol groups (Supplementary Fig. S5B). The reaction of HION with boric acid in the presence of a base led to numerous additional signals in the ^{11}B-NMR spectrum (Fig. 6A) and ^{1}H-NMR spectrum (Supplementary Fig. S7A). Importantly, these signals were not observed when the analysis was done with boric acid and base alone (Fig. 6B) or when the control experiments were performed in the absence of boric acid (Supplementary Fig. S7, B and C). These results suggested the formation and therefore the existence of additional boron compounds formed between boric acid and HION (Fig. 6). Attempts to identify the nature of these additional boron compounds were unsuccessful, suggesting that such a complex is unstable. In the presence of air, HION reacted to isatin, which was not dependent on the presence of boric acid (Supplementary Fig. S6).

Discussion

Identification of genomic loci involved in boron homeostasis in maize

Previous analyses of genetic variation in various plant species that detected QTLs or genomic regions associated with boron deficiency or toxicity tolerance, identified mostly boron transporter-related genes (Sutton et al. 2007; Zeng et al. 2008; Schnurbusch et al. 2010; Pallotta et al. 2014; Pommerrenig et al. 2018; He et al. 2021; Jia et al. 2021). Notably, the significantly associated SNPs on chr4 and chr7 in the GWAS analysis did not harbor any of the published boron transporter genes in maize, which are located on chr1 (*Zmtls1* and *Zmrte*) and on chr3 (*Zmrte2*) (Chatterjee et al. 2014, 2017; Durbak et al. 2014; Leonard et al. 2014). It is likely that passive, protein-independent boron transport was still prevailing in the low boron field conditions, therefore masking any potential influence of active or facilitated boron transporters.

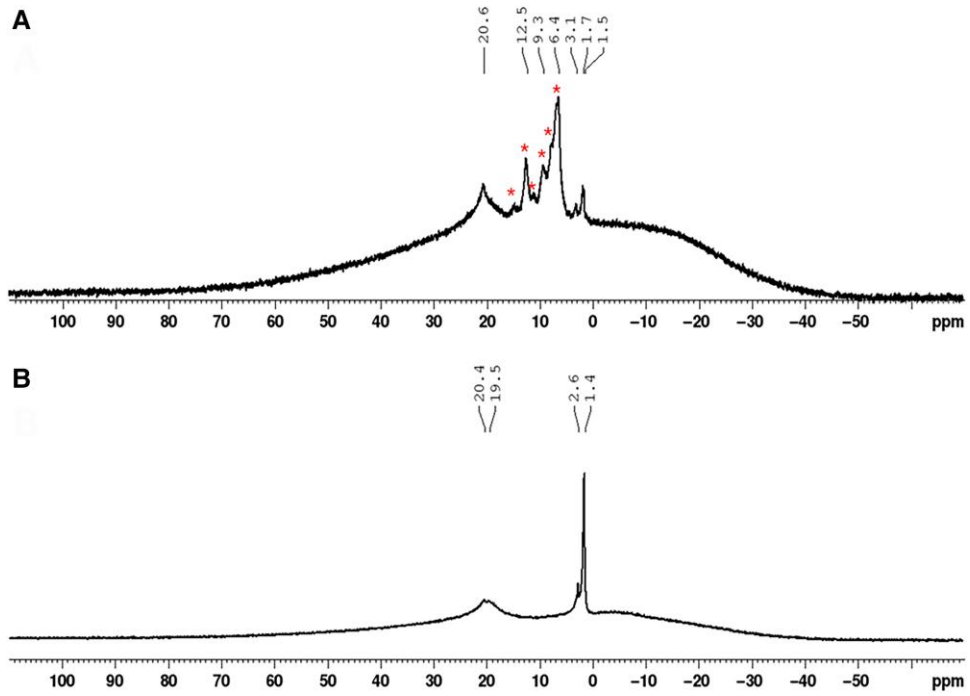

Figure 6. Boric acid reacts with HION to form additional boron species. **A)** The ^{11}B-NMR spectra showing the crude product of the reaction between HION and boric acid in the presence of a base and **B)** the crude product of the control experiment performed in the absence of HION. Signals assigned to the additional species are marked with an asterisk.

Similar studies using boron concentrations from seed as input have either detected specific boron transporters, like *Zmrte2* (Wu et al. 2021) and uncharacterized genes in maize (Schaefer et al. 2018) or peanut (Zhang et al. 2019), highlighting the potential contribution of non-boron transporter-related genes regulating boron homeostasis in plants.

Studies in rice, barley, and peanut have detected various cytochrome P450 proteins (with unknown function or putative iron-binding function) to be associated with either boron efficiency traits or boron concentration (Hassan et al. 2010; de Abreu Neto et al. 2017; Zhang et al. 2019), yet *bx* genes, which encode substrate specific cytochrome P450 proteins in grasses, have to our knowledge not been detected as potential candidates influencing boron-related processes in plants previously. Our study suggests that particularly *bx3* represents a molecular player associated with boron homeostasis in maize.

While we did not further test the additional GWAS hits detected (Table 1), the identification of a gene encoding a gibberellin receptor GID1L2 (GRMZM2G003246) on chr7 is worth mentioning. A functional role of gibberellin signaling in shaping the maize ionome had been suggested before (Schaefer et al. 2018) and it seems possible that gibberellin signaling or perception might be involved in boron concentration variation. Indeed, a rice GWAS analysis for boron toxicity tolerance also detected a gibberellin receptor (de Abreu Neto et al. 2017), providing evidence for the aforementioned hypothesis and for the applicability of our approach to detect molecular players involved in boron homeostasis. In addition, this finding adds to the importance of phytohormones in the boron response of plants (Martín-Rejano et al. 2011; Abreu et al. 2014; Camacho-Cristóbal et al. 2015; Li et al. 2015; Matthes and Torres-Ruiz 2016; Eggert and von Wirén 2017; Poza-Viejo et al. 2018; Gómez-Soto et al. 2019; Zhang et al. 2021; Matthes et al. 2022, 2023; Pommerrenig et al. 2022) and complements the reports of connections between the adaptation of plants to low or excess boron and gibberellins (Alva et al. 2015; Eggert and von Wirén 2017).

The unprecedented association between the benzoxazinoid pathway and boron levels is a surprising discovery, particularly because it suggests *bx3* as a non-boron transporter-related gene associated with boron homeostasis in maize. We detected reduced DIMBOA levels and upregulation of various *bx* biosynthesis genes in the boron transporter mutant *Zmtls1* (Table 2), which corroborates previous results showing a transcriptional feedback inhibition of benzoxazinoid biosynthesis genes by DIMBOA (Ahmad et al. 2011). However, altered boron levels and the leaf tip necrosis phenotypes were most pronounced in *bx3* mutants, compared with *bx1* or *bx2* mutants, although all 3 mutants have reduced DIMBOA levels. Besides a reduction of DIMBOA, the *bx3* mutant, unlike *bx1* or *bx2* mutants, was reported to accumulate the intermediate ION (Abramov et al. 2021). Since the benzoxazinoid pathway is blocked from ION on in the *bx3* mutant, it can be assumed that not just DIMBOA but also the direct product of BX3, namely HION, is depleted in the *bx3* mutant. Therefore, a depletion of HION or a shift in the ION to HION ratio might be of greater importance for the observed boron-related phenotypes than reduced DIMBOA levels in the *bx3* mutant. This makes it tempting to speculate about a causal connection between these intermediates (ION and/or HION) rather than DIMBOA and enhanced boron levels in the *bx3* mutant. This hypothesis is supported by the finding that transgenic Arabidopsis lines, that overexpress *bx1* and *bx2* and therefore accumulate ION (Abramov et al. 2021), also showed elevated boron levels in rosette leaves and a leaf tip necrosis phenotype (Fig. 5), similar to what was observed in the maize *bx3* mutant (Figs. 1 and 2). In the transgenic Arabidopsis lines, ION was further shown to be hydroxylated and glucosylated by endogenous Arabidopsis enzymes to yield the metabolite, indoline-2-one-5-β-D-glucopyranoside (5HIONG; Abramov et al. 2021). Therefore, the Arabidopsis boron-related phenotypes might

not just be connected to enhanced ION levels, but also to different intermediates/metabolites, like 5HIONG and/or ratio shifts of ION to such additional metabolites. Furthermore, the detection of additional boron species using ^{11}B-NMR and ^{1}H-NMR analyses of HION and boric acid mixtures (Fig. 6) provide compelling evidence for the ability of HION to form a complex with boric acid. While the identity of the additional boron species and proof for such a complex *in planta* remains elusive, it is tempting to speculate that a mechanistic link between boron levels and the benzoxazinoid pathway might be connected to the formation of boron–benzoxazinoid complexes, hence affecting boron homeostasis. While this remains intriguing and speculative the association of boron-related processes with the benzoxazinoid pathway opens up exciting lines of research in both areas.

Elevated boron levels toxic, beneficial, or both?

The *bx3* mutant, grown in low boron field conditions, showed elevated boron concentrations in the ear leaves, yet boron toxicity phenotypes were subtle at maturity (reduced plant height, increased tillering) (Fig. 1; Supplementary Fig. S3), suggesting that the enhanced boron levels were not high enough to be detrimental to plant performance. On the contrary, strong leaf senescence phenotypes were observed at the seedling stage (Figs. 1H and 2), indicating that elevated boron levels are more detrimental during juvenile vegetative development, although there are also additional factors that contribute to the leaf senescence phenotype (Fig. 2; Supplementary Fig. S3). Boron requirements are higher during reproductive development compared with vegetative development in maize (Lordkaew et al. 2011; Durbak et al. 2014) and *bx* gene expression is higher during seedling development (Frey et al. 1995, 1997), providing explanations for the leaf senescence phenotype observed in *bx3* seedlings, but not in mature plants. Since boron soil levels at the field site in Bonn-Endenich can be considered low (soil boron concentration: 0.27 mg/kg), it seems possible that the enhanced boron concentration in *bx3* mutants at maturity might counteract soil induced boron deficiency in contrast to provoking toxicity symptoms. This hypothesis is supported by the finding that specific tassel traits, like TL and length of CS, but also ear traits, like ear length, were significantly longer in *bx3* compared with B73 plants (Fig. 1G; Supplementary Table S5). This observation further complements published results, showing that boron supplementation increases tassel and ear size (Durbak et al. 2014; Leonard et al. 2014; Matthes et al. 2018). Our findings, therefore, allow a future assessment of *bx3* and potentially other *bx* genes as suitable molecular candidates for the adaptation of maize to low boron soil conditions.

Conclusion

Understanding the molecular regulation of boron homeostasis in crops remains a challenging task. By using a GWAS approach in combination with mutant and chemical analyses, we showed that the benzoxazinoid pathway is linked to boron homeostasis likely through *bx3* and the pathway intermediates ION and HION.

Materials and methods

Germplasm and plant growing conditions

In total, 277 inbred lines of the 282 Goodman-Buckler association panel (Flint-Garcia et al. 2005), consisting of diverse maize (*Zea mays* L.) lines including tropical, sub-tropical, temperate, sweet corn, and popcorn lines, were grown in a randomized complete block design in the summers of 2017 and 2018 at Genetics Farm of the University of Missouri (Columbia, Missouri, USA). Soil boron concentration in both years was 0.39 mg/kg as evaluated with the azomethine H method (Lohse 1982) by the Soil and Plant Testing Laboratory of the University of Missouri, which can be considered low considering the recommendation to apply boron to field maize, when soil levels are <0.75 ppm (Heckmann 2009).

The alleles used for the respective mutants were *Bx3::Mu* (*bx3*) (Frey et al. 1997), *bx1::Mu* (*bx1*) (Frey et al. 1997), *bx2::Ds* (*bx2*) (Tzin et al. 2017), and *tls1-ref* (*tls1*) (Durbak et al. 2014). The *bx1*, *bx3*, and *tls1* mutants were backcrossed at least 3 times to B73. Homozygous wild-types (B73) originating from the individual lines were used as controls. The *bx2* mutants were in a1-m3 background in the W22 inbred line, and the corresponding a1-m3 wild-type, also in the W22 background, was used as control. The *bx2* mutants and the corresponding wild-type (W22) were obtained from Dr. Georg Jander and Kevin Ahern (Boyce Thompson Institute, USA). In homozygous *bx3* plants, no DIMBOA can be detected and therefore can be considered null mutants (Frey et al. 1997). Homozygous *bx3* mutants from segregating lines were selected through genotyping using bx3_+540_F (5′-CAC CAA GAA GGT GCA GTC CT-3′), bx3_+1144_R (5′-GTA GCT GGA CTT ACC ACC AAG A-3′), and TIR6 (5′-AGA GAA GCC AAC GCC AWC GCC TCY ATT TCG TC-3′) primers. Genotyping for *tls1* was done as previously described (Durbak et al. 2014).

Unless otherwise stated, all maize greenhouse and growth chamber experiments were done with ED73 soil (Einheitserdewerke Werkverband e.V., Sinntal-Altengronau, Germany).

The transgenic Arabidopsis (*Arabidopsis thaliana*) lines, overexpressing parts of the maize benzoxazinoid pathway, namely *pSUR2::Bx1Bx2*, *pSUR2::Bx1Bx2xNahG*, and *p35S::Bx3* are described in Abramov et al. (2021). Seeds of the transgenic lines and the *Col-0* control were sown on 1% H_2O Agarose plates and stratified for 4 d at 4 °C in the dark. Afterwards, seeds were allowed to germinate for 7 d under long day conditions (light: 16 h, 22 °C, dark: 8 h, 17 °C, 40% humidity, light intensity = 65 $\mu E/m^2/s$), before seedlings were transferred to soil (Floragard B fein, sand, Perligran G mix, 10:1:1).

Boron concentration measurements

For the GWAS experiment in total, 277 inbred lines of the Goodman-Buckler association panel (Flint-Garcia et al. 2005) were used. In 2017 and 2018, leaves from the node subtending the ear shoot (referred to as ear leaves) from 5 plants per inbred line were collected after flowering, pooled, and about 2 cm of the leaves from the tip were discarded. The remaining leaf blades were dried at 60 °C and ground to a fine powder. Boron concentration in individual lines was analyzed subsequently by the azomethine H method (Lohse 1982) by the Soil and Plant Testing Laboratory at the University of Missouri.

The *bx3* mutants in the B73 background and the B73 inbreds (control) or *bx3* segregating lines were grown in the summers of 2020, 2021, and 2023 at the field station of the University of Bonn (Bonn-Endenich, Germany), where soil boron concentration was 0.27 mg/kg as assessed using a cold 0.01 M $CaCl_2$ extraction protocol and a miniaturized curcumin method for analysis (Wimmer and Goldbach 1999). Four ear leaves of *bx3* mutants, the B73 inbreds or the wild-type sibling controls were pooled separately, 2 cm of the leaf tips were discarded and the remaining leaf blades dried at 60 °C, and ground to a fine powder (3 biological replicates). For the Arabidopsis samples, whole rosettes were taken before bolting and dried at 60 °C before grinding to a fine powder

(3 to 4 biological replicates). Plant samples (500 mg maize or Arabidopsis) were digested with nitric acid in a CEM Mars 5 microwave digestion system (CEM Corporation, Matthews, North Carolina, USA) and boron concentration was analyzed by a miniaturized curcumin method (Wimmer and Goldbach 1999).

Genome-wide association study

The outlier removal, optimal transformation and BLUP calculation for the trait were performed as described in Slaten et al. (2020). The genotypic dataset was previously described in Shrestha et al. (2022). Briefly, the association panel was previously genotyped with the Illumina MaizeSNP50 BeadChip (Cook et al. 2012) and also with a genotyping-by-sequencing approach (Elshire et al. 2011) as described and utilized in Lipka et al. (2013). SNPs were filtered using minor allele frequency >0.05 and a total of 458,775 SNPs from both datasets were used for the GWAS analysis. We used FarmCPU model (Liu et al. 2016) to conduct GWAS and Bonferroni correction was used to correct for multiple testing at 5%. The candidate gene list was obtained using a 200 kb window size (100 kb on either side) of the significant SNPs. This interval was chosen to cover the long range LD in maize and also to compensate for low marker coverage as described in Ching et al. (2002), Flint-Garcia et al. (2003), Yan et al. (2009), and Shrestha et al. (2022). The physical locations and annotations of the genes were based on v2 of the maize B73 annotation.

Correlation analysis between boron concentrations and GWAS candidate gene expression in the Goodman-Buckler association panel

For the correlation analysis between leaf boron concentration and target gene expression levels, Pearson correlation tests were performed. We used gene expression data from Kremling et al. (2018). The authors collected 3′ RNA-sequencing data from 7 different tissues from 255 inbred lines of the Goodman-Buckler association panel. The normalized gene expression levels of candidate genes were used and correlated with back-transformed BLUPs of leaf boron concentrations of 277 lines of the Goodman-Buckler association panel (Supplementary Table S1).

Phenotypic analyses

Plant height measurements were taken at maturity from the soil level up to the tip of the tassel (total plant height = PH) and to the leaf collar of the flag leaf (plant height to flag leaf = FL). In addition, the number of primary tillers was scored. Plant height at seedling stage was determined from the pot soil level to the top of the leaf whorl. Developmental stages were assessed by using V-stages (Abendroth et al. 2011) and leaf number is given as the number of fully developed leaves plus all leaves that have emerged from the whorl.

TL was determined by measuring the length from the tassel node (node where the tassel is inserted in the stem at the base of the flag leaf) to the tip of the tassel. Peduncle length (PL) was determined by measuring the length of the tassel from the tassel node to the first branch. Branching area (BA) was determined by measuring the length of the main spike between the first and the last branch. Branch number (BN) is the total number of primary tassel branches. The length of CS was determined by subtracting PL and BA from TL.

Boron toxicity symptoms in seedling leaves were assessed using an adapted leaf bronzing score (de Abreu Neto et al. 2017), where 0 = no phenotype, 1 = leaf tips senesced, 2 = leaf tip and edges senesced (with or without leaf rolling), 3 = senescence reaches into leaf blade (with or without leaf rolling), 4 = any or all symptoms of categories 1 to 3 including aberrant leaf morphology, and 5 = fully senesced leaf (Supplementary Fig. S4).

The percentage of the senesced leaf area (boron fertilization experiment) was assessed 14 DAP (developmental stage V2 with 3 to 4 emerged leaves). The entire leaf blade of leaf one was cut and photographed, while for leaf 2, 5 cm of the leaf tip were cut and photographed. Image analysis was done with ImageJ (Schneider et al. 2012). The thresholds of all images were adjusted to either provide the full leaf area or the area of senescence (Supplementary Fig. S8). Out of these 2 values, the percentage of the senesced leaf area for every leaf was calculated.

Boron fertilization

B73 and *bx3* seedlings in the B73 background were grown in ED73 soil in a walk-in growth chamber (26 °C day, 16 °C night, 16 h day, 8 h light, 70% humidity) for 14 d and watered with either ultra-pure water (Merck Millipore, Burlington, USA), Peter's fertilizer (ICL specialty fertilizers, Tel-Aviv, Israel), Peter's fertilizer +0.5 mM boric acid, or Peter's fertilizer +1 mM boric acid. For the regular strength of Peter's fertilizer, nitrogen levels were adjusted to 238 ppm, which resulted in a final boron concentration of 0.08 ppm (Matthes et al. 2018). The plants were watered every other day, where 1 L of the respective solution was given to 24 plants (12 plants per genotype). The experiment was repeated 3 times.

DIMBOA levels in the *tls1* mutant

The boron transporter mutant *Zmtls1* (Durbak et al. 2014; Leonard et al. 2014) and wild-type siblings were grown in the Sears greenhouse facility at the University of Missouri, Columbia, USA (16/8 h light/dark cycle with an average day temperature of 30.5 °C, an average night temperature of 25 °C, and average humidity of 40% (day) and 60% (night)) and were continuously fertilized with Peter's fertilizer (ICL specialty fertilizers, Tel-Aviv, Israel), where nitrogen levels were adjusted to 238 ppm, resulting in boron concentrations of 0.08 ppm (Matthes et al. 2018). Developing leaves were dissected as described in Matthes et al. (2022) and analyzed for DIMBOA concentrations using liquid chromatography-mass spectrometry by the proteomics and metabolomics core facility at the University of Nebraska—Lincoln, USA. For details, see Supplementary Methods.

Boron-(H)ION complex formation

A solution of boric acid (2.6 mg/mL in D2O, pH 6, 540 μL, 22.5 μmol, 1.0 eq.) was added to a solution of ION (Sigma-Aldrich) (50 mg/mL in DMSO, 60 μL, 22.5 μmoL, 1.0 eq.) and kept at room temperature for 80 h. ^{11}B-NMR spectra were recorded after mixing, 18 and 80 h. Further experiments were performed with a boric acid solution, adjusted to pH 8 using 0.5 M NaOH solution, either at room temperature or 80 °C. Spectra were recorded on a Bruker Avance Neo 400 MHz with CryoProbe. Chemical shifts are given in ppm.

A solution of boric acid (2.3 mg/mL in D2O, pH 8 (adjusted using 0.5 M NaOH solution), 540 μL, 20.1 μmol, 1.0 eq.) was added to a solution of HION (Sigma-Aldrich) (50 mg/mL in DMSO, 60 μL, 20.1 μmol, 1.0 eq.) and kept either at room temperature or 80 °C. ^{11}B-NMR spectra were recorded after mixing, 3, 18, and 40 h. Further experiments were performed with 10 eq. HION (500 mg/mL in DMSO, 60 μL, 201 μmol, 10 eq.), 0.5 eq. and 0.2 eq. HION (respective stock solutions). The oxidized product isatin was isolated using preparative thin layer chromatography (CH/AcOEt 1:1).

Control experiments were performed in the absence of boric acid and using dimethylformamide instead of DMSO, also giving isatin as a product.

Under an argon atmosphere, tetrabutylammonium hydroxide (90.0 μL, 184 μmoL, 55 w% solution in water, 0.55 eq) was added to a degassed solution of HION (Sigma-Aldrich) (50.0 mg, 335 μmol, 1.00 eq) and boric acid (11.4 mg, 184 μmol, 0.55 eq.) in dimethylformamide (15 mL). The resulting solution was stirred at 130 °C for 16 h. Subsequently, the solvent was removed under reduced pressure using a cooling trap (<0.001 mbar, 100 °C). The yellow-brown color of the crude product mixture changes immediately to a strong violet color upon contact with air. The ^{11}B-NMR and ^{1}H-NMR spectra of the yellow-brown mixture were measured in a quartz glass NMR tube under argon atmosphere, using anhydrous and degassed acetonitrile-d_3 as a solvent.

To verify the origin of additional species in these spectra, the control experiments were performed (i) between the base and boric acid in the absence of HION and (ii) between HION and the base in the absence of boric acid, and the crude products were analyzed by ^{1}H and ^{11}B-NMR spectroscopy.

The spectra were recorded on a Bruker Avance 400 NMR spectrometer. Chemical shifts are given in ppm.

Statistical analysis

Statistical significance of the boron concentrations in the *bx3* mutant, the various growth trait phenotypes between *bx3* and B73 siblings, and the DIMBOA levels in the *tls1* mutant in comparison to non-mutant control lines was assessed in Microsoft Excel using Student's *t*-test (Student 1908) at a significance level of $P < 0.05$.

Statistical significance at a significance level of $P < 0.05$ was determined for the different boron fertilization treatments and the different genotypic categories in the Arabidopsis lines using analysis of variance with post hoc multiple testing correction applying the Tukey or Benjamini-Hochberg algorithms using the multcompView (Piepho 2004), agricolae (de Menidburu and Yaseen 2020), and emmeans (Lenth 2022) packages in R.

Accession numbers

Sequence data from this article can be found in the GenBank/EMBL data libraries or the MaizeGDB database under the following accession numbers: *Zmbx3*, LOC103652724, Zm00001eb165550; *Zmbx1*, LOC542117, Zm00001eb165610; *Zmbx2*, LOC100192631, Zm00001eb165620; *Zmtls1*, LOC541885, Zm00001eb043650.

Acknowledgments

We are indebted to the Soil and Plant Testing Laboratory of the University of Missouri, to Angelika Veits and Nur Gömec (University of Bonn—Plant Nutrition) for help with boron measurements. We further thank Chris Browne and his staff, as well as Helmut Rehkopf and Christa Schulz for exceptional plant care during the Missouri and Bonn field seasons, respectively. We are grateful to Laine Weiskopf for assisting in leaf material grinding, to Sherry Flint-Garcia and her team for help with the propagation and providing seeds of the 282 Goodman-Buckler association panel, and to Georg Jander and Kevin Ahern for providing seeds for the *bx2* mutant and the respective W22 inbred control. We thank the Proteomics & Metabolomics Facility (RRID:SCR_021314), Nebraska Center for Biotechnology at the University of Nebraska-Lincoln for the DIMBOA analysis. The facility and instrumentation are supported by the Nebraska Research Initiative.

Author contributions

V.S.: BLUPs and back-transformed BLUPs generation, GWAS analysis, correlation analysis, data analysis. L.C: Boron concentration measurements in soil, *bx3* mutants and Arabidopsis lines, data analysis, phenotypic analysis. C.S.: Phenotypic analysis of Arabidopsis lines and *bx3* mutants. J.N., T.D.: Boron–benzoxazinoid complex experiments. G. M., Z. D., T. K.: Boron analysis 282 Goodman-Buckler association panel. A.A: Generation and propagation of the Arabidopsis lines used. M.F., A.N.K., H.J., G.S., F.H., P.M., R.A.: Experimental design, student supervision, and data analysis. M.M.: Conceived and designed the study, experimental design, data analysis, student supervision, and writing of the manuscript with input from all authors. All authors approved of the final version of this manuscript.

Supplementary data

The following materials are available in the online version of this article.

Supplementary Materials and Methods.

Supplementary Figure S1. Phenotype of the *Zmtls1* mutant grown in the field in Bonn-Endenich or in the greenhouse and boron concentrations of *bx3* mutants.

Supplementary Figure S2. Phenotypes induced by boron supplementation and boron concentration in WT and *bx3* ear leaves grown in the greenhouse.

Supplementary Figure S3. Leaf necrosis and tassel phenotypes of the *bx3* mutant grown in the field Bonn-Endenich (2020).

Supplementary Figure S4. Scoring scheme for assessing leaf necrosis.

Supplementary Figure S5. Benzoxazinoid biosynthesis pathway in maize and lactam/lactim tautomerism of HION.

Supplementary Figure S6. Reactions of indolin-2-one (ION) and 3-hydroxy-ION in presence of air.

Supplementary Figure S7. Boric acid reacts with HION to form additional boron species. **A)** The ^{1}H-NMR spectra showing the crude mixture of the reaction of HION with boric acid in the presence of a base, **B)** the control experiment without boric acid, and **C)** pure HION.

Supplementary Figure S8. Image segmentation using ImageJ (Schneider et al. 2012).

Supplementary Table S1. Boron concentration of maize ear leaves in 277 lines of the 282 Goodman-Buckler association.

Supplementary Table S2. Descriptive statistics summary of boron concentrations (μg/g dw) obtained from the 277 back-transformed BLUPs of the 282 Goodman-Buckler association panel. dw, dry weight.

Supplementary Table S3. Correlation between gene expression of candidate genes with boron concentration in 277 lines of the 282 Goodman-Buckler association panel.

Supplementary Table S4. IPC-OES analysis of various nutrients in B73 and *bx3* mutants.

Supplementary Table S5. Phenotypes at maturity of *bx1*, *bx2*, *bx3* mutants, and their respective inbred line controls (B73, W22).

Supplementary Table S6. Vegetative phenotypes of *bx3* mutants and B73 control plants 14 and 25 days after planting (DAP).

Supplementary Table S7. Vegetative phenotypes of *bx3* mutants and B73 control plants 14 days after planting (DAP) with different watering regimes.

Supplementary Table S8. Correlation analysis of *bx* gene expression with boron concentration in the 282 Goodman-Buckler association panel.

Supplementary Table S9. Phenotypic analysis of *bx1*, *bx2*, *bx3* mutants, and their respective inbred line controls (B73, W22) 14, 18, and 25 days after planting (DAP).

Supplementary Table S10. Leaf necrosis score of Arabidopsis lines heterologously expressing parts of the maize benzoxazinoid pathway and *Col-0*.

Funding

This work was supported by the Agriculture and Food Research Initiative Grant 2015-06592 from the USDA/National Institute of Food and Agriculture to P.M. and by the German Research Foundation (DFG: MA 9520/1-1 and MA 9520/2-1 to M.S.M.). G.S. acknowledges funding by the DFG under Germany's Excellence Strategy—EXC 2070–390732324 (PhenoRob) and A.N.-K. thanks the DFG for an Emmy-Noether Fellowship (NO 1459/1-1) and the Hector Fellow Academy (HFA) for financial support. J.N. thanks the Hector Fellow Academy (HFA) for a Ph.D. scholarship.

Conflict of interest statement. None declared.

Data availability

All data are incorporated into the article and its online supplementary material.

References

Abendroth LJ, Elmore RW, Boyer MJ, Marlay SK (2011) Corn growth and development. Ext. Publ. #PMR-1009. https://store.extension.iastate.edu/Product/Corn-Growth-and-Development.

Abramov A, Hoffmann T, Stark TD, Zheng L, Lenk S, Hammerl R, Lanzl T, Dawid C, Schön CC, Schwab W, *et al.* Engineering of benzoxazinoid biosynthesis in *Arabidopsis thaliana*: metabolic and physiological challenges. *Phytochemistry*. 2021:192:112947. https://doi.org/10.1016/j.phytochem.2021.112947

Abreu I, Poza L, Bonilla I, Bolaños L. Boron deficiency results in early repression of a cytokinin receptor gene and abnormal cell differentiation in the apical root meristem of *Arabidopsis thaliana*. *Plant Physiol Biochem*. 2014:77:117–121. https://doi.org/10.1016/j.plaphy.2014.02.008

Ahmad S, Veyrat N, Gordon-Weeks R, Zhang Y, Martin J, Smart L, Glauser G, Erb M, Flors V, Frey M, *et al.* Benzoxazinoid metabolites regulate innate immunity against aphids and fungi in maize. *Plant Physiol*. 2011:157(1):317–327. https://doi.org/10.1104/pp.111.180224

Alva O, Roa-Roco RN, Pérez-Díaz R, Yánez M, Tapia J, Moreno Y, Ruiz-Lara S, González E, Gerós H. Pollen morphology and boron concentration in floral tissues as factors triggering natural and GA-induced parthenocarpic fruit development in grapevine. *PLoS One*. 2015:10(10):e0139503. https://doi.org/10.1371/journal.pone.0139503

Aquea F, Federici F, Moscoso C, Vega A, Jullian P, Haseloff J, Arce-Johnson P. A molecular framework for the inhibition of Arabidopsis root growth in response to boron toxicity. *Plant Cell Environ*. 2012:35(4):719–734. https://doi.org/10.1111/j.1365-3040.2011.02446.x

Begum RA, Fry SC. Boron bridging of rhamnogalacturonan-II in Rosa and Arabidopsis cell cultures occurs mainly in the endomembrane system and continues at a reduced rate after secretion. *Ann Bot*. 2022:130(5):703–715. https://doi.org/10.1093/aob/mcac119

Brdar-Jokanović M. Boron toxicity and deficiency in agricultural plants. *Int J Mol Sci*. 2020:21(4):1424. https://doi.org/10.3390/ijms21041424

Brown PH, Shelp BJ. Boron mobility in plants. *Plant Soil*. 1997:193(2):85–101. https://doi.org/10.1023/A:1004211925160

Camacho-Cristóbal JJ, Martín-Rejano EM, Herrera-Rodríguez MB, Navarro-Gochicoa MT, Rexach J, González-Fontes A. Boron deficiency inhibits root cell elongation via an ethylene/auxin/ROS-dependent pathway in Arabidopsis seedlings. *J Exp Bot*. 2015:66(13):3831–3840. https://doi.org/10.1093/jxb/erv186

Chatterjee M, Liu Q, Menello C, Galli M, Gallavotti A. The combined action of duplicated boron transporters is required for maize growth in boron-deficient conditions. *Genetics*. 2017:206(4):2041–2051. https://doi.org/10.1534/genetics.116.198275

Chatterjee M, Tabi Z, Galli M, Malcomber S, Buck A, Muszynski M, Gallavotti A. The boron efflux transporter ROTTEN EAR is required for maize inflorescence development and fertility. *Plant Cell*. 2014:26(7):2962–2977. https://doi.org/10.1105/tpc.114.125963

Ching A, Caldwell KS, Jung M, Dolan M, Oscar S, Smith H, Tingey S, Morgante M, Rafalski AJ. SNP frequency, haplotype structure and linkage disequilibrium in elite maize inbred lines. *BMC Genet*. 2002:14:1–14. https://doi.org/10.1186/1471-2156-3-19

Choi EY, Kolesik P, McNeill A, Collins H, Zhang Q, Huynh BL, Graham R, Stangoulis J. The mechanism of boron tolerance for maintenance of root growth in barley (*Hordeum vulgare* L.). *Plant Cell Environ*. 2007:30(8):984–993. https://doi.org/10.1111/j.1365-3040.2007.01693.x

Chormova D, Fry SC. Boron bridging of rhamnogalacturonan-II is promoted *in vitro* by cationic chaperones, including polyhistidine and wall glycoproteins. *New Phytol*. 2016:209(1):241–251. https://doi.org/10.1111/nph.13596

Chormova D, Messenger DJ, Fry SC. Boron bridging of rhamnogalacturonan-II, monitored by gel electrophoresis, occurs during polysaccharide synthesis and secretion but not post-secretion. *Plant J*. 2014:77(4):534–546. https://doi.org/10.1111/tpj.12403

Cook JP, McMullen MD, Holland JB, Tian F, Bradbury P, Ross-Ibarra J, Buckler ES, Flint-Garcia SA. Genetic architecture of maize kernel composition in the nested association mapping and inbred association panels. *Plant Physiol*. 2012:158(2):824–834. https://doi.org/10.1104/pp.111.185033

de Abreu Neto BJ, Hurtado-perez MC, Wimmer MA, Frei M. Genetic factors underlying boron toxicity tolerance in rice: genome-wide association study and transcriptomic analysis. *J Exp Bot*. 2017:68(3):687–700. https://doi.org/10.1093/jxb/erw423

de Bruijn WJC, Gruppen H, Vincken JP. Structure and biosynthesis of benzoxazinoids: plant defence metabolites with potential as antimicrobial scaffolds. *Phytochemistry*. 2018:155:233–243. https://doi.org/10.1016/j.phytochem.2018.07.005

de Menidburu F, Yaseen M. agricolae: statistical procedures for agricultural research. R package version 1.4.0. 2020. https://github.com/myaseen208/agricolae.

Durbak AR, Phillips KA, Pike S, O'Neill MA, Mares J, Gallavotti A, Malcomber ST, Gassmann W, McSteen P. Transport of boron by the *tassel-less1* aquaporin is critical for vegetative and reproductive development in maize. *Plant Cell*. 2014:26(7):2978–2995. https://doi.org/10.1105/tpc.114.125898

Eaton FM. Deficiency, toxicity, and accumulation of boron in plants. *J Agric Res*. 1944:69:237–277.

Eggert K, von Wirén N. Response of the plant hormone network to boron deficiency. *New Phytol*. 2017:216(3):868–881. https://doi.org/10.1111/nph.14731

Elshire RJ, Glaubitz JC, Sun Q, Poland JA, Kawamoto K, Buckler ES, Mitchell SE. A robust, simple genotyping-by-sequencing (GBS) approach for high diversity species. *PLoS One*. 2011:6(5):e19379. https://doi.org/10.1371/journal.pone.0019379

Esim N, Tiryaki D, Karadagoglu O, Atici O. Toxic effects of boron on growth and antioxidant system parameters of maize (*Zea mays* L.) roots. *Toxicol Ind Health*. 2013:29(9):800–805. https://doi.org/10.1177/0748233712442729

Feng Y, Cui R, Wang S, He M, Hua Y, Shi L, Ye X, Xu F. Transcription factor BnaA9.WRKY47 contributes to the adaptation of *Brassica napus* to low boron stress by up-regulating the boric acid channel gene *BnaA3.NIP5;1*. *Plant Biotechnol J*. 2020:18(5):1241–1254. https://doi.org/10.1111/pbi.13288

Flint-Garcia SA, Thornsberry JM, Buckler ESI. Structure of linkage disequilibrium in plants. *Annu Rev Plant Biol*. 2003:54(1):357–374. https://doi.org/10.1146/annurev.arplant.54.031902.134907

Flint-Garcia SA, Thuillet AC, Yu J, Pressoir G, Romero SM, Mitchell SE, Doebley J, Kresovich S, Goodman MM, Buckler ES. Maize association population: a high-resolution platform for quantitative trait locus dissection. *Plant J*. 2005:44(6):1054–1064. https://doi.org/10.1111/j.1365-313X.2005.02591.x

Florean M, Luck K, Hong B, Nakamura Y, O'Connor SE, Köllner TG. Reinventing metabolic pathways: independent evolution of benzoxazinoids in flowering plants. *Proc Natl Acad Sci U S A*. 2023:120(42):e2307981120. https://doi.org/10.1073/pnas.2307981120

Frey M, Chomet P, Glawischnig E, Stettner C, Grün S, Winklmair A, Eisenreich W, Bacher A, Meeley RB, Briggs SP, *et al.* Analysis of a chemical plant defense mechanism in grasses. *Science*. 1997:277(5326):696–699. https://doi.org/10.1126/science.277.5326.696

Frey M, Kliem R, Saedler H, Gierl A. Expression of a cytochrome P450 gene family in maize. *Mol Genet Genomics*. 1995:246(1):100–109. https://doi.org/10.1007/BF00290138

Frey M, Schullehner K, Dick R, Fiesselmann A, Gierl A. Benzoxazinoid biosynthesis, a model for evolution of secondary metabolic pathways in plants. *Phytochemistry*. 2009:70(15–16):1645–1651. https://doi.org/10.1016/j.phytochem.2009.05.012

Gómez-Soto D, Galván S, Rosales E, Bienert P, Abreu I, Bonilla I, Bolaños L, Reguera M. Insights into the role of phytohormones regulating *pAtNIP5;1* activity and boron transport in *Arabidopsis thaliana*. *Plant Sci*. 2019:287:110198. https://doi.org/10.1016/j.plantsci.2019.110198

Hamilton R. A corn mutant deficient in 2,4-dihydroxy-7-methoxy-1,4-benzoxazin-3-one with an altered tolerance of atrazine. *Weeds*. 1964:12(1):27–30. https://doi.org/10.2307/4040633

Hassan M, Oldach K, Baumann U, Langridge P, Sutton T. Genes mapping to boron tolerance QTL in barley identified by suppression subtractive hybridization. *Plant Cell Environ*. 2010:33(2):188–198. https://doi.org/10.1111/j.1365-3040.2009.02069.x

Hayes JE, Pallotta M, Garcia M, Öz MT, Rongala J, Sutton T. Diversity in boron toxicity tolerance of Australian barley (*Hordeum vulgare* L.) genotypes. *BMC Plant Biol*. 2015:15(1):231. https://doi.org/10.1186/s12870-015-0607-1

He M, Wang S, Zhang C, Liu L, Zhang J, Qiu S, Wang H, Yang G, Xue S, Shi L, *et al.* Genetic variation of *BnaA3.NIP5;1* expressing in the lateral root cap contributes to boron deficiency tolerance in *Brassica napus*. *PLoS Genet*. 2021:17(7):e1009661. https://doi.org/10.1371/journal.pgen.1009661

Heckmann JR. Boron: needs of soils and crops in New Jersey. Rutgers NJAES Cooperative Extension; 2009.

Hiroguchi A, Sakamoto S, Mitsuda N, Miwa K. Golgi-localized membrane protein AtTMN1/EMP12 functions in the deposition of rhamnogalacturonan II and I for cell growth in Arabidopsis. *J Exp Bot*. 2021:72(10):3611–3629. https://doi.org/10.1093/jxb/erab065

Housh AB, Matthes MS, Gerheart A, Wilder SL, Kil K, Schueller M, GuthrieJM, Mcsteen P, Ferrieri R. Assessment of a ^{18}F-phenylboronic acid radiotracer for imaging boron in maize. *Int J Mol Sci*. 2020:21(3):976. https://doi.org/10.3390/ijms21030976

Hu L, Mateo P, Ye M, Zhang X, Berset JD, Handrick V, Radisch D, Grabe V, Köllner TG, Gershenzon J, *et al.* Plant iron acquisition strategy exploited by an insect herbivore. *Science*. 2018:361(6403):694–697. https://doi.org/10.1126/science.aat4082

Huai Z, Peng L, Wang S, Zhao H, Shi L, Xu F. Identification and characterization of an *Arabidopsis thaliana* mutant *lbt* with high tolerance to boron deficiency. *Front Plant Sci*. 2018:9:736. https://doi.org/10.3389/fpls.2018.00736

Jefferies SP, Barr AR, Karakousis A, Kretschmer JM, Manning S, Chalmers KJ, Nelson JC, Islam AKMR, Langridge P. Mapping of chromosome regions conferring boron toxicity tolerance in barley (*Hordeum vulgare* L.). *Theor Appl Genet*. 1999:98(8):1293–1303. https://doi.org/10.1007/s001220051195

Jefferies SP, Pallotta MA, Paull JG, Karakousis A, Kretschmer JM, Manning S, Islam AKMR, Langridge P, Chalmers KJ. Mapping and validation of chromosome regions conferring boron toxicity tolerance in wheat (*Triticum aestivum*). *Theor Appl Genet*. 2000:101(5–6):767–777. https://doi.org/10.1007/s001220051542

Jia Z, Bienert MD, von Wirén N, Bienert GP. Genome-wide association mapping identifies *HvNIP2;2/HvLsi6* accounting for efficient boron transport in barley. *Physiol Plant*. 2021:171(4):809–822. https://doi.org/10.1111/ppl.13340

Kasajima I, Fujiwara T. Identification of novel *Arabidopsis thaliana* genes which are induced by high levels of boron. *Plant Biotechnol*. 2007:24(3):355–360. https://doi.org/10.5511/plantbiotechnology.24.355

Kasajima I, Ide Y, Yokota Hirai M, Fujiwara T. WRKY6 is involved in the response to boron deficiency in *Arabidopsis thaliana*. *Physiol Plant*. 2010:139(1):80–92. https://doi.org/10.1111/j.1399-3054.2010.01349.x

Kato Y, Miwa K, Takano J, Wada M, Fujiwara T. Highly boron deficiency-tolerant plants generated by enhanced expression of NIP5;1, a boric acid channel. *Plant Cell Physiol*. 2009:50(1):58–66. https://doi.org/10.1093/pcp/pcn168

Kobayashi M, Matoh T, Azuma J. Two chains of rhamnogalacturonan II are cross-linked by borate-diol ester bonds in higher plant cell walls. *Plant Physiol*. 1996:110(3):1017–1020. https://doi.org/10.1104/pp.110.3.1017

Kremling KAG, Chen SY, Su MH, Lepak NK, Romay MC, Swarts KL, Lu F, Lorant A, Bradbury PJ, Buckler ES. Dysregulation of expression correlates with rare-allele burden and fitness loss in maize. *Nature*. 2018:555(7697):520–523. https://doi.org/10.1038/nature25966

Landi M, Margaritopoulou T, Papadakis IE, Araniti F. Boron toxicity in higher plants: an update. *Planta*. 2019:250(4):1011–1032. https://doi.org/10.1007/s00425-019-03220-4

Lenth RV. emmeans: estimated marginal means, aka least-squares means. R package version 1.7.2. 2022. https://CRAN.Rproject.org/package=emmeans.

Leonard A, Holloway B, Guo M, Rupe M, Yu G, Beatty M, Zastrow-Hayes G, Meeley R, Llaca V, Butler K, *et al.* *Tassel-less1* encodes a boron channel protein required for inflorescence development in maize. *Plant Cell Physiol*. 2014:55(6):1044–1054. https://doi.org/10.1093/pcp/pcu036

Li K, Kamiya T, Fujiwara T. Differential roles of PIN1 and PIN2 in root meristem maintenance under low-B conditions in *Arabidopsis thaliana*. *Plant Cell Physiol*. 2015:56(6):1205–1214. https://doi.org/10.1093/pcp/pcv047

Lipka AE, Gore MA, Magallanes-Lundback M, Mesberg A, Lin H, Tiede T, Chen C, Robin Buell C, Buckler ES, Rocheford T, *et al.* Genome-wide association study and pathway-level analysis of tocochromanol levels in maize grain. *G3 (Bethesda, Md.)*. 2013:3(8):1287–1299. https://doi.org/10.1534/g3.113.006148

Liu X, Huang M, Fan B, Buckler ES, Zhang Z. Iterative usage of fixed and random effect models for powerful and efficient genome-wide association studies. *PLoS Genet*. 2016:12(2):e1005767. https://doi.org/10.1371/journal.pgen.1005767

Lohse G. Microanalytical azomethine-H method for boron determination in plant tissue. *Commun Soil Sci Plant Anal*. 1982:13(2):127–134. https://doi.org/10.1080/00103628209367251

Lordkaew S, Dell B, Jamjod S, Rerkasem B. Boron deficiency in maize. *Plant Soil*. 2011:342(1–2):207–220. https://doi.org/10.1007/s11104-010-0685-7

Lv Q, Wang L, Wang JZ, Li P, Chen YL, Du J, He YK, Bao F. SHB1/HY1 alleviates excess boron stress by increasing BOR4 expression level and maintaining boron homeostasis in Arabidopsis roots. *Front Plant Sci*. 2017:8:790. https://doi.org/10.3389/fpls.2017.00790

Marschner P. ed. *Marschner's mineral nutrition of higher plants*. 3rd ed. Amsterdam: Elsevier Ltd; 2012.

Martín-Rejano EM, Camacho-Cristóbal JJ, Herrera-Rodríguez MB, Rexach J, Navarro-Gochicoa MT, González-Fontes A. Auxin and ethylene are involved in the responses of root system architecture to low boron supply in Arabidopsis seedlings. *Physiol Plant*. 2011:142(2):170–178. https://doi.org/10.1111/j.1399-3054.2011.01459.x

Matoh T, Kawaguchi S, Kobayashi M. Ubiquity of a borate-rhamnogalacturonan II complex in the cell walls of higher plants. *Plant Cell Physiol*. 1996:37(5):636–640. https://doi.org/10.1093/oxfordjournals.pcp.a028992

Matthes M, Torres-Ruiz RA. Boronic acid treatment phenocopies *monopteros* by affecting PIN1 membrane stability and polar auxin transport in *Arabidopsis thaliana* embryos. *Development*. 2016:143(21):4053–4062. https://doi.org/10.1242/dev.131375

Matthes MS, Best NB, Robil JM, McSteen P. Enhancement of developmental defects in the boron-deficient maize mutant *tassel-less1* by reduced auxin levels. *J Plant Nutr Soil Sci*. 2023. https://doi.org/10.1002/jpln.202300155

Matthes MS, Darnell Z, Best NB, Guthrie K, Robil JM, Amstutz J, Durbak A, McSteen P. Defects in meristem maintenance, cell division, and cytokinin signaling are early responses in the boron deficient maize mutant *tassel-less1*. *Physiol Plant*. 2022:174(2):e13670. https://doi.org/10.1111/ppl.13670

Matthes MS, Robil JM, McSteen P. From element to development: the power of the essential micronutrient boron to shape morphological processes in plants. *J Exp Bot*. 2020:71(5):1681–1693. https://doi.org/10.1093/jxb/eraa042

Matthes MS, Robil JM, Tran T, Kimble A, Mcsteen P. Increased transpiration is correlated with reduced boron deficiency symptoms in the maize *tassel-less1* mutant. *Physiol Plant*. 2018:163(3):344–355. https://doi.org/10.1111/ppl.12717

Miwa K, Takano J, Fujiwara T. Improvement of seed yields under boron-limiting conditions through overexpression of BOR1, a boron transporter for xylem loading, in *Arabidopsis thaliana*. *Plant J*. 2006:46(6):1084–1091. https://doi.org/10.1111/j.1365-313X.2006.02763.x

Noguchi K, Yasumori M, Imai T, Naito S, Matsunaga T, Oda H. *bor1-1*, an *Arabidopsis thaliana* mutant that requires a high level of boron. *Plant Physiol*. 1997:115(3):901–906. https://doi.org/10.1104/pp.115.3.901

O'Neill MA, Eberhard S, Albersheim P, Darvill AG. Requirement of borate cross-linking of cell wall rhamnogalacturonan-II for Arabidopsis growth. *Science*. 2001:294(5543):846–849. https://doi.org/10.1126/science.1062319

O'Neill MA, Warrenfeltz D, Kates K, Pellerin P, Doco T, Darvill AG, Albersheim P. Rhamnogalacturonan-II, a pectic polysaccharide in the walls of growing plant cell, forms a dimer that is covalently cross-linked by a borate ester. In vitro conditions for the formation and hydrolysis of the dimer. *J Biol Chem*. 1996:271(37):22923–22930. https://doi.org/10.1074/jbc.271.37.22923

Onuh AF, Miwa K. Regulation, diversity and evolution of boron transporters in plants. *Plant Cell Physiol*. 2021:62(4):590–599. https://doi.org/10.1093/pcp/pcab025

Onuh AF, Miwa K. Mutations in type II Golgi-localized proton pyrophosphatase AVP2;1/VHP2;1 affect pectic polysaccharide rhamnogalacturonan-II and alter root growth under low boron condition in *Arabidopsis thaliana*. *Front Plant Sci*. 2023:14:1255486. https://doi.org/10.3389/fpls.2023.1255486

Pallotta M, Schnurbusch T, Hayes J, Hay A, Baumann U, Paull J, Langridge P, Sutton T. Molecular basis of adaptation to high soil boron in wheat landraces and elite cultivars. *Nature*. 2014:514(7520):88–91. https://doi.org/10.1038/nature13538

Paull JG, Rathjen AJ, Cartwright B. Major gene control of tolerance of bread wheat (*Triticum aestivum* L.) to high concentrations of soil boron. *Euphytica*. 1991:55(3):217–228. https://doi.org/10.1007/BF00021242

Peng L, Shi L, Cai H, Xu F, Zeng C. Transcriptional profiling reveals adaptive responses to boron deficiency stress in Arabidopsis. *Z Naturforsch—Sect C J Biosci*. 2012:67:510–524. https://doi.org/10.1515/znc-2012-9-1009

Piepho HP. An algorithm for a letter-based representation of all-pairwise comparisons. *J Comput Graph Stat*. 2004:13(2):456–466. https://doi.org/10.1198/1061860043515

Pommerrenig B, Faber M, Hajirezaei M-R, von Wirén N, Bienert GP. Cytokinins as boron deficiency signals to sustain shoot development in boron-efficient oilseed rape. *Physiol Plant*. 2022:174(5):e13776. https://doi.org/10.1111/ppl.13776

Pommerrenig B, Junker A, Abreu I, Bieber A, Fuge J, Willner E, Bienert MD, Altmann T, Bienert GP. Identification of rapeseed (*Brassica napus*) cultivars with a high tolerance to boron-deficient conditions. *Front Plant Sci*. 2018:9:1142. https://doi.org/10.3389/fpls.2018.01142

Poza-Viejo L, Abreu I, González-García MP, Allauca P, Bonilla I, Bolanos L, Reguera M. Boron deficiency inhibits root growth by controlling meristem activity under cytokinin regulation. *Plant Sci*. 2018:270:176–189. https://doi.org/10.1016/j.plantsci.2018.02.005

Reid RJ, Hayes JE, Post A, Stangoulis JCR, Graham RD. A critical analysis of the causes of boron toxicity in plants. *Plant Cell Environ*. 2004:27(11):1405–1414. https://doi.org/10.1111/j.1365-3040.2004.01243.x

Sakamoto T, Inui YT, Uraguchi S, Yoshizumi T, Matsunaga S, Mastui M, Umeda M, Fukui K, Fujiwara T. Condensin II alleviates DNA damage and is essential for tolerance of boron overload stress in Arabidopsis. *Plant Cell*. 2011:23(9):3533–3546. https://doi.org/10.1105/tpc.111.086314

Schaefer RJ, Michno JM, Jeffers J, Hoekenga O, Dilkes B, Baxter I, Myersc CL. Integrating coexpression networks with GWAS to prioritize causal genes in maize. *Plant Cell*. 2018:30(12):2922–2942. https://doi.org/10.1105/tpc.18.00299

Schneider CA, Rasband WS, Eliceiri KW. NIH image to ImageJ: 25 years of image analysis. *Nat Methods*. 2012:9(7):671–675. https://doi.org/10.1038/nmeth.2089

Schnurbusch T, Hayes J, Hrmova M, Baumann U, Ramesh SA, Tyerman SD, Langridge P, Sutton T. Boron toxicity tolerance in barley through reduced expression of the multifunctional aquaporin *HvNIP2;1*. *Plant Physiol*. 2010:153(4):1706–1715. https://doi.org/10.1104/pp.110.158832

Sechet J, Htwe S, Urbanowicz B, Agyeman A, Feng W, Ishikawa T, Colomes M, Kumar KS, Kawai-yamada M, Dinneny JR, *et al.*Suppression of Arabidopsis GGLT1 affects growth by reducing the L-galactose content and borate cross-linking of rhamnogalacturonan-II. *Plant J*. 2018:96(5):1036–1050. https://doi.org/10.1111/tpj.14088

Shrestha V, Yobi A, Slaten ML, Chan YO, Holden S, Gyawali A, Flint-Garcia S, Lipka AE, Angelovici R. Multiomics approach reveals a role of translational machinery in shaping maize kernel amino acid composition. *Plant Physiol*. 2022:188(1):111–133. https://doi.org/10.1093/plphys/kiab390

Slaten ML, Chan YO, Shrestha V, Lipka AE, Angelovici R. HAPPI GWAS: holistic analysis with pre- and post-integration GWAS. *Bioinformatics*. 2020:36(17):4655–4657. https://doi.org/10.1093/bioinformatics/btaa589

Sommer AL, Sorokin H. Effects of the absence of boron and of some other essential elements on the cell and tissue structure of the root tips of *Pisum sativum*. *Plant Physiol*. 1928:3(3):237–260.1. https://doi.org/10.1104/pp.3.3.237

Student. The probable error of a mean. *Biometrika*. 1908:6(1):1–25. https://doi.org/10.2307/2331554

Sutton T, Baumann U, Hayes J, Collins NC, Shi BJ, Schnurbusch T, Hay A, Mayo G, Pallotta M, Tester M, *et al.* Boron-toxicity tolerance in barley arising from efflux transporter amplification. *Science*. 2007:318(5855):1446–1449. https://doi.org/10.1126/science.1146853

Takano J, Wada M, Ludewig U, Schaaf G, von Wiren N, Fujiwara T. The Arabidopsis major intrinsic protein NIP5;1 is essential for efficient boron uptake and plant development under boron limitation. *Plant Cell*. 2006:18(6):1498–1509. https://doi.org/10.1105/tpc.106.041640

Tzin V, Fernandez-Pozo N, Richter A, Schmelz EA, Schoettner M, Schäfer M, Ahern KR, Meihls LN, Kaur H, Huffaker A, *et al.* Dynamic maize responses to aphid feeding are revealed by a time series of transcriptomic and metabolomic assays. *Plant Physiol*. 2015:169(3):1727–1743. https://doi.org/10.1104/pp.15.01039

Tzin V, Hojo Y, Strickler SR, Bartsch LJ, Archer CM, Ahern KR, Zhou S, Christensen SA, Galis I, Mueller LA, *et al.* Rapid defense responses in maize leaves induced by *Spodoptera exigua* caterpillar feeding. *J Exp Bot*. 2017:68(16):4709–4723. https://doi.org/10.1093/jxb/erx274

Uraguchi S, Kato Y, Hanaoka H, Miwa K, Fujiwara T. Generation of boron-deficiency-tolerant tomato by overexpressing an *Arabidopsis thaliana* borate transporter AtBOR1. *Front Plant Sci*. 2014:5:125. https://doi.org/10.3389/fpls.2014.00125

Verwaaijen B, Alcock TD, Spitzer C, Liu Z, Fiebig A, Bienert MD, Bräutigam A, Bienert GP. The *Brassica napus* boron deficient inflorescence transcriptome resembles a wounding and infection response. *Physiol Plant*. 2023:175(6):1–18. https://doi.org/10.1111/ppl.14088

Warington K. The effect of boric acid and borax on the broad bean and certain other plants. *Ann Bot*. 1923:37(4):629–672. https://doi.org/10.1093/oxfordjournals.aob.a089871

Wilder SL, Scott S, Waller S, Powell A, Benoit M, Guthrie JM, Schueller MJ, Awale P, McSteen P, Matthes MS, *et al.* Carbon-11 radiotracing reveals physiological and metabolic responses of maize grown under different regimes of boron treatment. *Plants*. 2022:11(3):241. https://doi.org/10.3390/plants11030241

Wimmer MA, Goldbach HE. A miniaturized curcumin method for the determination of boron in solutions and biological samples. *J Plant Nutr Soil Sci*. 1999:162(1):15–18. https://doi.org/10.1002/(SICI)1522-2624(199901)162:1<15::AID-JPLN15>3.0.CO;2-P

Wouters FC, Gershenzon J, Vassão DG. Benzoxazinoids: reactivity and modes of action of a versatile class of plant chemical defenses. *J Braz Chem Soc*. 2016:27:1379–1397. https://doi.org/10.5935/0103-5053.20160177

Wu D, Tanaka R, Li X, Ramstein GP, Cu S, Hamilton JP, Robin Buell C, Stangoulis J, Rocheford T, Gore MA. High-resolution genome-wide association study pinpoints metal transporter and chelator genes involved in the genetic control of element levels in maize grain. *G3 (Bethesda, Md.)*. 2021:11(4):jkab059. https://doi.org/10.1093/g3journal/jkab059

Xu F, Wang Y, Meng J. Mapping boron efficiency gene(s) in *Brassica napus* using RFLP and AFLP markers. *Plant Breed*. 2001:120(4):319–324. https://doi.org/10.1046/j.1439-0523.2001.00583.x

Yan J, Shah T, Warburton ML, Buckler ES, Mcmullen MD, Crouch J. Genetic characterization and linkage disequilibrium estimation of a global maize collection using SNP markers. *PLoS One*. 2009:4(12):e8451. https://doi.org/10.1371/journal.pone.0008451

Zeng C, Han Y, Shi L, Peng L, Wang Y, Xu F, Meng J. Genetic analysis of the physiological responses to low boron stress in *Arabidopsis thaliana*. *Plant Cell Environ*. 2008:31(1):112–122. https://doi.org/10.1111/j.1365-3040.2007.01745.x

Zhang C, He M, Jiang Z, Liu T, Wang C, Wang S, Xu F. Arabidopsis transcription factor STOP1 directly activates expression of *NOD26-LIKE MAJOR INTRINSIC PROTEIN5;1*, and is involved in the regulation of tolerance to low-boron stress. *J Exp*. 2024:75:2574–2583. https://doi.org/10.1093/jxb/erae038

Zhang C, He M, Wang S, Chu L, Wang C, Yang N, Ding G, Cai H, Shi L, Xu F. Boron deficiency-induced root growth inhibition is mediated by brassinosteroid signalling regulation in Arabidopsis. *Plant J*. 2021:107(2):564–578. https://doi.org/10.1111/tpj.15311

Zhang H, Wang ML, Schaefer R, Dang P, Jiang T, Chen C. GWAS and coexpression network reveal ionomic variation in cultivated peanut. *J Agric Food Chem*. 2019:67(43):12026–12036. https://doi.org/10.1021/acs.jafc.9b04939

Zhao Z, Wu L, Nian F, Ding G, Shi T, Zhang D, Shi L, Xu F, Meng J. Dissecting quantitative trait loci for boron efficiency across multiple environments in *Brassica napus*. *PLoS One*. 2012:7(9):e45215. https://doi.org/10.1371/journal.pone.0045215

4 General discussion

Boron is an essential micronutrient and therefore crucial for plant development (Warington, 1923). After a century of study, boron deficiency-induced phenotypic and physiological responses in many species have been documented, the primary function of boron in plants to crosslink cell wall rhamnogalacturonan II (RG-II) has been found, and boron transporters which contribute to boron homeostasis have been identified in many species (Marschner, 2023). However, the linkages between the phenotypes and the molecular functions of boron have not been fully revealed. Reported phenotypic responses of maize roots to boron deficiency were obscure and sometimes contradictory, and the underlying molecular mechanisms remain largely unexplored. Therefore, boron deficiency mimics, such as phenylboronic acid (PBA), have been proposed. Moreover, additional mechanisms except for boron transporters are known to contribute to boron homeostasis in maize.

This thesis reports two boron-related studies in the maize root and shoot respectively. In chapter 2, the boron deficiency-induced root defects and the usability of PBA as a boron deficiency mimic is tested. PBA reduces primary root length and lateral root density, similar to boron deficiency treatment, but more severe. The PBA-induced lateral root defects are stable, pronounced, boron-related, but are not due to RG-II dimerization defects. *In vitro*, PBA does not interfere with the boric acid-mediated RG-II crosslinking, nor crosslinks RG-II by itself. *In planta*, PBA could be oxidized and supply boric acid to form RG-II dimers.

In chapter 3, a novel boron homeostasis regulator unrelated to boron transporters is identified. The benzoxazinoid biosynthesis gene *benzoxazinless3* (*bx3*) is associated with boron homeostasis in maize ear leaves. BX3 converts indolin-2-one (ION) into 3-hydroxy-ION (HION) in the biosynthesis pathway of benzoxazinoids, a category of defense compounds in maize. Mutation of *bx3* leads to enhanced leaf tip necrosis and higher boron levels in leaves compared to the wild type plants, which are likely related to the benzoxazinoid intermediates ION and HION.

4.1 PBA induces defects of primary root development similar to boron deficiency, but more severe

Previous boron deficiency studies have mostly been focused on the primary root, where an inhibition of primary root elongation is one of the typical boron deficiency phenotypes, as reported for example in Arabidopsis (Bolanos et al., 2023; Chu et al., 2025). In this thesis, the primary root elongation defects induced by boron deficiency were marginal in maize seedlings (Chapter 2, Figs. 2), showcasing a unique response of the maize root system to boron deficiency.

This might be due to the lower abundance of RG-II and lower demand of boron in maize compared to that in dicotyledons (Matsunaga et al., 2004). Compared to the boron deficiency-induced primary root elongation defect, the 0.4 mM PBA-induced defect was more severe (Chapter 2, Figs. 2A, S2A-B). However, the PBA-induced inhibition of primary root length was not consistently detected across biological replicates (Chapter 2, Figs. 3F, S4A, S4C, S4E, S5A, S8D), suggesting additional factors affecting the effects of PBA on primary root elongation. The PBA-induced primary root inhibition had also been observed in Arabidopsis (Hays et al., 2024). In contrast, 50 μM PBA promoted the primary root growth in bean plants (Odhnoff, 1961). These findings suggest, that the effects of PBA on primary root elongation are species-specific.

The impact of boron on maize lateral root development is highlighted by both the effects of the boron deficiency treatment and the PBA treatment in this thesis. Boron deficiency is known to negatively affect lateral root formation in maize and pea (Wang et al., 2006; Housh et al., 2020; Wilder et al., 2022). In Arabidopsis, although the lateral root number decreases in boron-deficient conditions (Duran et al., 2018; Alcock et al., 2025), the lateral root density increases in most investigated accessions (Alcock et al., 2025). This inconsistency suggests there might be species-specific differences of the effects of boron deficiency on lateral root development, and a general understanding of the effects requires consistent and standardized phenotyping strategies.

Unlike the species-specific effects of boron deficiency on lateral roots, the negative effects of PBA on lateral roots are pronounced and conserved. In maize seedlings, PBA induced root lateral density defects similar to boron deficiency, and PBA induced significant reduction of lateral root primordia number (Chapter 2, Figs.1-2, S2). Consistently, PBA reduces lateral root density in Arabidopsis and bean (Odhnoff, 1961; Hays et al., 2024).

The initiation of maize lateral roots is tightly modulated by auxin (Dresselhaus et al., 2025). Indeed, auxin levels were reduced in maize roots under both boron deficiency and PBA treatments (Chapter 2, Figs. 3, 5). However, application of auxin did not rescue the lateral root defects induced by boron deficiency or PBA treatment, nor inhibition of auxin biosynthesis enhanced those lateral root defects (Chapter 2, Figs. 3, 6, S4-5, S8), suggesting that the auxin level reduction is not causal for the observed lateral root defects. Moreover, while boron deficiency negatively affects lateral root development in Arabidopsis (Duran et al., 2018; Alcock et al., 2025), auxin levels or signaling are up-regulated in Arabidopsis roots under boron deficiency (Martin-Rejano et al., 2011; Li et al., 2015; Camacho-Cristobal et al., 2015; Herrera-

Rodriguez et al., 2022; Tao et al., 2023). The boron deficiency-induced root responses and their correlation to the auxin cascade, therefore, seem to be species-specific.

To explore the mechanisms how PBA affects root development in maize, a GWAS was conducted (Chapter 2, Fig. 7). GWAS results using lateral root density ratios between PBA treatment and water control identified two *Lateral Organ Boundaries Domain* (*LBD*) genes and some auxin-related genes including *Auxin Response Factors* (*ARFs*; Chapter 2, Table S4). One of the detected *LBD* genes (Chapter 2, Table S4), *ROOTLESS CONCERNING CROWN AND SEMINAL ROOTS1* (*RTCS1*; *ZmLBD2*), regulates crown and seminal roots development under the control of ARF (Majer and Hochholdinger, 2011; Xu et al., 2015). *ZmLBD17* is boron toxicity-responsive in maize roots (Chen et al., 2022). Oilseed rape *LBD41* is boron deficiency-responsive, and associated with boron efficiency-related traits (Hua et al., 2017; Zhang et al., 2024). These findings suggest that boron might interfere with lateral root development through the auxin-LBD-mediated regulation (Du and Scheres, 2018; Orosa-Puente et al., 2018; Soyano et al., 2019), which will be interesting to test in the future by characterization of mutants of such candidate genes.

4.2 PBA is at least partially intact *in planta*

The usability of PBA as a boron deficiency mimic in plants is challenged by the oxidative instability of PBA. At the presence of H_2O_2, PBA can be oxidized to phenol and boric acid (Graham et al., 2021). The presence of RG-II dimers following PBA-treatment supports that PBA might be deboronated and does not induce boron deficiency *in planta* (Chapter 2, Fig. 4; Hays et al., 2024). On the other hand, many evidence suggests that PBA is still intact in organisms, at least partially.

Theoretically, H_2O_2 deboronates PBA in a 1:1 ratio *in vitro* (Graham et al., 2021). The amount of phenotypically effective PBA, therefore, should at least excess the amount of H_2O_2 *in planta*. However, the normal range of H_2O_2 in plants is considered at the range of 0.1 - 0.5 mM (Sharova et al., 2024), whereas 50 µM PBA significantly inhibits Arabidopsis primary roots (Hays et al., 2024), and 0.1 mM PBA significantly inhibits Arabidopsis hypocotyl bending (Jewaria et al., 2025). In addition, the PBA deboronation rate decreases with decreasing pH (Saxon and Peng, 2022). Meanwhile, there's an inducing effect of PBA on H_2O_2 accumulation, which should not occur if PBA simply quenches H_2O_2 (Chapter 2, Fig. 5). Moreover, the PBA-induced lateral root density defects were specific to the boric acid moiety in maize (Chapter 2; Figs. 6, S6B). In Arabidopsis, PBA inhibits the boric acid-induced BOR1 degradation (Matthes and Torres-Ruiz, 2016), and induces a root curvature phenotype (Hays et al., 2024). Such

effects have not been observed under boric acid or phenol treatments (Chapter 2, Figs. 6, S6; Xu et al., 2012; Landi et al., 2019), suggesting that the observed PBA-induced defects in plants are cause by unoxidized PBA.

Collectively, these findings suggest that the interaction between PBA and H_2O_2 *in planta* is not as simple as the redox reaction *in vitro*. Moreover, the reactive oxygen species (ROS) processes are stimulated by PBA, likely in a tissue-specific manner (Chapter 2, Fig. 7). The inducing effect of PBA on H_2O_2 accumulation is interesting, considering PBA and phenol are both reductive chemicals. In tomato leaves, PBA treatment increases the activities of four ROS scavenging enzymes with peroxidase included (Mathan, 1965; 1967), which might be a feedback result of PBA-induced H_2O_2 accumulation. Moreover, the effects of PBA on peroxidase seem to be specific. The horseradish peroxidase can interact with PBA (Liu et al., 2005), and PBA affinity separation isolated a peroxidase from Arabidopsis roots (Wimmer et al., 2009). These findings suggest direct molecular interactions between PBA and peroxidases, likely through the glycosyl group on peroxidases. Interestingly, in this thesis, from the lateral root density ratio GWAS, two closely linked peroxidase genes, maize *peroxidase50* (Zm00001eb226360) and maize *peroxidase56* (Zm00001eb226340) were identified (Chapter 2, Table S4; Wang et al., 2015). The *peroxidase50* gene is expressed preferentially in the root tips and is stress-responsive (Stelpflug et al., 2016; Hoopes et al., 2019).

4.3 The PBA-induced root defects are not caused by defective RG-II dimerization

One surprising finding made in this thesis is that PBA does not promote nor inhibit RG-II *in vitro* (Chapter 2; Fig. 4, Table S2). The maize RG-II analysis suggests that PBA does not integrate into pectin *in vivo* (Chapter 2; Fig. 4). In parallel, RG-II dimers were also detected in a rosa cell culture system treated with PBA and without boric acid, and the benzene ring did not present in the RG-II isolated from that cell culture (Sharma and Urbanowicz, personal communication). Therefore, PBA, although with a pKa lower than that of boric acid, does not have advantage over boric acid on the RG-II binding affinity. The results from this thesis does not support the hypothesis that PBA interferes with RG-II dimerization (Bassil et al., 2004; Hays et al., 2024). In this thesis, the typical RG-II peaks in chromatograms, however, could not be defined or quantified from the maize root samples (Chapter 2; Fig.4A). The highly esterified or branched components of maize root cell walls might hinder the release of RG-II by enzymes (Kozlova et al., 2020). Therefore, optimization of the RG-II purification is required. In order to eliminate the interference of boric acid derived by PBA oxidation, it would be worthwhile to conduct the *in vivo* RG-II analysis with oxidatively stable PBA species, such as 2-

carboxyphenylboronic acid (Grahams et al., 2021).

4.4 *Bx3* is a novel boron homeostasis regulator in maize

Previous studies have indicated that boron homeostasis is not solely regulated by boron transporters, however, the knowledge of transporter-independent mechanisms remains elusive and fragmentary (de Abreu Neto et al., 2017; Huai et al., 2018; Matthes et al., 2018; Hiroguchi et al., 2021; Jia et al., 2021; Wu et al., 2021; Onuh and Miwa, 2023). In maize, the GWAS of ear leaf boron levels did not identify any boron transporter genes among the significant loci (Chapter 3, Table 1). Instead, an association was found between boron homeostasis and the benzoxazinoid biosynthesis pathway. Benzoxazinoids are defense compounds that have never been reported to associate with boron-related processes. In addition to the benzoxazinoid-related genes detected on chromosome 4, there were several other non-boron transporter genes located in the additional significantly associated locus on chromosome 7 (Chapter 3, Table 1). Among them, a gibberellin receptor gene appears particularly noteworthy. Gibberellin levels have been reported to change in response to boron deficiency (Eggert and von Wirén, 2017; Su et al., 2019; Guo et al., 2025b). Gibberellins can induce the expression of the Arabidopsis vacuole boron channel gene *Tonoplast Intrinsic Protein 5;1* and alleviate boron toxicity (Pang et al., 2010; 2017). Gibberellin receptor genes have been identified to be induced by boron deficiency in poplar, associated with boron toxicity tolerance in rice, and grain-ionome-associated in maize (de Abreu Neto et al., 2017; Schaefer et al., 2018; Su et al., 2019). These findings highlight the importance of phytohormones for boron deficiency and toxicity responses Whether the gibberellin signaling is associated with boron homeostasis in maize remains to be validated.

4.5 The boron-benzoxazinoid biosynthesis association is likely mediated by the biosynthesis intermediates

The functional diversity of benzoxazinoids have been actively researched and expanded in recent years (Li et al., 2025). In the aspects of mineral elements, benzoxazinoids chelate iron, aluminum, molybdenum and arsenic, and modify the speciation and bioavailability of these elements (Poschenrieder et al., 2005; Hu et al., 2018a, b; Zhao et al., 2019; Hu et al., 2021; Caggìa et al., 2024). Notably, most of such studies are focused on the benzoxazinoids in the soil or rhizosphere, which are predominately 2,4-dihydroxy-7-methoxy-1,4-benzoxazin-3-one (DIMBOA) and DIMBOA-glucoside, together with the DIMBOA degradation product 6-methoxybenzoxazolin-2-one (Hu et al., 2018a). For example, DIMBOA forms Fe(III)$(DIMBOA)_2$ and Fe(III)$(DIMBOA)_3$ at the surface of maize roots, and promotes the iron

content in the maize xylem (Hu et al., 2018a). In this thesis, the association between boron and the benzoxazinoid biosynthesis pathway is likely mediated by upstream biosynthesis intermediates. Among the tested *benzoxazinless* (*bx*) mutants *bx1*, *bx2* and *bx3*, the correlation to boron homeostasis is specific to *bx3* (Chapter 3, Fig. 4). The *bx3* gene encodes an enzyme required to convert ION into HION. Therefore, the mutation of *bx3* leads to the accumulation of ION and a lack of HION (Chapter 3, Fig. 3.1). *bx3* mutants had elevated boron levels and necrosis in leaves compared to the wildtype (Chapter 3, Fig. 2). Moreover, overexpression of *BX1*and *BX2* in Arabidopsis, a species lacking the benzoxazinoid pathway, resulted in accumulation of ION (Abramov et al., 2021). Interestingly, the *BX1*and *BX2* overexpression Arabidopsis showed elevated boron levels and leaf necrosis phenotypes similar to *bx3*, suggesting boron homeostasis might be related to these intermediates (Chapter 3, Figs. 2, 5). Furthermore, the *in vitro* complexation between boric acid and HION, although unstable and unconfirmed *in vivo*, raises the question whether such interactions might influence the mobility or bioavailability of boron, similar to the DIMBOA-iron interaction (Chapter 3, Figs.6, S8; Hu et al., 2018a). These findings highlight the importance of not only the end products, but also the diverse activities of intermediates in the benzoxazinoid biosynthesis pathway.

4.6 Potential of the benzoxazinoid pathway in boron deficiency adaptation

Several observations suggest that manipulating the benzoxazinoid biosynthesis pathway might help to improve maize adaptation to boron deficiency, which is important as boron deficiency is a worldwide problem reducing the yield of maize (Shorrocks, 1997; Lordkaew et al., 2011; Brdar-Jokanović, 2020). The *bx3* gene expression was upregulated in the boron transporter mutant *tassel-less1* (Chapter 3, Table2). The *bx3* mutant seedlings displayed leaf tip necrosis resembling a typical boron toxicity symptom, and the severity was intensified with increasing boron levels (Chapter 3, Figs 2-3). Further phenotypic analysis in different growth conditions demonstrated the specific correlation between benzoxazinoid biosynthesis and boron homeostasis, but also suggested that the relationships between boron levels, benzoxazinoid biosynthesis, and plant phenotypes are complex, may also depend on developmental stages and environmental conditions. In a low-boron field, the elevated boron in *bx3* seemed to be not toxic to the mature plants, and might even benefit the reproductive development in specific aspects (Chapter 3, Fig.1; Table S5). Moreover, the elevated leaf boron levels in the Arabidopsis *BX1*and *BX2* overexpression lines indicate this potential is possible to be transferred to species without the benzoxazinoid pathway (Chapter 3, Fig. 5).

The *bx3* gene also provides a new nexus connecting boron and plant defense. Previous studies

had suggested some indirect connections between boron homeostasis and defense: herbivore attack reduces boron concentrations in birch leaves, and the defense metabolic responses are weakened under boron deficiency (Ruuhola et al., 2011). Boron-deficient citrus leaves are more attractive to herbivores due to altered volatiles (Dong et al., 2023). Boron deficiency induces infection-like transcriptomic responses in oilseed rape (Verwaaijen et al., 2023). From these reports no genetic mechanism is demonstrated. Nevertheless, given the knowledge that the benzoxazinoid biosynthesis pathway is responsive to diverse additional environmental stimuli (Guo et al., 2025a), these correlations raise the possibility that the benzoxazinoid pathway could serve as a regulatory hub for systemically coordinating maize performance under multiple environmental stresses, and connecting boron homeostasis to even broader stress adaptation.

5 References

Aibara, I., Hirai, T., Kasai, K., Takano, J., Onouchi, H., Naito, S., Fujiwara, T., and Miwa, K. (2018). Boron-dependent translational suppression of the borate exporter BOR1 contributes to the avoidance of boron toxicity. Plant Physiol. **177**:759–774.

Alcock, T. D., Bienert, M. D., Junker, A., Meyer, R. C., Tschiersch, H., Kudamala, S., von Wirén, N., Altmann, T., and Bienert, G. P. (2025). *Arabidopsis thaliana* exhibits wide within-species variation in tolerance to boron limitation and root and shoot trait resilience associate with a pleiotropic locus. New Phytol. **doi:** 10.1111/nph.70570.

Aquea, F., Federici, F., Moscoso, C., Vega, A., Jullian, P., Haseloff, J., and Arce-Johnson, P. (2012). A molecular framework for the inhibition of Arabidopsis root growth in response to boron toxicity. Plant Cell Environ. **35**:719–734.

Asad, A., Bell, R. W., Dell, B., and Huang, L. (1997). Development of a boron buffered solution culture system for controlled studies of plant boron nutrition. Plant Soil **188**:21–32.

Barnes, W. J., Koj, S., Black, I. M., Archer-Hartmann, S. A., Azadi, P., Urbanowicz, B. R., Peña, M. J., and O'Neill, M. A. (2021). Protocols for isolating and characterizing polysaccharides from plant cell walls: a case study using rhamnogalacturonan-II. Biotechnol. Biofuels Bioprod. **14**:142.

Bar-Peled, M., Urbanowicz, B. R., and O'Neill, M. A. (2012). The synthesis and origin of the pectic polysaccharide rhamnogalacturonan II – insights from nucleotide sugar formation and diversity. Front. Plant Sci. **3**:92.

Bassil, E., Hu, H., and Brown, P. H. (2004). Use of phenylboronic acids to investigate boron function in plants. Possible role of boron in transvacuolar cytoplasmic strands and cell-to-wall adhesion. Plant Physiol. **136**:3383–3395.

Begum, R. A., and Fry, S. C. (2023). Arabinogalactan-proteins as boron-acting enzymes, cross-linking the rhamnogalacturonan-II domains of pectin. Plants **12**(23):3921

Bharadwaj, V. S., Crowley, M. F., Peña, M. J., Urbanowicz, B., and O'Neill, M. (2020). Mechanism and reaction energy landscape for apiose cross-linking by boric acid in rhamnogalacturonan II. J. Phys. Chem. B **124**:10117–10125.

Bienert, M. D., Junker, A., Melzer, M., Altmann, T., von Wirén, N., and Bienert, G. P. (2023). Boron deficiency responses in maize (*Zea mays* L.) roots. J. Plant Nutr. Soil Sci. Advance online publication (09.11.2023) **doi**: 10.1002/jpln.202300173.

Bolaños, L., Abreu, I., Bonilla, I., Camacho-Cristobal, J. J., and Reguera, M. (2023). What can boron deficiency symptoms tell us about its function and regulation? Plants **12**:777.

Brdar-Jokanović, M. (2020). Boron toxicity and deficiency in agricultural plants. Int. J. Mol. Sci. **21**:1424.

Caggìa, V., Wälchli, J., Deslandes-Hérold, G., Mateo, P., Robert, C. A. M., Guan, H., Bigalke, M., Spielvogel, S., Mestrot, A., Schlaeppi, K., et al. (2024). Root-exuded specialized metabolites reduce arsenic toxicity in maize. Proc. Natl. Acad. Sci. U.S.A. **121**:e2314261121.

Camacho-Cristóbal, J. J., Rexach, J., and González-Fontes, A. (2008). Boron in plants: Deficiency and toxicity. J. Integr. Plant Biol. **50**:1247–1255.

Camacho-Cristobal, J. J., Martin-Rejano, E. M., Herrera-Rodriguez, M. B., Navarro-Gochicoa,

M. T., Rexach, J., and Gonzalez-Fontes, A. (2015). Boron deficiency inhibits root cell elongation via an ethylene/auxin/ROS-dependent pathway in Arabidopsis seedlings. J. Exp. Bot. **66**:3831–40.

Chatterjee, M., Tabi, Z., Galli, M., Malcomber, S., Buck, A., Muszynski, M., and Gallavotti, A. (2014). The boron efflux transporter ROTTEN EAR is required for maize inflorescence development and fertility. Plant Cell **26**:2962–2977.

Chatterjee, M., Liu, Q., Menello, C., Galli, M., and Gallavotti, A. (2017). The combined action of duplicated boron transporters is required for maize growth in boron-deficient conditions. Genetics **206**:2041–2051.

Chen, H., Zhang, Q., He, M., Wang, S., Shi, L., and Xu, F. (2018). Molecular characterization of the genome-wide BOR transporter gene family and genetic analysis of *BnaC04.BOR1;1c* in *Brassica napus*. BMC Plant Biology **18**:193.

Chen, X., Smith, S. M., Shabala, S., and Yu, M. (2023). Phytohormones in plant responses to boron deficiency and toxicity. J. Exp. Bot. **74**:743–754.

Choi, E.-Y., Kolesik, P., Mcneill, A., Collins, H., Zhang, Q., Huynh, B.-L., Graham, R., and Stangoulis, J. (2007). The mechanism of boron tolerance for maintenance of root growth in barley (*Hordeum vulgare* L.). Plant Cell Environ. **30**:984–993.

Chormova, D., Messenger, D. J., and Fry, S. C. (2014). Boron bridging of rhamnogalacturonan-II, monitored by gel electrophoresis, occurs during polysaccharide synthesis and secretion but not post-secretion. Plant J. **77**:534–546.

Chu, L., Shrestha, V., Schäfer, C. C., Niedens, J., Meyer, G. W., Darnell, Z., Kling, T., Dürr-Mayer, T., Abramov, A., Frey, M., et al. (2025a). Association of the benzoxazinoid pathway with boron homeostasis in maize. Plant Physiol. **197**:kiae611.

Chu, L., Schäfer, C. C., and Matthes, M. S. (2025b). Molecular mechanisms affected by boron deficiency in root and shoot meristems of plants. J. Exp. Bot. **76**:1866–1878.

Cotton, T. E. A., Pétriacq, P., Cameron, D. D., Meselmani, M. A., Schwarzenbacher, R., Rolfe, S. A., and Ton, J. (2019). Metabolic regulation of the maize rhizobiome by benzoxazinoids. ISME J **13**:1647–1658.

de Abreu Neto, J. B., Hurtado-Perez, M. C., Wimmer, M. A., and Frei, M. (2017). Genetic factors underlying boron toxicity tolerance in rice: genome-wide association study and transcriptomic analysis. J. Exp. Bot. **68**:687–700.

Dell, B., and Huang, L. (1997). Physiological response of plants to low boron. Plant Soil **193**:103–120.

Dong, Z., Liu, X., Srivastava, A. K., Tan, Q., Low, W., Yan, X., Wu, S., Sun, X., and Hu, C. (2023). Boron deficiency mediates plant–insect (*Diaphorima citri*) interaction by disturbing leaf volatile organic compounds and cell wall functions. Tree Physiol. **43**:597–610.

Dordas, C., Chrispeels, M. J., and Brown, P. H. (2000). Permeability and channel-mediated transport of boric acid across membrane vesicles isolated from squash roots. Plant Physiol. **124**:1349–1362.

Dresselhaus, T., Balboni, M., Berg, L., Dolata, A., Hochholdinger, F., Huang, Y., Jiang, G., von Korff, M., Ku, J.-C., van der Linde, K., et al. (2025). How meristems shape plant architecture in cereals—Cereal Stem Cell Systems (CSCS) Consortium. Plant Cell **37**:koaf150.

Du, Y., and Scheres, B. (2018). Lateral root formation and the multiple roles of auxin. J. Exp. Bot.

69:155–167.

Duran, C., Arce-Johnson, P., and Aquea, F. (2018). Methylboronic acid fertilization alleviates boron deficiency symptoms in *Arabidopsis thaliana*. Planta **248**:221–229.

Durbak, A. R., Phillips, K. A., Pike, S., O'Neill, M., Mares, J., Gallavotti, A., Malcomber, S. T., Gassmann, W., and McSteen, P. (2014). Transport of boron by the *tassel-less1* aquaporin is critical for vegetative and reproductive development in maize. Plant Cell **26**:2978–2995.

Eggert, K., and von Wirén, N. (2017). Response of the plant hormone network to boron deficiency. New Phytol. **216**:868–881.

Eltinge, E. T. (1936). Effect of boron deficiency upon the structure of *Zea mays*. Plant Physiol. **11**:765–778.

Esim, N., Tiryaki, D., Karadagoglu, O., and Atici, O. (2013). Toxic effects of boron on growth and antioxidant system parameters of maize (*Zea mays* L.) roots. Toxicol. Ind. Health **29**:800–805.

Eticha, D., Stass, A., and Horst, W. J. (2005). Cell-wall pectin and its degree of methylation in the maize root-apex: significance for genotypic differences in aluminium resistance. Plant Cell Environ. **28**:1410–1420.

Fang, K., Gao, S., Zhang, W., Xing, Y., Cao, Q., and Qin, L. (2016). Addition of phenylboronic acid to *Malus domestica* pollen tubes alters calcium dynamics, disrupts actin filaments and affects cell wall architecture. PLoS ONE **11**:e0149232.

Fleischer, A., O'Neill, M. A., and Ehwald, R. (1999). The pore size of non-graminaceous plant cell walls is rapidly decreased by borate ester cross-linking of the pectic polysaccharide rhamnogalacturonan II. Plant Physiol. **121**:829–838.

Frey, M., Schullehner, K., Dick, R., Fiesselmann, A., and Gierl, A. (2009). Benzoxazinoid biosynthesis, a model for evolution of secondary metabolic pathways in plants. Phytochemistry **70**:1645–1651.

García-Sánchez, F., Simón-Grao, S., Martínez-Nicolás, J. J., Alfosea-Simón, M., Liu, C., Chatzissavvidis, C., Pérez-Pérez, J. G., and Cámara-Zapata, J. M. (2020). Multiple stresses occurring with boron toxicity and deficiency in plants. J. Harzard. Mater. **397**:122713.

Garg, O. K., Sharma, A. N., and Kona, G. R. S. S. (1979). Effect of boron on the pollen vitality and yield of rice plants (*Oryza Sativa* L. var. Jaya). Plant Soil **52**:591–594.

Gfeller, V., Thoenen, L., and Erb, M. (2024). Root-exuded benzoxazinoids can alleviate negative plant-soil feedbacks. New Phytol. **241**:2575–2588.

Goldberg, S. (1997). Reactions of boron with soils. Plant Soil **193**:35–48.

Gomez-Soto, D., Galvan, S., Rosales, E., Bienert, P., Abreu, I., Bonilla, I., Bolanos, L., and Reguera, M. (2019). Insights into the role of phytohormones regulating *pAtNIP5;1* activity and boron transport in *Arabidopsis thaliana*. Plant Sci. **287**:110198.

González-Fontes, A., Rexach, J., Quiles-Pando, C., Herrera-Rodríguez, M. B., Camacho-Cristóbal, J. J., and Navarro-Gochicoa, M. T. (2013). Transcription factors as potential participants in the signal transduction pathway of boron deficiency. Plant Signal. Behav. **8**:e26114.

Graham, B. J., Windsor, I. W., Gold, B., and Raines, R. T. (2021). Boronic acid with high oxidative stability and utility in biological contexts. Proc. Natl. Acad. Sci. U.S.A. **118**:e2013691118.

Guo, D., Liu, Z., Raaijmakers, J. M., Xu, Y., Yang, J., Erb, M., Zhang, J., Zhu, Y.-G., Xu, J., and Hu, L. (2025a). Linalool-triggered plant-soil feedback drives defense adaptation in dense maize plantings. Science **389**:eadv6675.

Guo, X., Zhang, H., Duan, C., Yue, M., Zhao, Y., Wu, F., Zhang, P., Wen, P., Wu, M., and Xu, J. (2025b). Integrative physiological, metabolomic, and transcriptomic insights into strawberry adaptation to boron deficiency stress. Plant Physiol. Biochem. **229**:PtC110599.

Hanaoka, H., Uraguchi, S., Takano, J., Tanaka, M., and Fujiwara, T. (2014). OsNIP3;1, a rice boric acid channel, regulates boron distribution and is essential for growth under boron-deficient conditions. Plant J. **78**:890–902.

Hays, Q., Ropitaux, M., Gügi, B., Vallois, A., Baron, A., Vauzeilles, B., Lerouge, P., Anderson, C. T., and Lehner, A. (2024). Phenylboronic acid interacts with pectic rhamnogalacturonan-II and displays anti-auxinic effects during *Arabidopsis thaliana* root growth and development. J. Exp. Bot. Advance online publication (26.07.2024) **doi**:10.1093/jxb/erae315.

Hays, Q., Lerouge, P., Ropitaux, M., Anderson, C. T., and Lehner, A. (2025). Storming the barricades of rhamnogalacturonan-II synthesis and function. Plant Cell **37**:koaf088.

He, M., Wang, S., Zhang, C., Liu, L., Zhang, J., Qiu, S., Wang, H., Yang, G., Xue, S., Shi, L., et al. (2021). Genetic variation of *BnaA3.NIP5;1* expressing in the lateral root cap contributes to boron deficiency tolerance in *Brassica napus*. PLoS Genet. **17**:e1009661.

Herrera-Rodriguez, M. B., Camacho-Cristobal, J. J., Barrero-Rodriguez, R., Rexach, J., Navarro-Gochicoa, M. T., and Gonzalez-Fontes, A. (2022). Crosstalk of cytokinin with ethylene and auxin for cell elongation inhibition and boron transport in Arabidopsis primary root under boron deficiency. Plants **11**:2344.

Hiroguchi, A., Sakamoto, S., Mitsuda, N., and Miwa, K. (2021). Golgi-localized membrane protein AtTMN1/EMP12 functions in the deposition of rhamnogalacturonan II and I for cell growth in Arabidopsis. J. Exp. Bot. **72**:3611–3629.

Hoopes, G. M., Hamilton, J. P., Wood, J. C., Esteban, E., Pasha, A., Vaillancourt, B., Provart, N. J., and Buell, C. R. (2019). An updated gene atlas for maize reveals organ-specific and stress-induced genes. Plant J. **97**:1154–1167.

Housh, A. B., Matthes, M. S., Gerheart, A., Wilder, S. L., Kil, K.-E., Schueller, M., Guthrie, J. M., McSteen, P., and Ferrieri, R. (2020). Assessment of a ^{18}F-phenylboronic acid radiotracer for imaging boron in maize. Int. J. Biol. Macromol. **21**:976.

Hu, H., Brown, P. H., and Labavitch, J. M. (1996). Species variability in boron requirement is correlated with cell wall pectin. J. Exp. Bot. **47**:227–232.

Hu, L., Robert, C. A. M., Cadot, S., Zhang, X., Ye, M., Li, B., Manzo, D., Chervet, N., Steinger, T., van der Heijden, M. G. A., et al. (2018a). Root exudate metabolites drive plant-soil feedbacks on growth and defense by shaping the rhizosphere microbiota. Nat. Commun. **9**:2738.

Hu, L., Mateo, P., Ye, M., Zhang, X., Berset, J. D., Handrick, V., Radisch, D., Grabe, V., Köllner, T. G., Gershenzon, J., et al. (2018b). Plant iron acquisition strategy exploited by an insect herbivore. Science **361**:694–697.

Hu, L., Wu, Z., Robert, C. A. M., Ouyang, X., Züst, T., Mestrot, A., Xu, J., and Erb, M. (2021). Soil chemistry determines whether defensive plant secondary metabolites promote or suppress herbivore growth. Proc. Natl. Acad. Sci. U.S.A. **118**:e2109602118.

Hua, Y., Zhang, D., Zhou, T., He, M., Ding, G., Shi, L., and Xu, F. (2016). Transcriptomics-assisted

quantitative trait locus fine mapping for the rapid identification of a nodulin 26-like intrinsic protein gene regulating boron efficiency in allotetraploid rapeseed. Plant Cell Environ. **39**:1601–1618.

Hua, Y., Feng, Y., Zhou, T., and Xu, F. (2017). Genome-scale mRNA transcriptomic insights into the responses of oilseed rape (*Brassica napus* L.) to varying boron availabilities. Plant Soil **416**:205–225.

Huai, Z., Peng, L., Wang, S., Zhao, H., Shi, L., and Xu, F. (2018). Identification and characterization of an *Arabidopsis thaliana* mutant *lbt* with high tolerance to boron deficiency. Front. Plant Sci. **9**:736.

Huang, S., Konishi, N., Yamaji, N., Shao, J. F., Mitani-Ueno, N., and Ma, J. F. (2022). Boron uptake in rice is regulated post-translationally via a clathrin-independent pathway. Plant Physiol. **188**:1649–1664.

Ishii, T., and Matsunaga, T. (2001). Pectic polysaccharide rhamnogalacturonan II is covalently linked to homogalacturonan. Phytochem. **57**:969–974.

Ishii, T., and Ono, H. (1999). NMR spectroscopic analysis of the borate diol esters of methyl apiofuranosides. Carbohydr. Res. **321**:257–260.

Jewaria, P. K., Aryal, B., Begum, R. A., Wang, Y., Sancho-Andrés, G., Baba, A. I., Yu, M., Li, X., Lin, J., Fry, S. C., et al. (2025). Reduced RG-II pectin dimerization disrupts differential growth by attenuating hormonal regulation. Sci. Adv. **11**:eads0760.

Jia, Z., Bienert, M. D., von Wirén, N., and Bienert, G. P. (2021). Genome-wide association mapping identifies *HvNIP2;2/HvLsi6* accounting for efficient boron transport in barley. Physiol. Plant. **171**:809–822.

Jiang, S., Escobedo, J. O., Kim, K. K., Alptürk, O., Samoei, G. K., Fakayode, S. O., Warner, I. M., Rusin, O., and Strongin, R. M. (2006). Stereochemical and regiochemical trends in the selective detection of saccharides. J. Am. Chem. Soc. **128**:12221–12228.

Jonczyk, R., Schmidt, H., Osterrieder, A., Fiesselmann, A., Schullehner, K., Haslbeck, M., Sicker, D., Hofmann, D., Yalpani, N., Simmons, C., et al. (2008). Elucidation of the final reactions of DIMBOA-glucoside biosynthesis in maize: Characterization of Bx6 and Bx7. Plant Physiol. **146**:1053–1063.

Jothi, M., and Takano, J. (2023). Understanding the regulatory mechanisms of B transport to develop crop plants with B efficiency and excess B tolerance. Plant Soil **487**:1–20.

Kakegawa, K., Ishii, T., and Matsunaga, T. (2005). Effects of boron deficiency in cell suspension cultures of *Populus alba* L. Plant Cell Rep. **23**:573–578.

Kakei, Y., Yamazaki, C., Suzuki, M., Nakamura, A., Sato, A., Ishida, Y., Kikuchi, R., Higashi, S., Kokudo, Y., Ishii, T., et al. (2015). Small-molecule auxin inhibitors that target YUCCA are powerful tools for studying auxin function. Plant J. **84**:827–837.

Kasai, K., Takano, J., Miwa, K., Toyoda, A., and Fujiwara, T. (2011). High boron-induced ubiquitination regulates vacuolar sorting of the BOR1 borate transporter in *Arabidopsis thaliana*. J. Biol. Chem. **286**:6175–6183.

Kobayashi, M., Matoh, T., and Azuma, Ji. (1996). Two chains of rhamnogalacturonan II are cross-linked byborate-diol ester bonds in higher plant cell walls. Plant Physiol. **110**:1017–1020.

Kozlova, L. V., Nazipova, A. R., Gorshkov, O. V., Petrova, A. A., and Gorshkova, T. A. (2020).

Elongating maize root: zone-specific combinations of polysaccharides from type I and type II primary cell walls. Sci. Rep. **10**:10956.

Kunin, R., and Preuss, A. F. (1964). Characterization of a boron-specific ion exchange resin. I&EC Prod. Res. Dev. **3**:304–306.

Landi, M., Margaritopoulou, T., Papadakis, I. E., and Araniti, F. (2019). Boron toxicity in higher plants: an update. Planta **250**:1011–1032.

Leonard, A., Holloway, B., Guo, M., Rupe, M., Yu, G., Beatty, M., Zastrow-Hayes, G., Meeley, R., Llaca, V., Butler, K., et al. (2014). *tassel-less1* encodes a boron channel protein required for inflorescence development in maize. Plant Cell Physiol. **55**:1044–1054.

Li, K., Kamiya, T., and Fujiwara, T. (2015). Differential roles of PIN1 and PIN2 in root meristem maintenance under low-B conditions in *Arabidopsis thaliana*. Plant Cell Physiol. **56**:1205–14.

Li, S., Yan, L., Venuste, M., Xu, F., Shi, L., White, P. J., Wang, X., and Ding, G. (2023). A critical review of plant adaptation to environmental boron stress: Uptake, utilization, and interplay with other abiotic and biotic factors. Chemosphere **338**:139474.

Lindsay, P., Swentowsky, K. W., and Jackson, D. (2024). Cultivating potential: Harnessing plant stem cells for agricultural crop improvement. Mol. Plant **17**:50–74.

Liu, S., Wollenberger, U., Halámek, J., Leupold, E., Stöcklein, W., Warsinke, A., and Scheller, F. W. (2005). Affinity interactions between phenylboronic acid-carrying self-assembled monolayers and flavin adenine dinucleotide or horseradish peroxidase. Chem. Eur. J. **11**:4239–4246.

Liu, K., Liu, L.-L., Ren, Y.-L., Wang, Z.-Q., Zhou, K.-N., Liu, X., Wang, D., Zheng, M., Cheng, Z.-J., Lin, Q.-B., et al. (2015). *Dwarf and tiller-enhancing 1* regulates growth and development by influencing boron uptake in boron limited conditions in rice. Plant Sci. **236**:18–28.

Lordkaew, S., Dell, B., Jamjod, S., and Rerkasem, B. (2011). Boron deficiency in maize. Plant Soil **342**:207–220.

Macho-Rivero, M. Á., Camacho-Cristóbal, J. J., Herrera-Rodríguez, M. B., Müller, M., Munné-Bosch, S., and González-Fontes, A. (2017). Abscisic acid and transpiration rate are involved in the response to boron toxicity in Arabidopsis plants. Physiol. Plant. **160**:21–32.

Macho-Rivero, M. A., Herrera-Rodríguez, M. B., Brejcha, R., Schäffner, A. R., Tanaka, N., Fujiwara, T., González-Fontes, A., and Camacho-Cristóbal, J. J. (2018). Boron toxicity reduces water transport from root to shoot in Arabidopsis plants. Evidence for a reduced transpiration rate and expression of major PIP aquaporin genes. Plant Cell Physiol. **59**:841–849.

Majer, C., and Hochholdinger, F. (2011). Defining the boundaries: structure and function of LOB domain proteins. Trends Plant Sci. **16**:47–52.

Marfà, V., Gollin, D. J., Eberhard, S., Mohnen, D., Dan/ill, A., and Albersheim, P. (1991). Oligogalacturonides are able to induce flowers to form on tobacco explants. Plant J. **1**:217–225.

Markham, J. E., Lynch, D. V., Napier, J. A., Dunn, T. M., and Cahoon, E. B. (2013). Plant sphingolipids: function follows form. Curr. Opin. Plant Biol. **16**:350–357.

Marschner, H. (2023). *Marschner's Mineral Nutrition of Plants*. 4th ed. Amsterdam: Elsevier.

Martínez-Alvarez, V., González-Ortega, M. J., Martin-Gorriz, B., Soto-García, M., and Maestre-Valero, J. F. (2017). The use of desalinated seawater for crop irrigation in the Segura River

Basin (south-eastern Spain). Desalination **422**:153–164.

Martínez-Mazón, P., Bahamonde, C., Herrera-Rodríguez, M. B., Fernández-Ocaña, A. M., Rexach, J., González-Fontes, A., and Camacho-Cristóbal, J. J. (2023). Role of ABA in the adaptive response of Arabidopsis plants to long-term boron toxicity treatment. Plant Physiol. Bioch. **202**:107965.

Martin-Rejano, E. M., Camacho-Cristobal, J. J., Herrera-Rodriguez, M. B., Rexach, J., Navarro-Gochicoa, M. T., and Gonzalez-Fontes, A. (2011). Auxin and ethylene are involved in the responses of root system architecture to low boron supply in Arabidopsis seedlings. Physiol. Plant. **142**:170–8.

Mathan, D. S. (1965). Phenylboric acid, a chemical agent simulating the effect of the *Lanceolate* gene in the tomato. Am. J. Bot. **52**:185–192.

Mathan, D. S. (1967). Reversing the morphogenetic effect of phenylboric acid and of the lanceolate gene with actinomycin D in the tomato. Genetics **57**:15–23.

Matoh, T., Ishigaki, K., Mizutani, M., Matsunaga, W., and Takabe, K. (1992). Boron nutrition of cultured tobacco BY-2 cells: I. Requirement for and intracellular localization of boron and selection of cells that tolerate low levels of boron. Plant Cell Physiol. **33**:1135–1141.

Matoh, T., Kawaguchi, S., and Kobayashi, M. (1996). Ubiquity of a borate-rhamnogalacturonan II complex in the cell walls of higher plants. Plant Cell Physiol. **37**:636–640.

Matsunaga, T., Ishii, T., Matsumoto, S., Higuchi, M., Darvill, A., Albersheim, P., and O'Neill, M. A. (2004). Occurrence of the primary cell wall polysaccharide rhamnogalacturonan II in pteridophytes, lycophytes, and bryophytes. Implications for the evolution of vascular plants. Plant Physiol. **134**:339–351.

Matthes, M., and Torres-Ruiz, R. A. (2016). Boronic acid treatment phenocopies monopteros by affecting PIN1 membrane stability and polar auxin transport in *Arabidopsis thaliana* embryos. Development **143**:4053–4062.

Matthes, M. S., Robil, J. M., Tran, T., Kimble, A., and McSteen, P. (2018). Increased transpiration is correlated with reduced boron deficiency symptoms in the maize *tassel-less1* mutant. Physiol. Plant. **163**:344–355.

Matthes, M. S., Robil, J. M., and McSteen, P. (2020). From element to development: The power of the essential micronutrient boron to shape morphological processes in plants. J. Exp. Bot. **71**:1681–1693.

Matthes, M. S., Darnell, Z., Best, N. B., Guthrie, K., Robil, J. M., Amstutz, J., Durbak, A., and McSteen, P. (2022). Defects in meristem maintenance, cell division, and cytokinin signaling are early responses in the boron deficient maize mutant *tassel-less1*. Physiol. Plant. **174**:e13670.

Matthes, M. S., Best, N. B., Robil, J. M., and McSteen, P. (2023). Enhancement of developmental defects in the boron-deficient maize mutant *tassel-less1* by reduced auxin levels. J. Plant Nutr. Soil Sci. Advance online publication (22.09.2023) **doi**:10.1002/jpln.202300155.

Mitani, N., Yamaji, N., and Ma, J. F. (2008). Characterization of substrate specificity of a rice silicon transporter, Lsi1. Pflugers Arch. - Eur. J. Physiol. **456**:679–686.

Miwa, K., Wakuta, S., Takada, S., Ide, K., Takano, J., Naito, S., Omori, H., Matsunaga, T., and Fujiwara, T. (2013). Roles of BOR2, a boron exporter, in cross linking of rhamnogalacturonan II and root elongation under boron limitation in Arabidopsis. Plant Physiol. **163**:1699–1709.

Muro, K., Yamasaki, A., Matsumoto, M., Tanaka, Y.-K., Ogra, Y., Fujiwara, T., Yoshinari, A., and Takano, J. (2025). The polar-localized borate exporter BOR1 facilitates boron transport in tapetal cells to the developing pollen grains. Plant Physiol. **197**:kiaf100.

Nakagawa, Y., Hanaoka, H., Kobayashi, M., Miyoshi, K., Miwa, K., and Fujiwara, T. (2007). Cell-type specificity of the expression of *OsBOR1*, a rice efflux boron transporter gene, is regulated in response to boron availability for efficient boron uptake and xylem loading. Plant Cell **19**:2624–2635.

Noguchi, K., Yasumori, M., Imai, T., Naito, S., Matsunaga, T., Oda, H., Hayashi, H., Chino, M., and Fujiwara, T. (1997). *bor1-1*, an *Arabidopsis thaliana* mutant that requires a high level of boron. Plant Physiol. **115**:901–906.

Odhnoff, C. (1961). The influence of boric acid and phenylboric acid on the root growth of bean (*Phaseolus vutgaris*). Physiol. Plant. **14**:187–220.

Oiwa, Y., Kitayama, K., Kobayashi, M., and Matoh, T. (2013). Boron deprivation immediately causes cell death in growing roots of *Arabidopsis thaliana* (L.) Heynh. Soil. Sci. Plant. Nutr. **59**:621–627.

O'Neill, M. A., Warrenfeltz, D., Kates, K., Pellerin, P., Doco, T., Darvill, A. G., and Albersheim, P. (1996). Rhamnogalacturonan-II, a pectic polysaccharide in the walls of growing plant cell, forms a dimer that is covalently cross-linked by a borate ester: *In vitro* conditions for the formation and hydrolysis of the dimer. J. Biol. Chem. **271**:22923–22930.

O'Neill, M. A., Eberhard, S., Albersheim, P., and Darvill, A. G. (2001). Requirement of borate cross-linking of cell wall rhamnogalacturonan II for *Arabidopsis* growth. Science **294**:846–849.

O'Neill, M. A., Ishii, T., Albersheim, P., and Darvill, A. G. (2004). Rhamnogalacturonan II: Structure and function of a borate cross-linked cell wall pectic polysaccharide. Annu. Rev. Plant Biol. **55**:109–139.

Onuh, A. F., and Miwa, K. (2023). Mutations in type II Golgi-localized proton pyrophosphatase AVP2;1/VHP2;1 affect pectic polysaccharide rhamnogalacturonan-II and alter root growth under low boron condition in *Arabidopsis thaliana*. Front. Plant Sci. **14**:1255486.

Orosa-Puente, B., Leftley, N., von Wangenheim, D., Banda, J., Srivastava, A. K., Hill, K., Truskina, J., Bhosale, R., Morris, E., Srivastava, M., et al. (2018). Root branching toward water involves posttranslational modification of transcription factor ARF7. Science **362**:1407–1410.

Pang, Y., Li, L., Ren, F., Lu, P., Wei, P., Cai, J., Xin, L., Zhang, J., Chen, J., and Wang, X. (2010). Overexpression of the tonoplast aquaporin *AtTIP5;1* conferred tolerance to boron toxicity in *Arabidopsis*. J. Genet. Genomics **37**:389–397.

Pang, Y., Li, J., Qi, B., Tian, M., Sun, L., Wang, X., and Hao, F. (2017). Aquaporin AtTIP5;1 as an essential target of gibberellins promotes hypocotyl cell elongation in *Arabidopsis thaliana* under excess boron stress. Functional Plant Biol. **45**:305–314.

Perez Di Giorgio, J. A., Patrick Bienert, G., Daniel Ayub, N., Yaneff, A., Laura Barberini, M., Alejandro Mecchia, M., Amodeo, G., Cynthia Soto, G., and Prometeo Muschietti, J. (2016). Pollen-specific aquaporins NIP4;1 and NIP4;2 are required for pollen development and pollination in *Arabidopsis thaliana*. Plant Cell **28**:1053–1077.

Pizer, Richard., and Babcock, Lucia. (1977). Mechanism of the complexation of boron acids with catechol and substituted catechols. Inorg. Chem. **16**:1677–1681.

Pommerrenig, B., Junker, A., Abreu, I., Bieber, A., Fuge, J., Willner, E., Bienert, M. D., Altmann,

T., and Bienert, G. P. (2018). Identification of rapeseed (*Brassica napus*) cultivars with a high tolerance to boron-deficient conditions. Front. Plant Sci. **9**:1142.

Pommerrenig, B., Faber, M., Hajirezaei, M. R., von Wiren, N., and Bienert, G. P. (2022). Cytokinins as boron deficiency signals to sustain shoot development in boron-efficient oilseed rape. Physiol. Plant. **174**:e13776.

Ponnamperuma, F. N., and Yuan, W. L. (1966). Toxicity of boron to rice. Nature **211**:780–781.

Poschenrieder, C., Tolrà, R. P., and Barceló, J. (2005). A role for cyclic hydroxamates in aluminium resistance in maize? J. Inorg. Biochem. **99**:1830–1836.

Poza-Viejo, L., Abreu, I., Gonzalez-Garcia, M. P., Allauca, P., Bonilla, I., Bolanos, L., and Reguera, M. (2018). Boron deficiency inhibits root growth by controlling meristem activity under cytokinin regulation. Plant Sci. **270**:176–189.

Reid, R. J., Hayes, J. E., Post, A., Stangoulis, J. C. R., and Graham, R. D. (2004). A critical analysis of the causes of boron toxicity in plants. Plant Cell Environ. **27**:1405–1414.

Richter, A., Schroeder, A. F., Marcon, C., Hochholdinger, F., Jander, G., and Negin, B. (2024). Catechol acetylglucose: a newly identified benzoxazinoid-regulated defensive metabolite in maize. New Phytol. **244**:2474–2488.

Routray, P., Li, T., Yamasaki, A., Yoshinari, A., Takano, J., Choi, W. G., Sams, C. E., and Roberts, D. M. (2018). Nodulin Intrinsic Protein 7;1 is a tapetal boric acid channel involved in pollen cell wall formation. Plant Physiol. **178**:1269–1283.

Ruuhola, T., Leppänen, T., Julkunen-Tiitto, R., Rantala, M. J., and Lehto, T. (2011). Boron fertilization enhances the induced defense of silver birch. J. Chem. Ecol. **37**:460–471.

Sakcali, M. S., Kekec, G., Uzonur, I., Alpsoy, L., and Tombuloglu, H. (2015). Randomly amplified polymorphic-DNA analysis for detecting genotoxic effects of boron on maize (*Zea mays* L.). Toxicol. Ind. Health **31**:712–720.

Sanhueza, D., Begum, R. A., Albenne, C., Jamet, E., and Fry, S. C. (2022). An *Arabidopsis thaliana* arabinogalactan-protein (AGP31) and several cationic AGP fragments catalyse the boron bridging of rhamnogalacturonan-II. Biochem. J. **479**:1967–1984.

Saxon, E., and Peng, X. (2022). Recent advances in hydrogen peroxide responsive organoborons for biological and biomedical applications. ChemBioChem **23**:e202100366.

Schaefer, R. J., Michno, J.-M., Jeffers, J., Hoekenga, O., Dilkes, B., Baxter, I., and Myers, C. L. (2018). Integrating coexpression networks with GWAS to prioritize causal genes in maize. Plant Cell **30**:2922–2942.

Schnurbusch, T., Hayes, J., Hrmova, M., Baumann, U., Ramesh, S. A., Tyerman, S. D., Langridge, P., and Sutton, T. (2010). Boron toxicity tolerance in barley through reduced expression of the multifunctional aquaporin *Hv*NIP2;1. Plant Physiol. **153**:1706–1715.

Shao, J. F., Yamaji, N., Huang, S., and Ma, J. F. (2021). Fine regulation system for distribution of boron to different tissues in rice. New Phytol. **230**:656–668.

Sharova, E. I., Smolikova, G. N., and Medvedev, S. S. (2024). Determining hydrogen peroxide content in plant tissue extracts. Russ. J. Plant Physiol. **70**:216.

Shorrocks, V. M. (1997). The occurrence and correction of boron deficiency. Plant Soil **193**:121–148.

Song, G., Li, X., Munir, R., Khan, A. R., Azhar, W., Khan, S., and Gan, Y. (2021). *BnaA02.NIP6;1a* encodes a boron transporter required for plant development under boron deficiency in *Brassica napus*. Plant Physiol. Bioch. **161**:36–45.

Soyano, T., Shimoda, Y., Kawaguchi, M., and Hayashi, M. (2019). A shared gene drives lateral root development and root nodule symbiosis pathways in Lotus. Science **366**:1021–1023.

Stangoulis, J. C. R., Reid, R. J., Brown, P. H., and Graham, R. D. (2001). Kinetic analysis of boron transport in *Chara*. Planta **213**:142–146.

Stelpflug, S. C., Sekhon, R. S., Vaillancourt, B., Hirsch, C. N., Buell, C. R., de Leon, N., and Kaeppler, S. M. (2016). An expanded maize gene expression atlas based on RNA sequencing and its use to explore root development. Plant Genome **9**:1–16.

Su, W.-L., Liu, N., Mei, L., Luo, J., Zhu, Y.-J., and Liang, Z. (2019). Global transcriptomic profile analysis of genes involved in lignin biosynthesis and accumulation induced by boron deficiency in poplar roots. Biomolecules **9**:156.

Sutton, T., Baumann, U., Hayes, J., Collins, N. C., Shi, B. J., Schnurbusch, T., Hay, A., Mayo, G., Pallotta, M., Tester, M., et al. (2007). Boron-toxicity tolerance in barley arising from efflux transporter amplification. Science **318**:1446–1449.

Takano, J., and Tanaka, M. (2023). Boron-sensing mechanisms involved in boron transport regulation in plants. J. Plant Nutr. Soil Sci. Advance online publication (22.06.2023) **doi**:10.1002/jpln.202300029.

Takano, J., Noguchi, K., Yasumori, M., Kobayashi, M., Gajdos, Z., Miwa, K., Hayashi, H., Yoneyama, T., and Fujiwara, T. (2002). Arabidopsis boron transporter for xylem loading. Nature **420**:337–340.

Takano, J., Miwa, K., Yuan, L., von Wirén, N., and Fujiwara, T. (2005). Endocytosis and degradation of BOR1, a boron transporter of *Arabidopsis thaliana*, regulated by boron availability. Proc. Natl. Acad. Sci. U.S.A. **102**:12276–12281.

Takano, J., Wada, M., Ludewig, U., Schaaf, G., von Wiren, N., and Fujiwara, T. (2006). The Arabidopsis major intrinsic protein NIP5;1 is essential for efficient boron uptake and plant development under boron limitation. Plant Cell **18**:1498–1509.

Tanaka, M., Wallace, I. S., Takano, J., Roberts, D. M., and Fujiwara, T. (2008). NIP6;1 is a boric acid channel for preferential transport of boron to growing shoot tissues in *Arabidopsis*. Plant Cell **20**:2860–2875.

Tanaka, M., Takano, J., Chiba, Y., Lombardo, F., Ogasawara, Y., Onouchi, H., Naito, S., and Fujiwara, T. (2011). Boron-dependent degradation of *NIP5;1* mRNA for acclimation to excess boron conditions in *Arabidopsis*. Plant Cell **23**:3547–59.

Tao, L., Zhu, H., Huang, Q., Xiao, X., Luo, Y., Wang, H., Li, Y., Li, X., Liu, J., Jásik, J., et al. (2023). PIN2/3/4 auxin carriers mediate root growth inhibition under conditions of boron deprivation in Arabidopsis. Plant J. **115**:1357–1376.

Tapia-Quezada, C. E., Ruiz-Herrera, L. F., Huerta-Venegas, P. I., and López-Bucio, J. (2022). Mild high concentrations of boric acid repress leaf formation and primary root growth in Arabidopsis seedlings while showing anti-apoptotic effects in a mutant with compromised cell viability. J. Plant Growth Regul. **41**:3410–3420.

Tölle, J. B., Alcock, T. D., and Bienert, G. P. (2025). Borax promotes fertility of *Brassica napus* better than other boron species at suboptimal supply. J. Plant Nutr. Soil Sci. Advance online

publication (23.07.2025) **doi**:10.1002/jpln.70000.

Verwaaijen, B., Alcock, T. D., Spitzer, C., Liu, Z., Fiebig, A., Bienert, M. D., Bräutigam, A., and Bienert, G. P. (2023). The *Brassica napus* boron deficient inflorescence transcriptome resembles a wounding and infection response. Physiol. Plant. **175**:e14088.

Von Rad, U., Hüttl, R., Lottspeich, F., Gierl, A., and Frey, M. (2001). Two glucosyltransferases are involved in detoxification of benzoxazinoids in maize. Plant J. **28**:633–642.

Voxeur, A., and Fry, S. C. (2014). Glycosylinositol phosphorylceramides from *Rosa* cell cultures are boron-bridged in the plasma membrane and form complexes with rhamnogalacturonan II. Plant J. **79**:139–149.

Wang, G., Romheld, V., Li, C., and Bangerth, F. (2006). Involvement of auxin and CKs in boron deficiency induced changes in apical dominance of pea plants (*Pisum sativum* L.). J. Plant Physiol. **163**:591–600.

Wang, B., Guo, X., and Bai, P. (2014). Removal technology of boron dissolved in aqueous solutions – A review. Colloids Surf. A Physicochem. Eng. Asp. **444**:338–344.

Wang, Y., Wang, Q., Zhao, Y., Han, G., and Zhu, S. (2015). Systematic analysis of maize class III peroxidase gene family reveals a conserved subfamily involved in abiotic stress response. Gene **566**:95–108.

Wang, C., Tang, Z., Zhuang, J.-Y., Tang, Z., Huang, X.-Y., and Zhao, F.-J. (2020). Genetic mapping of ionomic quantitative trait loci in rice grain and straw reveals *OsMOT1;1* as the putative causal gene for a molybdenum QTL *qMo8*. Mol. Genet. Genomics **295**:391–407.

Wang, M.-Q., Wang, Y.-T., Peng, J.-S., Yu, Y.-X., Wen, T.-T., Liu, Z.-J., Qi, Z.-A., Zhang, X.-Y., He, S.-Y., Fang, Z.-J., et al. (2025). OsNIP3;1 mediates diurnal boron oscillation at rice vasculature tip. New Phytol. **247**:1493–1502.

Warington, K. (1923). The effect of boric acid and borax on the broad bean and certain other plants. Ann. Bot. **os-37**:629–672.

Wilder, S. L., Scott, S., Waller, S., Powell, A., Benoit, M., Guthrie, J. M., Schueller, M. J., Awale, P., McSteen, P., Matthes, M. S., et al. (2022). Carbon-11 radiotracing reveals physiological and metabolic responses of maize grown under different regimes of boron treatment. Plants **11**:241.

Wimmer, M. A., Lochnit, G., Bassil, E., Muhling, K. H., and Goldbach, H. E. (2009). Membrane-associated, boron-interacting proteins isolated by boronate affinity chromatography. Plant Cell Physiol. **50**:1292–304.

Wouters, F. C., Blanchette, B., Gershenzon, J., and Vassão, D. G. (2016). Plant defense and herbivore counter-defense: benzoxazinoids and insect herbivores. Phytochem. Rev. **15**:1127–1151.

Wu, D., Tanaka, R., Li, X., Ramstein, G. P., Cu, S., Hamilton, J. P., Buell, C. R., Stangoulis, J., Rocheford, T., and Gore, M. A. (2021). High-resolution genome-wide association study pinpoints metal transporter and chelator genes involved in the genetic control of element levels in maize grain. G3 (Bethesda). **11**:jkab059.

Xu, F., Wang, Y., Ying, W., and Meng, J. (2002). Inheritance of boron nutrition efficiency in *Brassica napus*. J. Plant Nutr. **25**:901–912.

Xu, J., Su, Z.-H., Chen, C., Han, H.-J., Zhu, B., Fu, X.-Y., Zhao, W., Jin, X.-F., Wu, A.-Z., and

Yao, Q.-H. (2012). Stress responses to phenol in *Arabidopsis* and transcriptional changes revealed by microarray analysis. Planta **235**:399–410.

Xu, C., Tai, H., Saleem, M., Ludwig, Y., Majer, C., Berendzen, K. W., Nagel, K. A., Wojciechowski, T., Meeley, R. B., Taramino, G., et al. (2015). Cooperative action of the paralogous maize lateral organ boundaries (LOB) domain proteins RTCS and RTCL in shoot-borne root formation. New Phytol. **207**:1123–1133.

Xu, W., Wang, P., Yuan, L., Chen, X., and Hu, X. (2021). Effects of application methods of boron on tomato growth, fruit quality and flavor. Horticulturae **7**:223.

Yan, J., Springsteen, G., Deeter, S., and Wang, B. (2004). The relationship among pKa, pH, and binding constants in the interactions between boronic acids and diols—it is not as simple as it appears. Tetrahedron **60**:11205–11209.

Yang, M., Lu, K., Zhao, F.-J., Xie, W., Ramakrishna, P., Wang, G., Du, Q., Liang, L., Sun, C., Zhao, H., et al. (2018). Genome-wide association studies reveal the genetic basis of ionomic variation in rice. Plant Cell **30**:2720–2740.

Yang, L.-T., Pan, J.-F., Hu, N.-J., Chen, H.-H., Jiang, H.-X., Lu, Y.-B., and Chen, L.-S. (2022). Citrus physiological and molecular response to boron stresses. Plants **11**:40.

Yao, J., Cui, R., Fang, B., Wang, S., Ye, X., Liu, Z., and Xu, F. (2025). Transcription factor *BnaA1.WRKY53* is involved in regulation of auxin-induced leaf curling under boron deficiency in *Brassica napus*. Crop J. **13**:1068–1080.

Zhang, D., Zhao, H., Shi, L., and Xu, F. (2014). Physiological and genetic responses to boron deficiency in *Brassica napus*: A review. Soil. Sci. Plant. Nutr. **60**:304–313.

Zhang, Q., Chen, H., He, M., Zhao, Z., Cai, H., Ding, G., Shi, L., and Xu, F. (2017). The boron transporter BnaC4.BOR1;1c is critical for inflorescence development and fertility under boron limitation in *Brassica napus*. Plant Cell Environ. **40**:1819–1833.

Zhang, H., Wang, M. L., Schaefer, R., Dang, P., Jiang, T., and Chen, C. (2019). GWAS and coexpression network reveal ionomic variation in cultivated peanut. J. Agric. Food Chem. **67**:12026–12036.

Zhang, C., He, M., Wang, S., Chu, L., Wang, C., Yang, N., Ding, G., Cai, H., Shi, L., and Xu, F. (2021). Boron deficiency-induced root growth inhibition is mediated by brassinosteroid signalling regulation in Arabidopsis. Plant J. **107**:564–578.

Zhang, Z., Zhai, H., Hua, Y., Wang, S., and Xu, F. (2024). Genome-wide association study integrated with transcriptome analysis to identify boron efficiency-related candidate genes and favorable haplotypes in *Brassica napus* L. J. Integr. Agric. Advance online publication (05.11.2024) **doi**:10.1016/j.jia.2024.11.013.

Zhao, Z., Gao, X., Ke, Y., Chang, M., Xie, L., Li, X., Gu, M., Liu, J., and Tang, X. (2019). A unique aluminum resistance mechanism conferred by aluminum and salicylic-acid-activated root efflux of benzoxazinoids in maize. Plant Soil **437**:273–289.

Zhao, S., Huq, Md. E., Fahad, S., Kamran, M., and Riaz, M. (2024). Boron toxicity in plants: understanding mechanisms and developing coping strategies; a review. Plant Cell Rep. **43**:238.

Zhou, T., Hua, Y., Huang, Y., Ding, G., Shi, L., and Xu, F. (2016). Physiological and transcriptional analyses reveal differential phytohormone responses to boron deficiency in *Brassica napus* genotypes. Front. Plant Sci. **7**:221.

Zhou, D., Shen, W., Cui, Y., Liu, Y., Zheng, X., Li, Y., Wu, M., Fang, S., Liu, C., Tang, M., et al. (2021). APICAL SPIKELET ABORTION (ASA) controls apical panicle development in rice by regulating salicylic acid biosynthesis. Front. Plant Sci. **12**:636877.

6 Appendix

6.1 Appendix for chapter 2

Supplementary tables for chapter 2

Supplementary tables for chapter 2 are available in the digital appendix on the bonndoc publication server: https://nbn-resolving.org/urn:nbn:de:hbz:5-89855

Supplementary figures for chapter 2

Figure S1

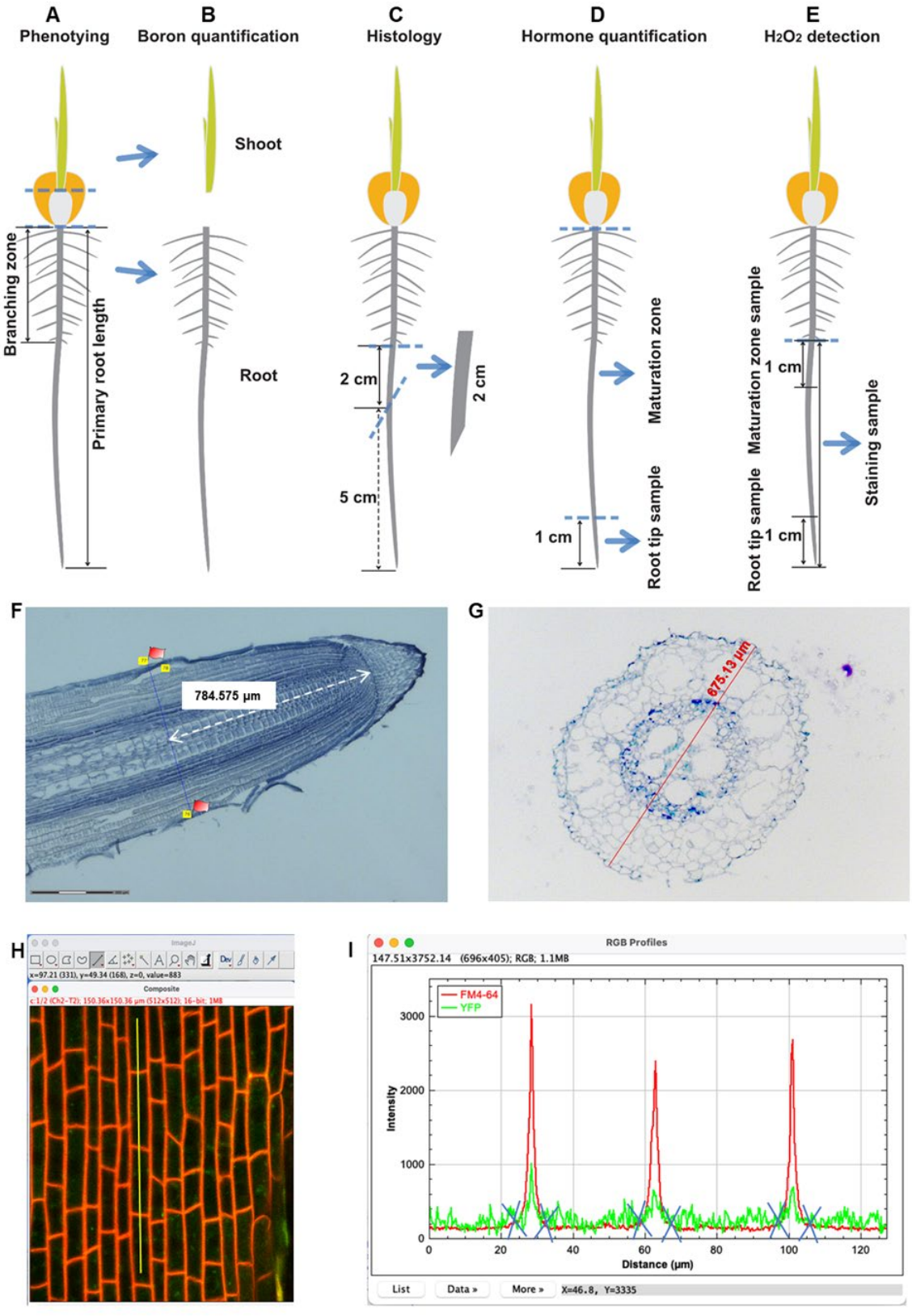

Figure legend on next page

Figure S1 Graphical representation of phenotyping and sampling strategies and quantification of meristem length, root diameter, and PIN1a-YFP or FM4-64 fluorescence following boron deficiency- and phenylboronic acid (PBA) treatments.

A, Primary root length and branching zone phenotyping. B-E, Sampling methods of boron quantification in root and shoot tissue (B), lateral root primordia and root diameter analysis (C), phytohormone quantification (D) and H_2O_2 detection via 3,3′-diaminobenzidine staining (E). F, Example of meristem length analysis using lateral root sections. G, Primary root diameter analysis using radial root sections. The sections in F - G are from the +B (50 μM boric acid) treatment and sampled 4 days after treatment (DAT) and stained using toluidine blue. H-I, Strategy for PIN1a-YFP and FM4-64 fluorescence quantification at the plasma membrane and in the cytosol using ImageJ (Scheinder et al., 2012) and R (R Core Team, 2021). Fluorescence was detected along a manually drawn line (see yellow line) across a cell file (H). The detected fluorescence intensity values were plotted against the distance from the starting point of the line (I). Membrane locations were manually selected for each image (as indicated by the blue X) and the respective fluorescence intensities at the membrane were calculated using the integrate()-function in R with the respective membrane locations. Related to Figure 2.

Figure S2

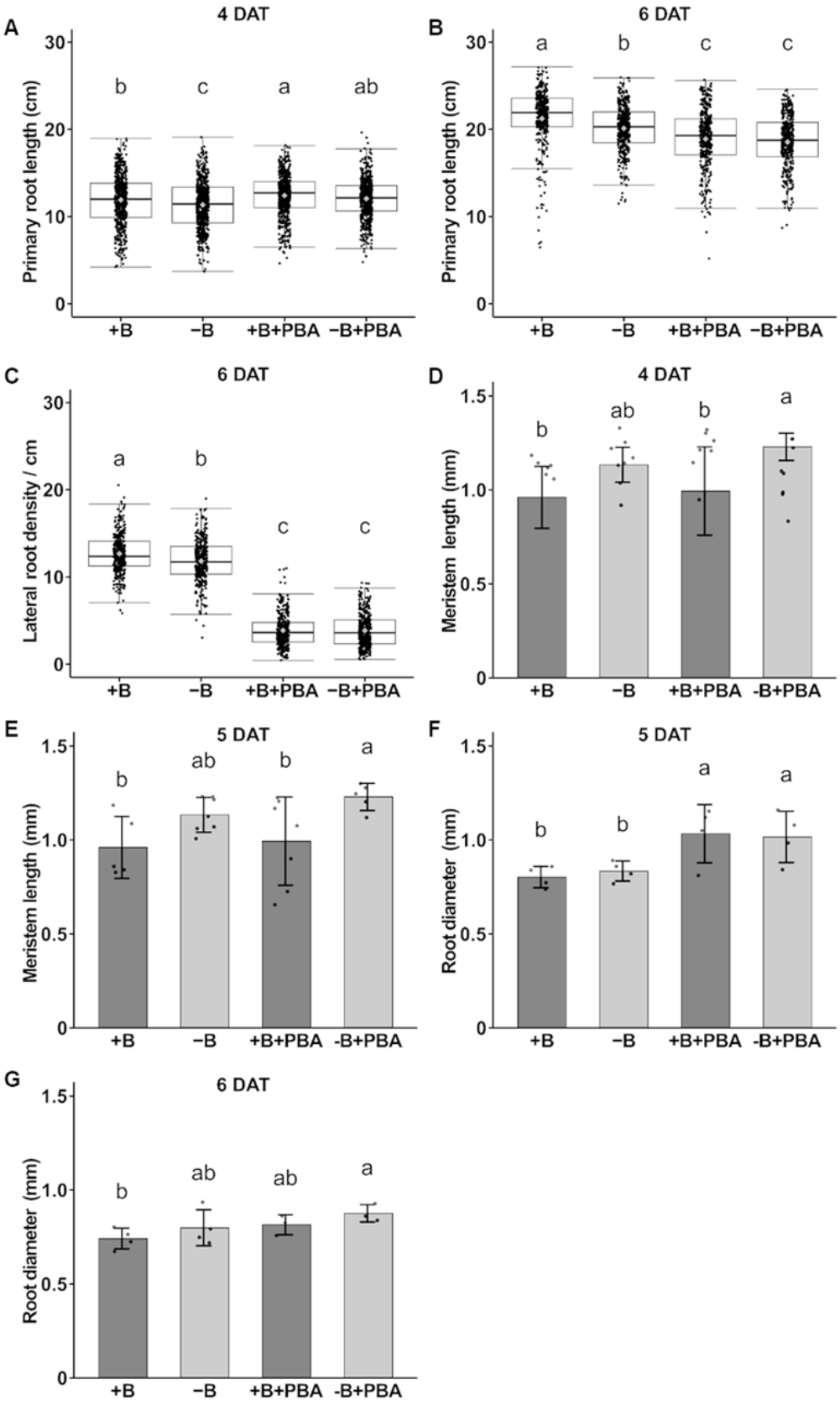

Figure legend on next page

Figure S2 Phenylboronic acid- (PBA) and boron deficiency-treatments induce primary root defects in maize. A-B, Boxplots of primary root length 4 (A) or 6 (B) days after treatments (DAT) of: 50 μM boric acid (+B), no boric acid (-B; 0 μM boric acid), 50 μM boric acid + 0.4 mM PBA (+B+PBA), or without boric acid + 0.4 mM PBA (-B+PBA). All treatments were made in Hoagland media. C, Boxplots of lateral root density of the same seedlings as indicated in B. For boxplots A-C, the grey diamond within each box represents the mean of 8 biological replicates (n > 40 per replicate per treatment). Different letters indicate statistically significant differences as determined by Tukey's test ($p \leq 0.05$). D-E, Bar plots of meristem length in the primary root tip 4 DAT (D) and 5 DAT (E). F-G, Bar plots of root diameter 5 DAT (F) or 6 DAT (G) of the 4 treatments as indicated in A-C. Data represent the mean ± standard deviation (n = 3 biological replicates). Different letters indicate significant differences as determined by Fisher's test ($p < 0.05$) following analysis of variance. Related to Figure 2.

Figure S3

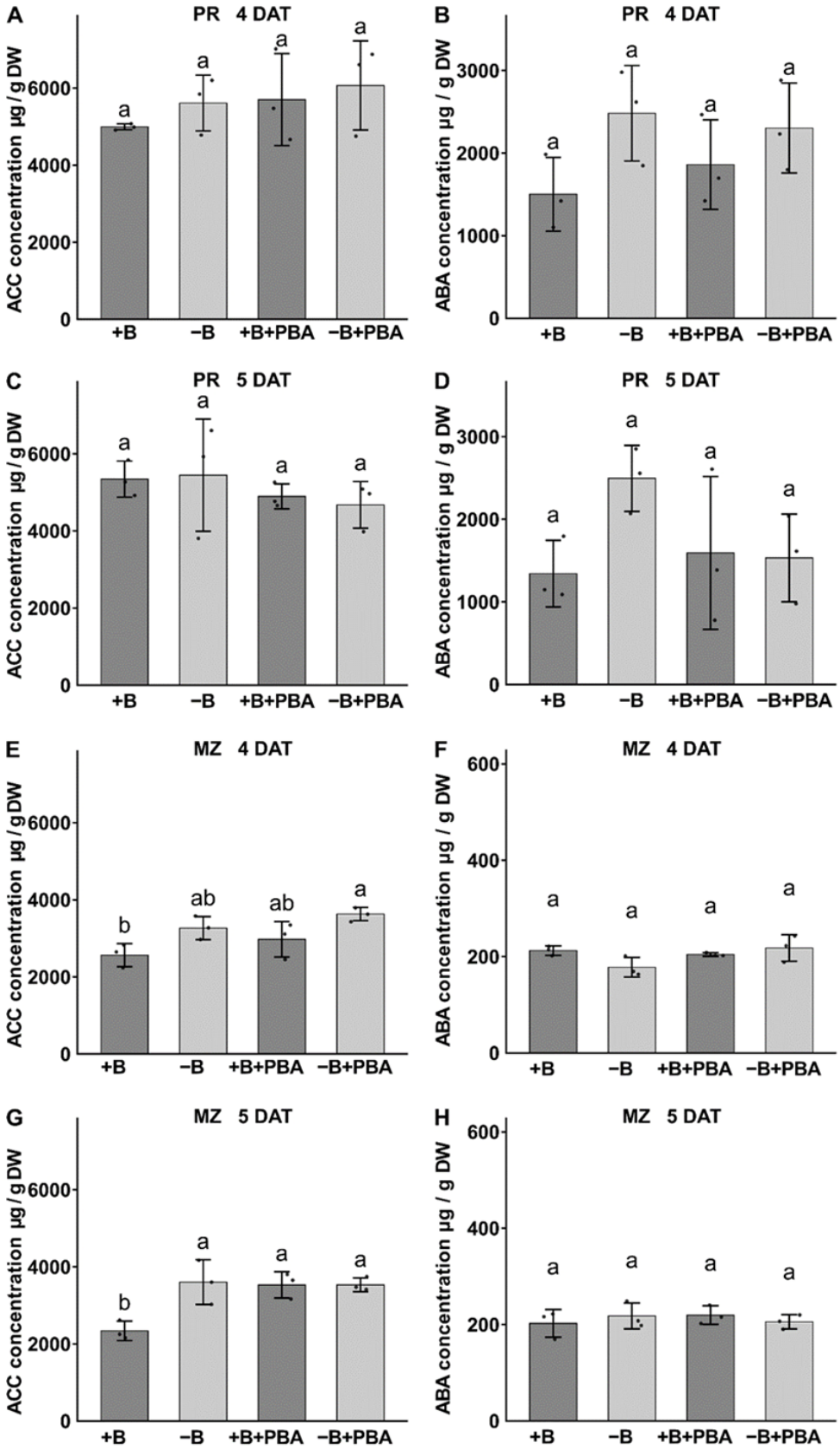

Figure legend on next page

Figure S3 Alterations of the levels of the ethylene precursor 1-amino-cyclopropane-1-carboxylic acid (ACC) and abscisic acid (ABA) following boron deficiency and phenylboronic acid (PBA) treatments. A-H, Boxplots of hormone concentrations in seedling roots 4 or 5 days after treatment (DAT) of: 50 μM boric acid (+B), without boric acid (-B; 0 μM boric acid), with 50 μM boric acid + 1 mM PBA (+B+PBA), or without boric acid + 1 mM PBA (-B+PBA). All treatments were done in Hoagland media. Samples were collected from primary root tips up to 1 cm (A - D) and the maturation zone (E - H). A-B, Concentrations of ACC (A) and ABA (B) in primary root tips 4 DAT. C-D, Concentrations of ACC (C) and ABA (D) in primary root tips 5 DAT. E-F, Concentrations of ACC (E) and ABA (F) in the maturation zone 4 DAT. G-H, Concentrations of ACC (G) and ABA (H) in the maturation zone 5 DAT. The bar plots in A - H represent the mean ± standard deviations (n = 3 biological replicates). Different letters indicate significant differences as determined by Tukey's test ($p \leq 0.05$) following analysis of variance. DW = dry weight, MZ = maturation zone, PR = primary root tip. Related to Figure 3

Figure S4

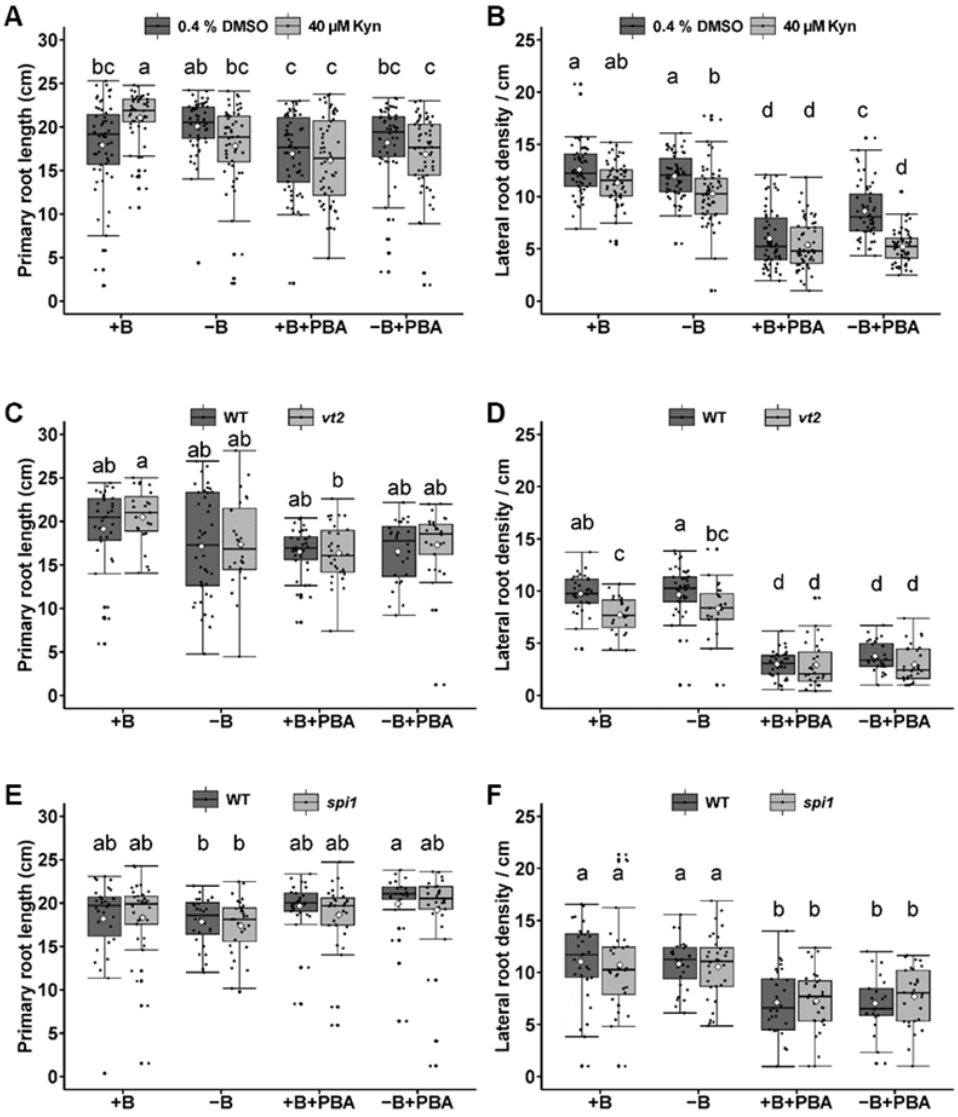

Figure S4 Effects of altered auxin biosynthesis on boron deficiency- and phenylboronic acid (PBA)-induced defects in maize roots. Boxplots of primary root length (A, C, E) and lateral root density (B, D, F) of seedlings 6 days after the indicated treatments of: 50 µM boric acid (+B), without boric acid (-B; 0 µM boric acid), 50 µM boric acid + 0.4 mM PBA (+B+PBA), or without boric acid + 0.4 mM PBA (-B+PBA). A-B, Effects of the auxin biosynthesis inhibitor L-kynurenine (Kyn; 40 µM) on boron deficiency- and PBA-induced defects regarding primary root length (A) and lateral root density (B). DMSO was added to the control conditions (0.4 %), since it was the solvent of Kyn. The white diamond in each boxplot represents the mean over 3 biological replicates (n ≥17 per replicate per treatment). C-F, Effects of boron deficiency and PBA on the primary roots of wild type and the auxin biosynthesis mutants *vanishing tassel2* (*vt2*; C-D) and *sparse inflorescence1 (spi1;* E-F). The white diamond in each boxplot represents the mean over 3 biological replicates (n ≥ 4 per replicate per treatment; C-D) or over 4 biological replicates (n ≥ 3 per replicate per treatment; E-F). In A-F, different letters indicate significant differences as determined by Tukey's test ($p \leq 0.05$). DMSO = dimethyl sulfoxide. Related to Figure 3.

Figure S5

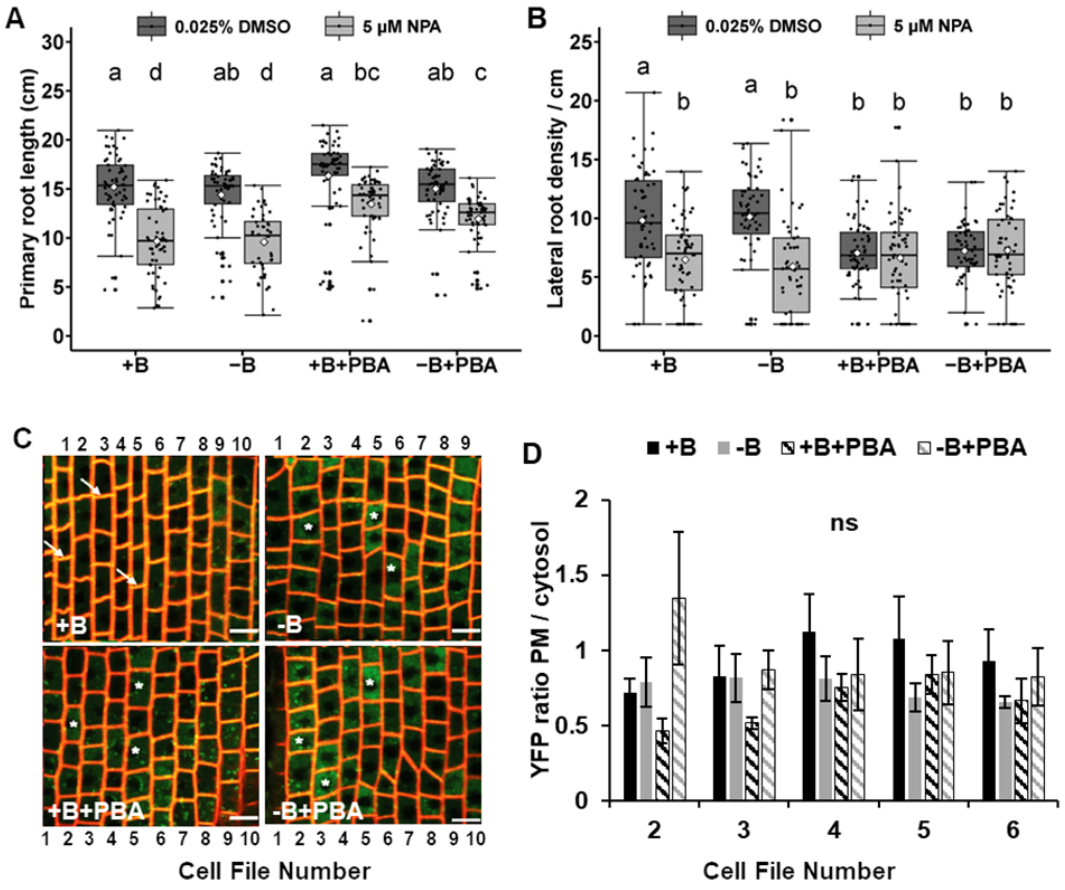

Figure S5 Involvement of auxin transport in boron deficiency- and phenylboronic acid (PBA)-induced defects in maize roots. A-B, Boxplots of primary root length (A) and lateral root density (B) 6 days after treatment of: 50 µM boric acid (+B), without boric acid (-B; 0 µM boric acid), with 50 µM boric acid + 0.4 mM PBA, or without boric acid + 0.4 mM PBA (-B+PBA) with or without the addition of 5 µM naphthylphthalamic acid (NPA). All treatments were done in Hoagland media. DMSO was added to the control conditions (0.025 %), since it was the solvent of NPA. The white diamond within each boxplot represents the mean of 4 biological replicates ($n \geq 17$ per replicate per treatment). Different letters indicate statistically significant differences as determined by Tukey's test ($p \leq 0.05$). C, Confocal laser scanning microscopy showing the subcellular localization of PIN1a-YFP in the primary root tip 6 days after the indicated boron or PBA treatments: +B, -B, +B+PBA, -B+PBA. D, Bar plots of PIN1a-YFP-fluorescence quantification at the plasma membrane versus the cytosol. The ratios between YFP-fluorescence at the plasma membrane versus the cytosol were determined individually for each cell file. Data are represented as means ± standard error of means ($n = 3$ - 5 biological replicates). Statistical significance ($p \leq 0.05$) was calculated using the Dunnett's test in R (compared to the +B control). Scale bars in C = 20 µm. DMSO = dimethyl sulfoxide, ns = not statistically significantly different, PM = plasma membrane.

Figure S6

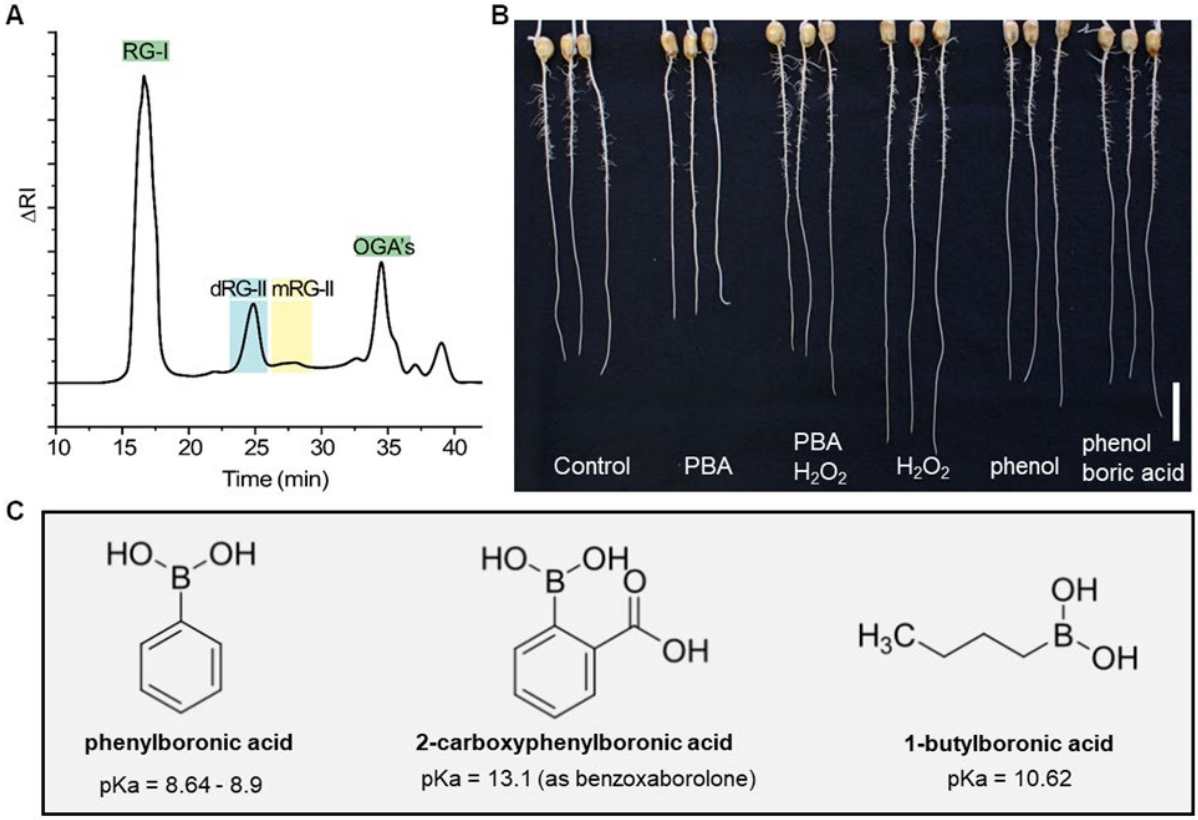

Figure S6 Phenylboronic acid (PBA)-induced root defects are likely not caused by the oxidation products of PBA. A, A typical size exclusion chromatography (SEC) profile of celery rhamnogalacturonan I (RG-I), RG-II (mRG-II = monomeric and dRG-II = RG-II dimers), and oligogalacturonic acids (OGA's). B, Original image underlying Figure 6: Representative image of primary roots 6 days after treatment of: Control (Hoagland solution), 1 mM PBA, 1 mM PBA + 1 mM H2O2, 1 mM H2O2, 1 mM phenol, 1 mM phenol + 1 mM boric acid. C, Chemical structures and acid dissociation constants (pKa) of phenylboronic acid (PBA; Sporzyński et al., 2024), 2-carboxyphenylboronic acid (2-CPBA; Graham et al., 2021) and 1-butylboronic acid (BBA; De Paola et al., 1999), RI = refractive index. Scale bar in B = 3 cm. Related to Figures 4, 6.

Figure S7

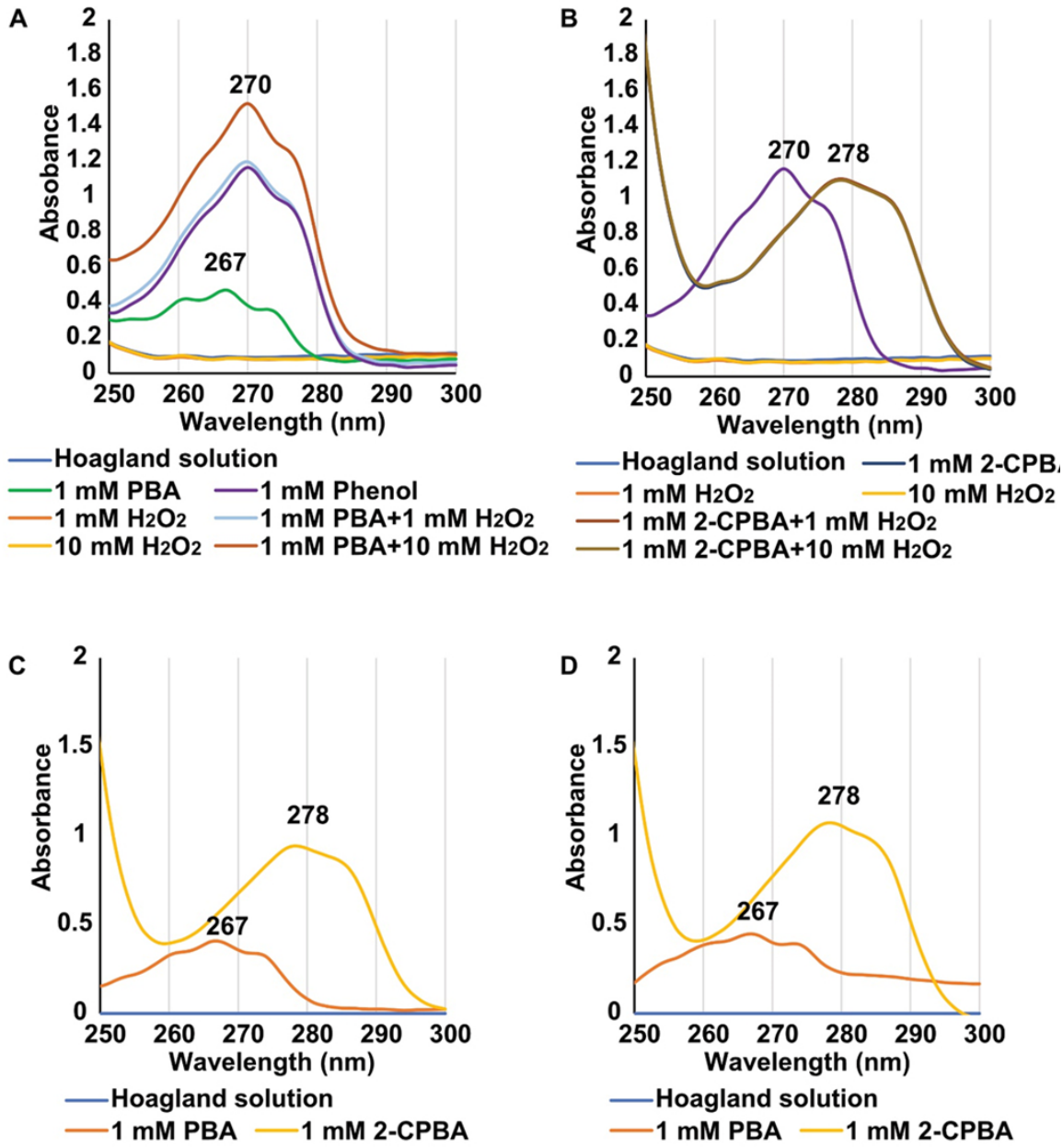

Figure S7 Phenol is not detected by ultraviolet (UV) spectroscopy in media containing phenylboronic acid (PBA) or 2-carboxyphenylboronic acid (2-CPBA). A, UV-spectra of 1 mM PBA, 1 mM phenol, and 1 mM PBA plus different concentrations of H_2O_2 (1 mM or 10 mM) in Hoagland solution. B, UV-spectra of 1 mM 2-CPBA, 1 mM phenol, and 1 mM 2-CPBA plus different concentrations of H_2O_2 (1 mM and 10 mM) in Hoagland solution. The solutions in A and B were incubated at 20 °C in the dark for 2 h. C - D, UV-spectra of Hoagland media containing 1 mM PBA (C) or 1 mM 2-CPBA (D) used in the seedling assays. Media in C and D was analyzed at the beginning of the treatment and 6 days after the treatment, which was the time point for most phenotyping assays.

Figure S8

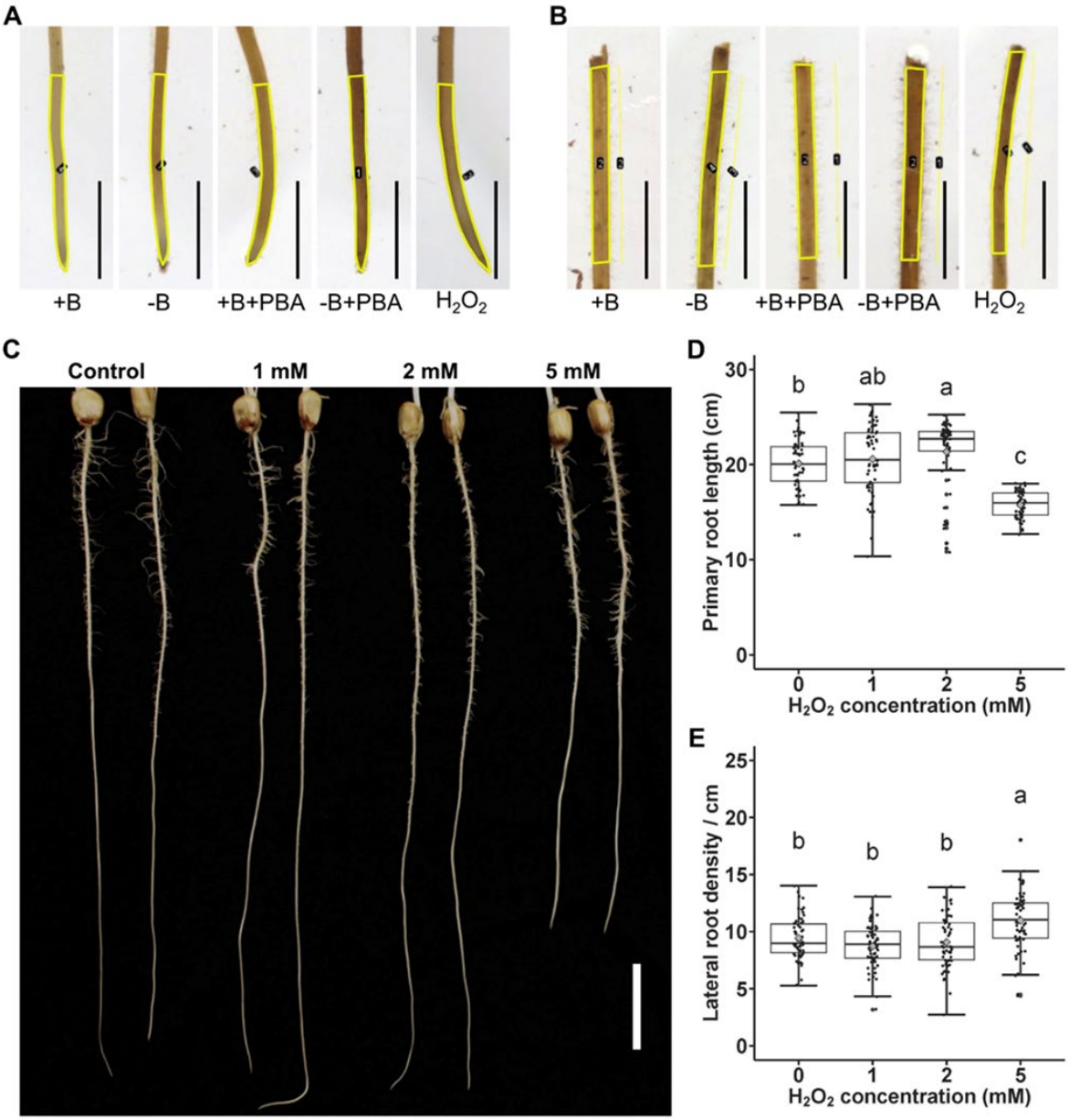

Figure S8 H_2O_2 treatment leads to maize primary root defects in a dose-dependent manner. A-B: Examples of 3,3′-diaminobenzidine-stained primary roots six days after the indicated treatments of: 50 µM boric acid (+B), without boric acid (-B; 0 µM boric acid), with 50 µM boric acid + 1 mM PBA, without boric acid + 1 mM PBA (-B+PBA), or with 1 mM H_2O_2 (H_2O_2). All treatments were done in Hoagland media. The yellow polygon selections in A - B indicate the quantified areas in the 1 cm root tip-samples (A) or in the lateral root formation zone-samples (1 cm below the branching zone; B). C, Representative image of primary roots 6 days after the indicated treatments of 0 mM, 1 mM, 2 mM, and 5 mM H_2O_2. D-E, Box plots of primary root length (D) and lateral root density (E) of seedlings 6 days after the indicated H_2O_2 treatments. The grey diamond in each boxplot represents the mean of 3 biological replicates with n ≥ 19 per replicate per treatment. Different letters indicate statistically significant differences as determined by Tukey's test ($p \leq 0.05$). The scale bar in A-B = 5 mm and in C = 3 cm. Related to Figures 5 and 6.

Figure S9

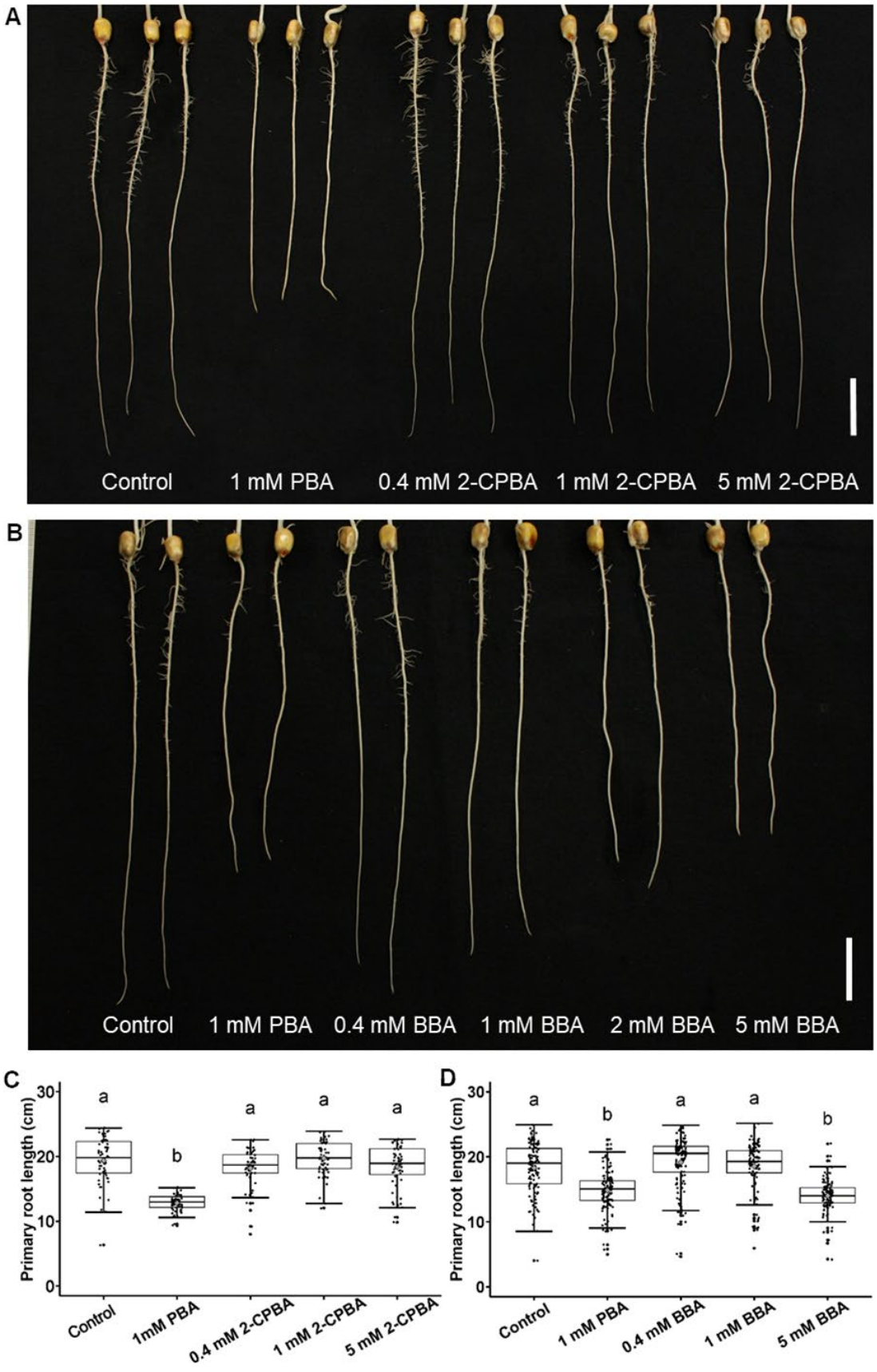

Figure legend on next page

Figure S9 2-Carboxyphenylboronic acid (2-CPBA) and 1-butylboronic acid (BBA) lead to similar primary root phenotypes as phenylboronic acid (PBA). A, Representative image of primary roots 6 days after treatment (DAT) of: Control (Hoagland media), 1 mM PBA, 0.4 mM 2-CPBA, 1 mM 2-CPBA, 5 mM 2-CPBA. B, Representative image of primary roots 6 DAT of: Control (Hoagland media), 1 mM PBA, 0.4 mM BBA, 1 mM BBA, 2 mM BBA, and 5 mM BBA. Shown are two roots per treatment representing two different B73 seed packs (biological replicates). C-D, Box plots of primary root length of the seedlings treated with 2-CPBA (C) or BBA (D) 6 DAT. The grey diamond within each boxplot represents the mean of 3 biological replicates (C) or 6 biological replicates (D) with $n \geq 17$ per replicate per treatment. Different letters indicate statistically significant differences as determined by Tukey's test ($p \leq 0.05$). The scale bars in A and B = 3 cm. Related to Figure 6.

Figure S10

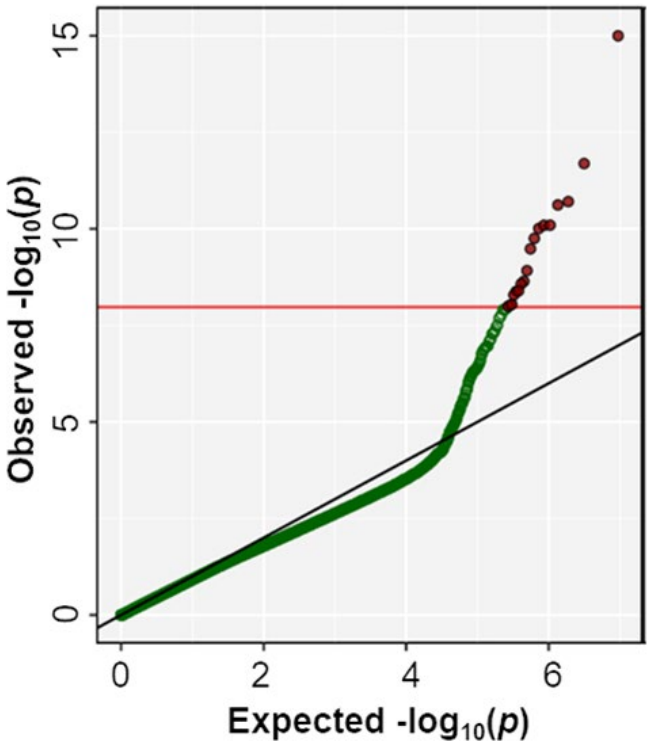

Figure S10 Quantile-quantile (QQ)-plot underlying the results of a genome-wide association study (FarmCPU model) with the lateral root density ratio data (1 mM phenylboronic acid versus H_2O control). The QQ-plot depicts the expected (x-axis) and observed (y-axis) -$\log_{10}p$-values. Related to Figure 7.

6.2 Appendix for chapter 3

Appendix for chapter 3 is available online:

https://academic.oup.com/plphys/article/197/1/kiae611/7887750#supplementary-data

7 Publications

7.1 Publications related to this thesis

- **Phenylboronic acid-induced defects in maize roots are independent of rhamnogalacturonan-II dimerization**

  Liuyang Chu, Deepak Sharma, Alexa Brox, Cay Christin Schäfer, Norman B. Best, Ha Ngoc Duong, Yen On Chan, Jutta Baldauf, Beatrice Klammer, Julia Brück, Felix Plotecki, Gabriel Schaaf, Ruthie Angelovici, Frank Hochholdinger, Breanna Urbanowicz, and Michaela S. Matthes

  Plant Physiology, in revision.

  Own contribution: Experimental design, performed the majority of the experiments, statistical analyses (except GWAS), interpretation of results, and writing of the manuscript.

- **Association of the benzoxazinoid pathway with boron homeostasis in maize.**

  Liuyang Chu†, Vivek Shrestha†, Cay Christin Schäfer, Jan Niedens, George W. Meyer, Zoe Darnell, Tyler Kling, Tobias Dürr-Mayer, Aleksej Abramov, Monika Frey, Henning Jessen, Gabriel Schaaf, Frank Hochholdinger, Agnieszka Nowak-Król, Paula McSteen, Ruthie Angelovici, Michaela S. Matthes

  Plant Physiology (2024). DOI:10.1093/plphys/kiae611 (published, †: co-first authors).

  Own contribution: Phenotypic analyses of maize mutants and Arabidopsis lines, boron quantification of soil and mutants, writing of the manuscript.

- **Molecular mechanisms affected by boron deficiency in root and shoot meristems of plants (review)**

  Liuyang Chu, Cay Christin Schäfer, and Michaela S. Matthes

  Journal of Experimental Botany (2025). DOI:10.1093/jxb/eraf036 (published, first author).

  Own contribution: Literature reading, interpretation and manuscript writing.

7.2 Presentations at conferences

- **Dissecting the boron deficiency response of maize roots using phenylboronic acid**

  2026 Maize Genetics Meeting. Feb.26-Mar.9, 2026, Cologne, Germany. (*Lightning talk presentation of the poster and poster presentation*)

- **Effects of phenylboronic acid on maize root development: Boron-related but independent of rhamnogalacturonan-II dimerization**

  International Symposium on Micronutrients in Crops and the 50th Anniversary Celebration of Micronutrient Research at Huazhong Agricultural University. Nov. 14-17, 2025. Wuhan, China. (*Invited oral presentation*)

- **Effects of phenylboronic acid on maize root development: Boron-related but rhamnogalacturonan II-independent?**

  2025 Maize Genetics Meeting. Mar.6-9, 2025, St. Louis, USA. (*Oral presentation at the pre-meeting Maize Development and Cell Biology Workshop and poster presentation at the main conference*)

- **Primary root development of maize (*Zea mays* L.) under boron deficiency.**

  56th Annual conference of the German Society of Plant Nutrition. Sep.2-4, 2024. Bonn, Germany. (*Lightning talk presentation of the poster and poster presentation*)

- **Boron deficiency leads to defects in maize lateral roots.**

  International Conference on 100 Years of Results in Boron Research in Plants. Sep. 22-23, 2023, Hohenheim, Germany. (*Oral presentation*).

- **Boron deficiency leads to lateral root defects in maize.**

  5th European Maize Meeting. June 14-16, 2023. Bologna, Italy. (*Poster presentation*).

- **Boron deficiency leads to lateral root defects in maize.**

  Molecular Biology of Plants 2023. Feb. 6-9, 2023. Hennef, Germany. (*Poster presentation*).

- **Characterization of boron deficiency-induced defects in the maize primary root.**

  International Conference of the German Society for Plant Sciences. Aug. 28 – Sep. 1, 2022. Bonn, Germany. (*Poster presentation*).

8 Acknowledgement

First, I would like to sincerely thank my supervisor Michaela for providing me with the opportunity to work on such interesting projects, and for her continuous guidance and support in both research and life. I am also grateful to Frank for his support regarding my position and study. I am also thankful to Gabriel, Claudia and Lukas for being in my thesis committee.

I would like to thank Gabriel for his valuable advice and support for both studies in this thesis. I would like to express my gratitude to all external collaborators (as listed among the co-authors in Chapters 2 and 3) for their indispensable contributions, and I am especially thankful to Micha and Gabriel for establishing and facilitating these collaborations.

I am deeply grateful to all members of the Crop Functional Genomics (CFG) and the Chemical Signaling (CS) groups for creating such a great environment and making my PhD experience wonderful. In particular, I would like to thank the technicians and students who contributed significantly to my studies: Alexa, Cay, Julia, Felix, and Bea for their help with experiments; Jutta and Marion for help with statistics; Helmut and Christa for their help in the field; and also thank Angelika, Nur, Ira, and Kerstin, for their support with boron measurements.

Many thanks to Peng and Caro for their insightful questions, suggestions, and generous help with plant resources. I would also like to acknowledge other current and former members of the CFG and CS groups: Xiaoming, Marcel, Li, Yaping, Zhihui, Danning, Alina, Yan, Annika, Junwen, Baogang, Wenxin, Mauritz, Ling, Xuelian, Xiaofang, Klea, Zamiga, Xiaolin, Ben, Anna, Michelle, José, Stephan, Maria, Britta, Claudia, Ute, and Madlen.

I am grateful to Frau Jessen and Frau Kreitz for their administrative support.

I am deeply thankful to my parents, my brother, and my friends for their constant encouragement and support.

Last but not least, I want to thank my master thesis supervisor, Prof. Dr. Fangsen Xu, who inspired my interest in the study of the micronutrient boron.